University of Alberta

Fault Diagnosis in Sampled-data Systems

by

Iman Izadi Najaf Abadi 

A thesis submitted to the Faculty of Graduate Studies and Research in partial fulfillment of the requirements for the degree of **Doctor of Philosophy**.

Department of Electrical and Computer Engineering

Edmonton, Alberta
Fall 2006

Your file Votre référence
ISBN: 978-0-494-23048-0
Our file Notre référence
ISBN: 978-0-494-23048-0

Abstract

In most applications, because of numerous advantages it offers, digital technology (computer, PLC, microcontroller etc.) is used to control industrial plants. These types of systems, where the process under control is continuous-time but the controller is digitally implemented, are called sampled-data systems. Faults can occur in sampled-data systems like any other control system. In order to prevent performance degradation, physical damage or failure, faults should be promptly detected. In this thesis fault diagnosis in sampled-data systems is studied. The sampled-data design can be carried out using direct or indirect design approaches. Direct design, emphasized in this research, does not involve any approximations.

Normally, to design a robust fault detection and isolation (FDI) scheme, a performance index which is a measure of the sensitivity of the FDI to faults and its robustness to unknown inputs and disturbances is defined and optimized. Different performance indices based on $\mathcal{H}_\infty$ and $\mathcal{H}_2$ norms are considered. Using the direct design approach and the so-called norm invariant transformation, it is shown that a sampled-data FDI problem can be converted to an equivalent discrete-time problem. This will form the foundation of a unifying framework for optimal sampled-data residual generator design.

Multirate systems are also abundant in industry. Here, several methods of residual generation based on multirate sampled data are developed. The

key feature of such residual generators is that they operate at a fast rate for prompt fault detection. The lifting technique is used to convert the multirate problem into an equivalent single-rate discrete-time problem with causality constraints.

It is generally believed that the optimal multirate design performs better than the optimal slow-rate and worse than the optimal fast-rate designs. This conjecture is theoretically proved in this thesis for general multirate control systems with norms of the closed-loop system as performance indices. However, it is shown that the common performance indices in FDI design do not satisfy this property. To resolve this, an alternative performance index is defined after formulating the FDI problem as a standard control problem.

Acknowledgements

I would like to express my sincere gratitude to my supervisors, Dr. Qing Zhao and Dr. Tongwen Chen, for their invaluable support. Dr. Zhao's incredible sense of exploring new ideas has been a major driving force in my research. Without her friendly supervision, generous encouragement and patient guidance this thesis would have never been written. As an excellent and knowledgable teacher and a brilliant researcher, Dr. Chen has taught me to be confident, clear and concise in teaching, organized and disciplined in research, and more importantly to develop a sense of professionalism from the early stages of my career. I thank both of them for giving me the opportunity to work in their research groups.

I am grateful to my sponsors, the Ministry of Science, Research and Technology of Iran and the Natural Sciences and Engineering Research Council of Canada. I also thank the members of my Candidacy and Final Oral Examining Committees: Dr. Alan Lynch, Dr. Horacio Marquez, Dr. Venkata Dinavahi, Dr. Nariman Sepehri, Dr. Amos Ben-Zvi and Dr. Scott Meadows, for their invaluable technical guidance.

Far too many people to acknowledge individually have assisted in so many ways during my work at the University of Alberta. They all have my sincere gratitude. In particular, I would like to thank Mehrdad Sahebsara, Amir-Kamal Dehghani, Masoud Abbaszadeh, Vahid Zahedzadeh, Adarsha Swarnakar, Hongbin Li, Amr Pertew and Jiandong Wang, all current or former members of the Advanced Control Systems Lab at the University of Alberta.

I would like to take this opportunity to thank my beloved parents and

brothers for their moral support, encouragement and patience. I'm extremely grateful to them. I also thank my in-laws for their constant support and help.

My most heartfelt acknowledgment must go to my wife Atefeh, whose warm companionship, patience, constant optimism, and support can never be appreciated enough. Words can not express my gratitude and everlasting love. And finally, a special thank-you to my son, Mohammad, for bringing hope, joy and a lot of noise to our life!

الاِمَامُ، الاَنيسُ الرَّفيقُ، وَالوالِدُ الشَّفِيقُ، وَالاَخُ الشَّقِيقُ (الكافى)

To the kindest father, the dearest brother, the most intimate friend.

To the most anticipated.

To *Imam Mahdi.*

Contents

List of Figures

List of Symbols

A^T	Transpose of matrix A
trace(A)	Trace of matrix A
rank(A)	Rank of matrix A
diag$\{a_1, \cdots, a_n\}$	$\begin{bmatrix} a_1 & & 0 \\ & \ddots & \\ 0 & & a_n \end{bmatrix}$
$\lambda_{\min}(A)$	Minimum eigenvalue of matrix A
$\lambda_{\max}(A)$	Maximum eigenvalue of matrix A
$\sigma_{\max}(A)$	Maximum singular value of matrix A
$\|A\|_2$	Induced 2-norm (spectral norm) of matrix A defined as $\|A\|_2 = \sigma_{\max}(A)$
$\delta(t)$	Continuous-time unit impulse function
$\delta_d(k)$	Discrete-time unit impulse function
$1(t)$	Continuous-time unit step function
$1_d(k)$	Discrete-time unit step function
x^*, f^*	Optimal solution and optimal value of the performance index $f(x)$
l.c.m.	Least common multiple
g.c.m.	Greatest common divisor

S_h	The ideal sampling operator with sampling period h
H_h	The (zero-order) hold operator with sampling period h
L_n	The (n-fold) lifting operator (page 49)
G	A linear time-invariant continuous-time system with impulse response function $g(t)$ and transfer function $G(s) = C(sI - A)^{-1}B + D = \left[\begin{array}{c\|c} A & B \\ \hline C & D \end{array}\right]$; or A linear time-invariant discrete-time system with impulse response function $g(k)$ and transfer function $G(z) = C(zI - A)^{-1}B + D = \left[\begin{array}{c\|c} A & B \\ \hline C & D \end{array}\right]$
$G_D(z)$	Step invariant transformation of $G(s)$ (page 27)
$G_I(z)$	Impulse invariant transformation of $G(s)$ (page 28)
$G_J(z)$	Norm invariant transformation of $G(s)$ (page 29)
$G_{\mathrm{BT}}(z)$	Bilinear (Tustin) transformation of $G(s)$ (page 32)
$\mathbb{N}$	Set of natural (nonnegative integer) numbers
$\mathbb{Z}$	Set of integer numbers
$\mathbb{R}$	Set of real numbers
$\mathbb{R}^n$	Set of real $n \times 1$ vectors
$\mathbb{R}^{n\times m}$	Set of real $n \times m$ matrices
$\mathcal{L}(\mathbb{R})$	Vector space of all continuous-time signals
$\|u\|_2$	The $\mathcal{L}_2$ norm of continuous-time signal $u(t) \in \mathcal{L}(\mathbb{R})$ defined as $\|u\|_2 = \left(\int_{-\infty}^{\infty} u^T(t) \cdot u(t)\, dt\right)^{1/2}$
$\mathcal{L}_2(\mathbb{R})$	Vector space of all continuous-time signals with finite $\mathcal{L}_2$ norm

$\|G(s)\|_2$	$\mathcal{H}_2$ norm of continuous-time transfer function $G(s)$ defined as $\|G(s)\|_2 = \left(\frac{1}{2\pi}\int_{-\infty}^{\infty} \text{trace}\left[G^T(-j\omega)G(j\omega)\right]\, d\omega\right)^{1/2}$
$\|G(s)\|_\infty$	$\mathcal{H}_\infty$ norm of continuous-time transfer function $G(s)$ defined as $\|G(s)\|_\infty = \sup_\omega \sigma_{\max}\left[G(j\omega)\right]$
$\ell(\mathbb{Z})$	Vector space of all discrete-time signals
$\|v\|_2$	The ℓ_2 norm of discrete-time signal $v(k) \in \ell(\mathbb{Z})$ defined as $\|v\|_2 = \left(\sum_{k=-\infty}^{\infty} v^T(k)\cdot v(k)\right)^{1/2}$
$\ell_2(\mathbb{Z})$	Vector space of all discrete-time signals with finite ℓ_2 norm
$\|G(z)\|_2$	$\mathcal{H}_2$ norm of discrete-time transfer function $G(z)$ defined as $\|G(z)\|_2 = \left(\frac{1}{2\pi}\int_0^{2\pi} \text{trace}\left[G^T(e^{-j\omega})G(e^{j\omega})\right]\, d\omega\right)^{1/2}$
$\|G(z)\|_\infty$	$\mathcal{H}_\infty$ norm of discrete-time transfer function $G(z)$ defined as $\|G(z)\|_\infty = \sup_\omega \sigma_{\max}\left[G(e^{j\omega})\right]$
$\mathcal{RH}_\infty$	Set of all real-rational, proper and stable continuous-time transfer functions; or Set of all real-rational, proper and stable discrete-time transfer functions

Conventions

- Continuous-time signals are represented by Roman letters, discrete-time signals by Greek letters.
- In block diagrams, continuous-time signals are represented by continuous lines, discrete-time signals by dotted lines.

Chapter 1

Introduction

1.1 Background

By definition a *fault* is a nonpermitted deviation of a characteristic property which leads to the inability to fulfil the intended purpose [7, 30]. Faults can occur in all of the components of a closed-loop control system including sensors, actuators, communication network and the process under control. Such faults disturb the normal operation of the control system and may result in unsatisfactory performance, instability, *failure* (complete breakdown of a system component or function) or even dangerous situations. Due to the increasing complexity of modern control systems and the growing demands for quality, cost efficiency, availability, reliability and safety, it is important that faults be promptly diagnosed and appropriate remedies be applied.

A monitoring system which is used to detect faults and determine their type, location, time of occurrence and significance is called a *fault diagnosis* system [7, 30]. The overall concept of fault diagnosis consists of the following three tasks [7, 19]:

- **Fault detection**: determination of the presence of a fault in a system and the time of its occurrence.
- **Fault isolation**: determination of the location of different faults, e.g., which sensor or actuator has become faulty.
- **Fault identification**: estimation of the type, magnitude and cause of the fault.

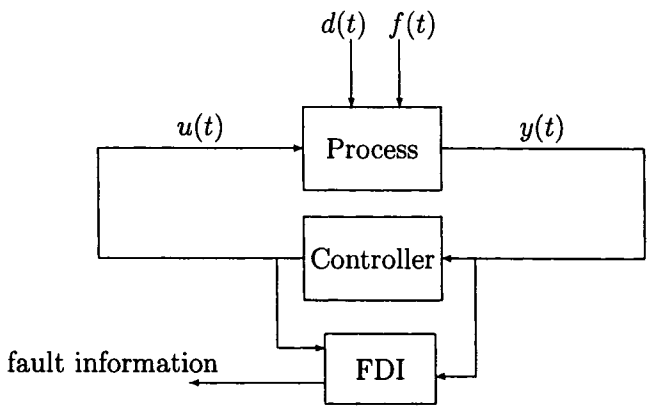

Figure 1.1: A typical fault detection and isolation scheme

Depending on the type of fault and the acceptable performance of a control system, these three tasks can be relatively important. However, fault detection is an absolute must for any practical system and fault isolation is almost equally important. On the other hand, fault identification may not be essential if no reconfiguration action is involved [7]. Hence, in the literature, fault diagnosis is often considered as *fault detection and isolation* (FDI). Research in fault diagnosis has been gaining attention during the past three decades in both theory and application, and numerous results are available in the literature. Many books, tutorial papers and surveys have also been written on the subject [7, 18, 19, 21, 22, 23, 24, 25, 41].

A typical scheme of fault detection and isolation in a control system is illustrated in Figure 1.1. In this scheme, besides the control signal $u(t)$, there are two other inputs to the process: unknown disturbance $d(t)$ and fault to be detected $f(t)$. The FDI uses process input $u(t)$ and process output $y(t)$ to detect the faults. Based on the information obtained from the FDI one can decide how to deal with the faults.

Various methods of fault diagnosis have been developed in the literature. These methods have also been categorized in various groups based on different criteria [19, 41]. Here, three main categories of fault detection methods are briefly introduced:

Hardware redundancy is a traditional approach to fault diagnosis. The method is based on using multiple lanes of sensors, actuators and computer

hardware/software to measure and control a particular variable. A voting scheme is then applied to decide if a fault has occurred and its likely location [31, 43, 47]. The use of hardware redundancy is common in highly sensitive systems like flight control [17]. While this method is very reliable, extra equipment and maintenance cost and the additional space required to accommodate the redundant hardware could be serious problems.

Signal based fault detection is the most frequently used diagnosis method in practice [4, 44]. The idea is to monitor the level of a particular signal and raise alarm when the signal reaches a certain threshold. This method is easy to implement but it has some serious drawbacks. Firstly, the method is not robust, i.e., in the event of noise, input variation and change of operating point, false alarms can possibly be raised. Secondly, a single fault can cause many system signals to exceed their limits, which makes fault isolation very difficult. In view of these drawbacks, some techniques have been recently proposed that combine the signal based approach with statistical methods, in order to improve the robustness and accuracy of fault detection [26].

Model based fault detection can be defined as detection and isolation of faults by comparing the systems' available measurements with *a priori* information represented by a mathematical model of the system (analytical redundancy). The difference between real measurements and estimates of these measurements are used to generate a residual quantity. Fault is then detected by setting a threshold on this residual quantity. A number of residuals can be designed for faults occurring in different locations of the system. The analysis of each individual residual leads to fault isolation. The main focus in this thesis is on model based methods of fault detection, which will be discussed in more details in Chapter 2.

Because of numerous advantages that digital technology and computers can offer, nowadays most of control and fault detection algorithms are implemented by computers. A combination of a real world continuous-time process and a digital controller is called a sampled-data system. Extensive research has been carried out on sampled-data systems and various approaches for controller design have been introduced [9]. Processes that are controlled in a sampled-data framework are also susceptible to faults. So the question that naturally

comes to mind is that how faults can be detected in a sampled-data framework. This question and other related issues in sampled-data fault detection are addressed in this thesis.

A relatively easy approach to the sampled-data FDI problem is to use the known continuous-time or discrete-time techniques. This is known as indirect design, and can be accomplished in two ways:

- One can first design a continuous-time FDI for the continuous-time system and then approximate it by a discrete-time FDI.
- Alternatively, one can first approximate the continuous-time system by a discrete-time one and then design a discrete-time FDI.

Because of the approximation involved in both designs, one might not get a satisfactory result [54]. In control system design, there exists another approach that enables us to directly design a discrete-time controller for the continuous-time system without making any approximations [9], known as direct design. The direct approach for controller design motivates us to investigate a direct method of FDI design for sampled-data systems. Some work has been recently done on this subject and interesting results are available [53, 56, 58]. In this thesis, a unifying and general approach is developed for FDI design in sampled-data systems by using the so-called norm invariant transformation. The approach is based on converting the original sampled-data problem to a discrete-time one.

In the study of sampled-data systems, an essential assumption is that all the inputs/outputs are generated/sampled synchronously at a single rate. However, this is not the case in many industrial situations where different control signals are generated at different rates and/or different process outputs are measured at different rates. These systems, known as multirate sampled-data systems, are again susceptible to faults. The next problem discussed in this thesis is how to design an FDI for multirate sampled-data systems. Some methods are already available in the literature [14, 15, 16, 49, 55, 57, 59]. In most of these methods, detection of faults can be substantially delayed because the fault information (residual) is generated at a slow rate. To reduce or eliminate the detection delay, an FDI scheme needs to generate the fault information at the fastest rate possible. The approach adopted here guaran-

tees that anytime a new piece of information arrives from the process, the FDI updates the residual.

One of the important properties of an FDI is that it should be insensitive to disturbance, noise and other unknown inputs in order to lower the false alarm rate. Meanwhile, the FDI should be adequately sensitive to faults so that it can properly detect even very small faults. Therefore, the most challenging trade-off in FDI design is to increase sensitivity to faults and robustness to other unknown inputs. Researchers try to address this trade-off by introducing and optimizing a performance index. Therefore, selection of an appropriate performance index and developing analytical or numerical optimization methods are fundamental steps in any robust FDI design. But what is exactly meant by an "appropriate" performance index? This is another subject that is investigated in this thesis.

One of the properties that is intuitively expected from an "appropriate" performance index is that: if more information (from the system) is available then better performance can be achieved. The precise mathematical statement of this property will be provided later in the thesis, but what is important for now is that, the popular and commonly used performance indices in FDI design do not satisfy this property. This will be shown via some examples. It will also be proved that the performance index used for controller design (some norm of the closed-loop system) is in fact "appropriate" in the sense that it satisfies the aforementioned property. Therefore, if one can formulate the FDI design problem as a controller design problem, then the control performance index can be readily used. In this thesis an approach is proposed to implement this idea and convert the sampled-data FDI problem to an equivalent sampled-data control problem.

1.2 Outline of the thesis

The rest of this thesis is organized as follows:

In Chapter 2, model based methods of fault detection are reviewed. After a brief discussion of how faults are modelled in dynamical systems, the concepts of residual and residual generation are introduced. The three main methods of model based residual generation which are: observer, parity space and factorization, are briefly reviewed. The issue of robust residual generation

and its methods are also addressed. Finally, the decoupling of residual from disturbance is discussed.

Chapter 3 is about fault detection in sampled-data systems. After reviewing the concepts of direct and indirect designs in sampled-data systems, the techniques to convert a continuous-time model to a discrete-time one are discussed. Generalizations of the concepts of $\mathcal{H}_\infty$ and $\mathcal{H}_2$ norms to sampled-data systems are given next. These concepts are then used to address the robustness of residual generators in sampled-data systems. The important contribution of this chapter is to provide a general formulation of the robust residual generator for sampled-data systems. This will be achieved by converting the sampled-data problem to a discrete-time problem, which can be solved using existing methods of discrete-time FDI design.

Chapter 4 is dedicated to fault detection in multirate systems. A multirate sampled-data system is converted to a single-rate discrete-time system using the lifting operation and direct design. This will form the basic framework for fault detection in multirate systems. Methods of residual generation are directly applicable to the equivalent discrete-time model. However, the result will be a slow-rate residual generator. Two methods of fast-rate residual generation are then proposed based on parity space and factorization (with $\mathcal{H}_\infty$ optimization) techniques, and the optimality and causality issues are addressed.

In Chapter 5, an analysis of the performance index in sampled-data control systems is given. $\mathcal{H}_\infty$ and $\mathcal{H}_2$ performances of sampled-data and linear periodically time-varying systems (LPTV) are defined. Then the theorems that compare the performances of slow-rate, fast-rate, and multirate systems are proposed and proved.

In Chapter 6, motivated by the results of Chapter 5, the performance indices used for sampled-data fault detection are studied. It is shown, through some examples, that the expected properties do not hold for these performance indices. To address this, the sampled-data FDI problem is converted to a standard control problem which can be solved using known techniques.

A summary of the thesis, final conclusions and some directions for future work are given in Chapter 7.

Chapter 2

Model Based Fault Diagnosis

The model based fault diagnosis approach makes explicit use of a mathematical model of the process. It has been receiving considerable attention during the past decades, both in research and application. A great variety of methods of model based FDI have been developed based on the use of mathematical models and modern control theory.

Two main steps in a successful model based FDI algorithm are:

- **Residual generation**: A residual generator uses the available input and output information of the process to generate a fault indicating signal (residual). The residual should be normally zero or close to zero when no fault is present, but different from zero when a fault occurs. This means that in ideal conditions, the residual is independent of the input and output of the system.

- **Residual evaluation (decision making)**: The residuals generated by residual generators are examined for the likelihood of faults and a decision is made based on that. An evaluation process may consist of a simple threshold test on the instantaneous values or moving averages of the residual. Alternatively methods of statistical decision theory (e.g., generalized likelihood ratio testing or sequential probability ratio testing) may be used to evaluate the residual.

Most of the work in the field of model based FDI is focused on the residual generation problem. The reason is that residual evaluation and decision making are relatively easy on well designed residuals. However, this does not

imply that the research on residual evaluation is not important. This thesis concentrates on model based residual generation.

Ideally the residual should only be sensitive to faults. If no modelling uncertainty is present, the dependency of the residual on the input and output of a system can be removed by proper design. In addition to the controlled input of a system (control signal), other unknown inputs (e.g., disturbance, measurement noise, etc.) can change the output of the system and hence the residual. This may cause a false alarm even when a fault has not occurred. A model based FDI has to be sensitive with respect to faults in order to detect incipient faults, but robust with respect to unknown inputs and modelling uncertainties in order to avoid false alarms. Thus, an important property of a model based FDI is the robustness against modelling uncertainty and disturbance. Robust FDI has become a central research issue over recent years.

2.1 Modelling of faulty systems

From the fault diagnosis point of view, it is useful to divide the faults into three categories [19]:

- Actuator faults
- Component faults
- Sensor faults

In model based methods, faults are commonly modelled as input signals. In addition, there are always other (unknown) inputs in the system due to disturbance, noise, etc. Model uncertainty, which always exists in real world problems, is also modelled by unknown input. So, in general, apart from the actual controlled input to the process, two other sets of inputs are considered: vector of faults to be detected and vector of unknown inputs (which represents disturbance, noise, model uncertainty, etc.).

In this research, linear time-invariant (LTI) multiple-input multiple-output (MIMO) dynamical systems are considered. A dynamical system with a possibility of fault occurrence can be modelled both by state space or transfer function equations.

State space model

The state space model of a faulty system is given as

$$\begin{cases} \dot{x}(t) = Ax(t) + Bu(t) + E_d d(t) + E_{f_a} f_a(t) + E_{f_c} f_c(t) \\ y(t) = Cx(t) + Du(t) + D_d d(t) + D_{f_a} f_a(t) + D_{f_s} f_s(t) \end{cases}$$

where $x(t) \in \mathbb{R}^n$ is the state vector, $u(t) \in \mathbb{R}^{n_u}$ the vector of control signal, $y(t) \in \mathbb{R}^m$ the vector of plant output, $d(t) \in \mathbb{R}^{n_d}$ the vector of unknown inputs (e.g., disturbance, noise, model mismatch, etc.), $f_a(t) \in \mathbb{R}^{n_{f_a}}$ the vector of actuator faults, $f_c(t) \in \mathbb{R}^{n_{f_c}}$ the vector of component faults and $f_s(t) \in \mathbb{R}^{n_{f_s}}$ the vector of sensor faults. A, B, C, D, E_d, D_d, E_{f_a}, D_{f_a}, E_{f_c} and D_{f_s} are known matrices of appropriate dimensions.

Combining all possible faults together, a general faulty system can be modelled as

$$\begin{cases} \dot{x}(t) = Ax(t) + Bu(t) + E_d d(t) + E_f f(t) \\ y(t) = Cx(t) + Du(t) + D_d d(t) + D_f f(t) \end{cases}$$

where $f(t) \in \mathbb{R}^{n_f}$ is the fault vector. Each element of the fault vector $f(t)$ corresponds to a specific component/actuator/sensor fault. E_f and D_f are known as fault entry matrices and represent the effect of faults on the system.

Transfer function model

Transfer functions may also be used to model a faulty system:

$$y(t) = G_u u(t) + G_d d(t) + G_f f(t), \tag{2.1}$$

where $u(t) \in \mathbb{R}^{n_u}$ is the input vector, $y(t) \in \mathbb{R}^m$ the output vector, $d(t) \in \mathbb{R}^{n_d}$ the vector of unknown inputs and $f(t) \in \mathbb{R}^{n_f}$ the vector of faults to be detected. $G_u(s)$, $G_d(s)$ and $G_f(s)$ are transfer functions of appropriate dimensions.

Discrete-time systems

Similar to the continuous-time models, one of the following models for discrete-time faulty systems might be used:

State space model: $$\begin{cases} x(k+1) = Ax(k) + Bu(k) + E_d d(k) + E_f f(k) \\ y(k) = Cx(k) + Du(d) + D_d d(k) + D_f f(k) \end{cases}$$

Transfer function model: $$y(k) = G_u u(k) + G_d d(k) + G_f f(k)$$

Here, $x(k) \in \mathbb{R}^n$, $u(k) \in \mathbb{R}^{n_u}$, $y(k) \in \mathbb{R}^m$, $d(k) \in \mathbb{R}^{n_d}$ and $f(k) \in \mathbb{R}^{n_f}$ are the state, control signal, plant output, unknown input and fault vectors respectively. A, B, C, D, E_d, D_d, E_f and D_f are known matrices of appropriate dimensions. $G_u(z)$, $G_d(z)$ and $G_f(z)$ are discrete-time LTI transfer functions of appropriate dimensions.

2.2 General structure of residual generator

In this section, the general structure of a residual generator in model based methods of FDI design is derived. The information used for residual generation in a continuous-time system is the measured output from sensors $y(t)$ and the control signal $u(t)$. A residual generator is a linear time-invariant process; its input consists of both input and output of the system under monitor and its output is the residual. A typical residual generator is then described by:

$$r(t) = \begin{bmatrix} Q_y & Q_u \end{bmatrix} \begin{bmatrix} y(t) \\ u(t) \end{bmatrix} = Q_y y(t) + Q_u u(t), \tag{2.2}$$

where $r(t) \in \mathbb{R}$ is the residual. $Q_y(s)$ and $Q_u(s)$ are stable LTI transfer function matrices.

First the simple case when no unknown input is present in the system is considered, i.e., $d \equiv 0$. By definition the residual is designed to become zero for the fault free case and nonzero for the faulty case:

$$\text{residual} = \begin{cases} \text{zero} & f \equiv 0, \\ \text{nonzero} & f \neq 0. \end{cases}$$

In other words $r \equiv 0$ if and only if $f \equiv 0$. To satisfy this condition, after substituting system model (2.1) in (2.2), Q_y and Q_u must satisfy the following constraint:

$$Q_y(s)G_u(s) + Q_u(s) = 0. \tag{2.3}$$

This condition parameterizes all linear residual generators. Satisfaction of condition (2.3) guarantees that the residual is independent of the controlled input of the process. Design of a residual generator is now summarized in the selection of Q_y and Q_u.

If the process is affected by unknown inputs (i.e., $d(t) \neq 0$), then in addition to condition (2.3) other constraints are raised. One now needs to generate a

residual that is as sensitive as possible to faults and as robust as possible to unknown inputs, which introduces the concept of robust FDI.

Different model based methods of residual generation vary in how they parameterize the residual generator (i.e., Q_y and Q_u) and how they tackle the robustness problem. Various methods have been developed in the literature, most of them belong to one of these main categories:

- observer based approach,
- parity space approach,
- factorization approach,
- parameter estimation approach.

Although these methods have been developed independently over decades, several researchers have pointed out that there are close relationships among the different approaches [19]. In this chapter, some of the methods that are emphasized in our research are briefly reviewed.

2.3 Observer based methods

A wide class of linear residual generators are observers. The idea is to use an observer to estimate the output of the plant and then compare the estimated output with the actual output to generate the residual. A typical observer based residual generator is formulated as:

$$\begin{cases} \dot{w}(t) = Fw(t) + Ky(t) + Ju(t) \\ r(t) = L_1 w(t) + L_2 y(t) + L_3 u(t) \end{cases}$$

$w(t) \in \mathbb{R}^{n_w}$ is the state vector of residual generator and $r(t) \in \mathbb{R}$ is the residual. Matrices F, K, J, L_1, L_2 and L_3 are designed to guarantee stability of the residual generator, satisfy the general condition (2.3) and make the effect of $d(t)$ on $r(t)$ zero or as small as possible. To do so different approaches are available: unknown input observers, fault detection filters and eigenstructure assignment, to name a few [21, 28, 42]. The methods are readily extendible to the discrete-time case [7].

2.4 Parity space approach

The parity space approach was originally introduced for discrete-time systems [11]. However, some attempts have been made to generalize it to the continuous-time case [40]. Here, the original form of parity space as introduced in [11] is considered for the following discrete-time system

$$\begin{cases} x(k+1) = Ax(k) + Bu(k) + E_d d(k) + E_f f(k) \\ y(k) = Cx(k) + Du(k) + D_d d(k) + D_f f(k) \end{cases}$$

It is assumed that (C, A) is observable.

A parity space based residual generator is formulated as:

$$r(k) = v_s\big(y_s(k) - H_{u,s}u_s(k)\big), \tag{2.4}$$

where

$$y_s(k) = \begin{bmatrix} y(k-s) \\ y(k-s+1) \\ \vdots \\ y(k) \end{bmatrix}, \quad u_s(k) = \begin{bmatrix} u(k-s) \\ u(k-s+1) \\ \vdots \\ u(k) \end{bmatrix},$$

$$H_{u,s} = \begin{bmatrix} D & 0 & \cdots & 0 & 0 \\ CB & D & \cdots & 0 & 0 \\ \vdots & \vdots & & \vdots & \vdots \\ CA^{s-1}B & CA^{s-2}B & \cdots & CB & D \end{bmatrix}.$$

Here, $r(k) \in \mathbb{R}$ is the residual and s is the order of parity relation. The design parameter $v_s \in \mathbb{R}^{1\times m(s+1)}$ is known as the parity vector. To satisfy the general residual generator condition (2.3), the parity vector v_s should satisfy

$$v_s H_{o,s} = 0, \quad H_{o,s} = \begin{bmatrix} C \\ CA \\ \vdots \\ CA^s \end{bmatrix}. \tag{2.5}$$

The set of all parity vectors that satisfy condition (2.5) is known as parity space P_s

$$P_s = \{v_s | v_s H_{o,s} = 0\}.$$

Substituting $y(k)$ from the plant model in (2.4) and using the condition (2.5), the dynamics of the residual generator is expressed by

$$r(k) = v_s\big(H_{d,s}d_s(k) + H_{f,s}f_s(k)\big), \quad v_s \in P_s$$

where

$$d_s(k) = \begin{bmatrix} d(k-s) \\ d(k-s+1) \\ \vdots \\ d(k) \end{bmatrix}, \quad f_s(k) = \begin{bmatrix} f(k-s) \\ f(k-s+1) \\ \vdots \\ f(k) \end{bmatrix},$$

$$H_{d,s} = \begin{bmatrix} D_d & 0 & \cdots & 0 & 0 \\ CE_d & D_d & \cdots & 0 & 0 \\ \vdots & \vdots & & \vdots & \vdots \\ CA^{s-1}E_d & CA^{s-2}E_d & \cdots & CE_d & D_d \end{bmatrix},$$

$$H_{f,s} = \begin{bmatrix} D_f & 0 & \cdots & 0 & 0 \\ CE_f & D_f & \cdots & 0 & 0 \\ \vdots & \vdots & & \vdots & \vdots \\ CA^{s-1}E_f & CA^{s-2}E_f & \cdots & CE_f & D_f \end{bmatrix}.$$

Now, the problem is how to find v_s. If there exists a parity vector $v_s \in P_s$ such that

$$v_s H_{d,s} = 0,$$
$$v_s H_{f,s} \neq 0,$$

then the residual $r(k)$ can be perfectly decoupled from the unknown input $d(k)$. Otherwise, the effect of $d(k)$ on $r(k)$ can be minimized by solving an optimization problem. A common choice of performance index for optimization is

$$J = \frac{\|v_s H_{d,s}\|_2}{\|v_s H_{f,s}\|_2} = \frac{v_s H_{d,s} H_{d,s}^T v_s^T}{v_s H_{f,s} H_{f,s}^T v_s^T}. \tag{2.6}$$

The numerator of J in (2.6) reflects the effect of unknown input $d(k)$ on the residual while the denominator reflects the effect of fault $f(k)$. By minimizing J a compromise is made between sensitivity to the fault and robustness to the disturbance. v_s is then designed by solving the optimization problem

$$\min_{v_s \in P_s} J. \tag{2.7}$$

The complete analytical solution of this optimization problem can be found in [11]. Here the optimal solution is given without proof.

Assume that N_B is the basis vector for parity space P_s (or the null space of $H_{o,s}$), i.e., for any parity vector v_s there exists a vector p_s such that $v_s =$

$p_s N_B$. Also assume that $\lambda_{\min}$ is the minimum generalized eigenvalue of the pair $\left(N_B H_{d,s} H_{d,s}^T N_B^T, N_B H_{f,s} H_{f,s}^T N_B^T\right)$ and $p_{s,\min}$ is the corresponding generalized eigenvector, i.e.,

$$p_{s,\min} N_B H_{d,s} H_{d,s}^T N_B^T = \lambda_{\min} p_{s,\min} N_B H_{f,s} H_{f,s}^T N_B^T.$$

Then $v_s^* = p_{s,\min} N_B$ is the optimal solution of (2.7) and $J^* = \lambda_{\min}$ is the optimal performance.

2.5 Factorization approach

As discussed earlier, any linear residual generator can be described as (2.2) with Q_y and Q_u satisfying (2.3). Here, a parametrization of all linear residual generators based on the coprime factorization of G_u is given [20].

Consider the LTI continuous-time process described by the transfer function model

$$y(t) = G_u u(t) + G_d d(t) + G_f f(t). \tag{2.8}$$

Let $\left(M_u(s), N_u(s)\right)$ be a left coprime factorization of $G_u(s)$, i.e., $M_u(s)$ and $N_u(s)$ are left coprime and they satisfy

$$G_u(s) = M_u^{-1}(s) N_u(s).$$

Then a parametrization of Q_y and Q_u is given as

$$\begin{aligned} Q_y(s) &= R(s) M_u(s), \\ Q_u(s) &= -R(s) N_u(s). \end{aligned}$$

In other words all linear residual generators for the continuous-time system in (2.8) can be parameterized as

$$r(t) = R\big(M_u y(t) - N_u u(t)\big), \tag{2.9}$$

where $R(s) \in \mathcal{RH}_\infty^{1\times m}$ is a designable post-filter. Let

$$G_u(s) = \left[\begin{array}{c|c} A & B \\ \hline C & D \end{array}\right].$$

Assuming (C, A) is observable, the left coprime factorization $\left(M_u(s), N_u(s)\right)$ can be parameterized as

$$M_u(s) = \left[\begin{array}{c|c} A - LC & L \\ \hline -C & I \end{array}\right],$$
$$N_u(s) = \left[\begin{array}{c|c} A - LC & B - LD \\ \hline C & D \end{array}\right],$$

where L is a free-to-choose matrix which ensures that $A - LC$ is Hurwitz. Note that when $G_u(s)$ is stable, one can choose $L = 0$ and thus $M_u(s) = I$ and $N_u(s) = G_u(s)$. In this case the general form of the residual generator is

$$r(t) = R(y(t) - G_u u(t)).$$

Design of the residual generator is now summarized in finding the stable transfer function matrix $R(s)$. Substituting the system model (2.8) into the residual generator (2.9), the dynamics of the residual generator can be expressed by

$$\begin{aligned} r(t) &= RM_u G_d d(t) + RM_u G_f f(t) \\ &= RM_u(G_d d(t) + G_f f(t)). \end{aligned}$$

This equation shows how the fault $f(t)$ and the unknown input $d(t)$ affect the residual. In the ideal case, the residual should only be sensitive to $f(t)$ which means that $d(t)$ should have no effect on the residual. If a post-filter $R(s)$ can be found such that

$$R(s)M_u(s)G_d(s) \equiv 0,$$
$$R(s)M_u(s)G_f(s) \not\equiv 0.$$

then perfect decoupling of the residual from the unknown input is possible (this case will be discussed later in Section 2.6). Otherwise, in order to compromise between the sensitivity of the residual to the fault and its robustness to the unknown input, one should design $R(s)$ to make $R(s)M_u(s)G_d(s)$ as small as possible (in some sense) while keeping $R(s)M_u(s)G_f(s)$ reasonably large. Using some definition of norm as a measure of the size of a system, $R(s)$ is to be found such that $\|R(s)M_u(s)G_d(s)\|$ becomes small while $\|R(s)M_u(s)G_f(s)\|$

remains large. This is usually achieved by solving an optimization problem. As a widely accepted approach the following optimization problem is considered

$$\min_{R(s)\in\mathcal{RH}_\infty^{l\times m}} \frac{\|R(s)M_u(s)G_d(s)\|}{\|R(s)M_u(s)G_f(s)\|}.$$

The solutions of this optimization problem for the common $\mathcal{H}_\infty$ and $\mathcal{H}_2$ norms are briefly review next.

2.5.1 $\mathcal{H}_\infty$ optimization

In the $\mathcal{H}_\infty$ approach the performance index is

$$J_{\infty/\infty} = \frac{\|R(s)M_u(s)G_d(s)\|_\infty}{\|R(s)M_u(s)G_f(s)\|_\infty},$$

and the optimization problem becomes

$$\min_{R(s)\in\mathcal{RH}_\infty} J_{\infty/\infty}. \tag{2.10}$$

The analytical solution of this optimization problem is given in [13, 20] which is briefly reviewed here.

Assume that $G_d(s)$ has no transmission zeros on the imaginary axis and at infinity (i.e., $G_d(j\omega)$ does not lose rank for all ω [5]). This assumption ensures that there exists a so-called co-inner-outer factorization of $M_u(s)G_d(s)$ such that

$$M_u(s)G_d(s) = G_{do}(s)G_{di}(s).$$

The co-inner $G_{di}(s)$ satisfies $G_{di}(j\omega)G_{di}^T(-j\omega) = I$. The co-outer $G_{do}(s)$ has a left inverse $G_{do}^{-1}(s) \in \mathcal{RH}_\infty$ such that $G_{do}^{-1}(s)G_{do}(s) = I$. Now define a change of variable as

$$R(s) = Q(s)G_{do}^{-1}(s),$$

where $Q(s) \in \mathcal{RH}_\infty$ is the new parameter. The performance index in terms of $Q(s)$ will be

$$J_{\infty/\infty} = \frac{\|Q(s)G_{di}(s)\|_\infty}{\|Q(s)G_{do}^{-1}(s)M_u(s)G_f(s)\|_\infty}.$$

Using the fact that

$$\|Q(s)G_{di}(s)\|_\infty = \|Q(s)\|_\infty,$$

and the submultiplicative property of $\mathcal{H}_\infty$ norm

$$\|Q(s)G_{do}^{-1}(s)M_u(s)G_f(s)\|_\infty \leq \|Q(s)\|_\infty \|G_{do}^{-1}(s)M_u(s)G_f(s)\|_\infty,$$

imply that

$$J_{\infty/\infty} = \frac{\|Q(s)\|_\infty}{\|Q(s)G_{do}^{-1}(s)M_u(s)G_f(s)\|_\infty} \geq \frac{\|Q(s)\|_\infty}{\|Q(s)\|_\infty \|G_{do}^{-1}(s)M_u(s)G_f(s)\|_\infty} = \frac{1}{\|G_{do}^{-1}(s)M_u(s)G_f(s)\|_\infty}.$$

Therefore, the optimal performance index is

$$J_{\infty/\infty}^* = \frac{1}{\|G_{do}^{-1}(s)M_u(s)G_f(s)\|_\infty}. \tag{2.11}$$

This optimal performance index can be achieved by selecting any stable $Q(s)$ that satisfies

$$\|Q(s)G_{do}^{-1}(s)M_u(s)G_f(s)\|_\infty = \|Q(s)\|_\infty \|G_{do}^{-1}(s)M_u(s)G_f(s)\|_\infty. \tag{2.12}$$

Conventionally $Q(s) = I$ is chosen, but in this thesis the general form of $Q(s)$ is considered.

In summary, the family of optimal solutions of the optimization problem in (2.10) is given as

$$R^*(s) = Q(s)G_{do}^{-1}(s),$$

where the parameter $Q(s) \in \mathcal{RH}_\infty$ satisfies (2.12). The optimal value of the performance index $J_{\infty/\infty}$ is given in (2.11).

This solution is obtained under the assumption that $G_d(s)$ has no transmission zeros on the imaginary axis and at infinity, which is too restrictive. For example if $G_d(s)$ is strictly proper, then it has zeros at infinity and $G_{do}(s)$ does not have a left inverse in $\mathcal{RH}_\infty$. An approach was delivered in [13] which extended this result to the case that $G_{do}(s)$ is not left invertible. There is also another parametrization of the solution in [20] that does not require the assumption that $G_d(s)$ has no zeros at infinity.

2.5.2 $\mathcal{H}_2$ optimization

For the $\mathcal{H}_2$ approach, the following performance index is considered

$$J_{2/2} = \frac{\|R(s)M_u(s)G_d(s)\|_2^2}{\|R(s)M_u(s)G_f(s)\|_2^2}.$$

Thus, the optimization problem becomes

$$\min_{R(s)\in\mathcal{RH}_\infty} J_{2/2}. \tag{2.13}$$

Using the definition of $\mathcal{H}_2$ norm, the performance index $J_{2/2}$ can be written as

$$J_{2/2} = \frac{\int_{-\infty}^{\infty} R(j\omega)M_u(j\omega)G_d(j\omega)G_d^T(-j\omega)M_u^T(-j\omega)R^T(-j\omega)d\omega}{\int_{-\infty}^{\infty} R(j\omega)M_u(j\omega)G_f(j\omega)G_f^T(-j\omega)M_u^T(-j\omega)R^T(-j\omega)d\omega}.$$

The analytical solution of this optimization problem is proposed in [12]. Here the optimal solution is given without proof.

Assume that $f_{\omega_0}(s)$ is an ideal frequency selector at frequency ω_0, i.e.,

$$\forall q(s) \in \mathcal{RH}_\infty^{1\times m},$$
$$\begin{cases} f_{\omega_0}(j\omega)q(j\omega) = 0, \quad \omega \neq \omega_0 \\ \int_{-\infty}^{\infty} f_{\omega_0}(j\omega)q(j\omega)q^T(-j\omega)f_{\omega_0}^T(-j\omega)d\omega = q(j\omega_0)q^T(-j\omega_0). \end{cases}$$

Also assume that $\lambda_{\min}(\omega)$ is the minimum generalized eigenvalue and $v_{\min}(j\omega)$ is the corresponding generalized eigenvector of the following generalized eigenvalue problem

$$v_{\min}(j\omega)M_u(j\omega)G_d(j\omega)G_d^T(-j\omega)M_u^T(-j\omega) = \lambda_{\min}(\omega)v_{\min}(j\omega)M_u(j\omega)G_f(j\omega)G_f^T(-j\omega)M_u^T(-j\omega).$$

Also assume that $\lambda_{\min}(\omega)$ has its minimum at frequency ω^*, i.e.,

$$\lambda_{\min}(\omega^*) = \inf_{\omega} \lambda_{\min}(\omega).$$

The optimal solution of the optimization problem in (2.13) is

$$R^*(s) = f_{\omega^*}(s)v_{\min}(s),$$

and the optimal value of the performance index is

$$J_{2/2}^* = \lambda_{\min}(\omega^*).$$

The ideal frequency selector $f_{\omega_0}(s)$ is not practically implementable. In practice usually a bandpass filter with a narrow frequency bandwidth is used to approximate the ideal frequency selector.

2.5.3 Discrete-time systems

The factorization approach for discrete-time systems is very similar to the continuous-time case. Consider the LTI discrete-time process described by

$$y(k) = G_u u(k) + G_d d(k) + G_f f(k). \tag{2.14}$$

Let $\big(M_u(z), N_u(z)\big)$ be a left coprime factorization of $G_u(z)$, i.e., $M_u(z)$ and $N_u(z)$ are left coprime and they satisfy

$$G_u(z) = M_u^{-1}(z) N_u(z).$$

Then all linear discrete-time residual generators can be parameterized as

$$r(k) = R\big(M_u y(k) - N_u u(k)\big), \tag{2.15}$$

where $R(z) \in \mathcal{RH}_\infty^{1\times m}$ is a designable post-filter. Substituting the system model into the residual generator (2.15) the dynamics of the residual generator is expressed by

$$r(k) = RM_u G_d d(k) + RM_u G_f f(k).$$

If a post-filter $R(z)$ can be found such that

$$\begin{aligned} R(z)M_u(z)G_d(z) &\equiv 0, \\ R(z)M_u(z)G_f(z) &\neq 0, \end{aligned}$$

then perfect decoupling of the residual from the unknown input is possible. Otherwise similar to the continuous-time case, $R(z)$ is designed by optimizing a performance index. Performance indices based on $\mathcal{H}_\infty$ and $\mathcal{H}_2$ norms are widely accepted.

In the $\mathcal{H}_\infty$ approach the performance index is described by

$$J_{\infty/\infty} = \frac{\|R(z)M_u(z)G_d(z)\|_\infty}{\|R(z)M_u(z)G_f(z)\|_\infty},$$

and the optimization problem becomes

$$\min_{R(z)\in\mathcal{RH}_\infty} J_{\infty/\infty}. \tag{2.16}$$

Assume that $G_d(z)$ has no transmission zeros on the unit circle, then there exists a co-inner-outer factorization of $M_u(z)G_d(z)$ such that

$$M_u(z)G_d(z) = G_{do}(z)G_{di}(z).$$

The co-inner $G_{di}(z)$ satisfies $G_{di}(e^{j\omega h})G_{di}^T(e^{-j\omega h}) = I$. The co-outer $G_{do}(z)$ has a left inverse $G_{do}^{-1}(z) \in \mathcal{RH}_\infty$ such that $G_{do}^{-1}(z)G_{do}(z) = I$. In Appendix A a method for calculating the co-inner-outer factorization of a discrete-time system is given.

Similar to the continuous-tim case, the optimal solution of the optimization problem in (2.16) is parameterized as

$$R^*(z) = Q(z)G_{do}^{-1}(z),$$

where the free parameter $Q(z) \in \mathcal{RH}_\infty$ satisfies

$$\|Q(z)G_{do}^{-1}(z)M_u(z)G_f(z)\|_\infty = \|Q(z)\|_\infty \|G_{do}^{-1}(z)M_u(z)G_f(z)\|_\infty.$$

The optimal value of the performance index is

$$J_{\infty/\infty}^* = \frac{1}{\|G_{do}^{-1}(z)M_u(z)G_f(z)\|_\infty}.$$

There is a major difference between this solution and the solution in the continuous-tim case. In continuous-time, the solution was obtained under the assumption that $G_d(s)$ has no transmission zeros on the imaginary axis and at infinity. The no-zero-at-infinity assumption is quite restrictive for the method can not be directly applied when $G_d(s)$ is strictly proper. In the discrete-time case, however, the only assumption required is that $G_d(z)$ has no transmission zeros on the unit circle. Therefore, $G_d(z)$ can be strictly proper, which will always be the case in sampled-data systems.

For the $\mathcal{H}_2$ approach, considering the following performance index

$$J_{2/2} = \frac{\|R(z)M_u(z)G_d(z)\|_2^2}{\|R(z)M_u(z)G_f(z)\|_2^2},$$

the optimization problem is

$$\min_{R(z)\in\mathcal{RH}_\infty} J_{2/2}. \tag{2.17}$$

Let $f_{\omega_0}(z)$ be an ideal discrete-time frequency selector defined as

$$\forall q(z) \in \mathcal{RH}_\infty^{1\times m},$$
$$\begin{cases} f_{\omega_0}(e^{j\omega h})q(e^{j\omega h}) = 0, \quad \omega \neq \omega_0 \\ \\ \displaystyle\int_0^{2\pi/h} f_{\omega_0}(e^{j\omega h})q(e^{j\omega h})q^T(e^{-j\omega h})f_{\omega_0}^T(e^{-j\omega h})d\omega = q(e^{j\omega_0 h})q^T(e^{-j\omega_0 h}). \end{cases}$$

Assume that $\lambda_{\min}(\omega)$ is the minimum generalized eigenvalue and $v_{\min}(e^{j\omega h})$ is the corresponding generalized eigenvector of the following generalized eigenvalue problem

$$v_{\min}(e^{j\omega h})M_u(e^{j\omega h})G_d(e^{j\omega h})G_d^T(e^{-j\omega h})M_u^T(e^{-j\omega h}) = \lambda_{\min}(\omega)v_{\min}(e^{j\omega h})M_u(e^{j\omega h})G_f(e^{j\omega h})G_f^T(e^{-j\omega h})M_u^T(e^{-j\omega h}).$$

Also assume that

$$\lambda_{\min}(\omega^*) = \inf_{\omega} \lambda_{\min}(\omega).$$

Then the optimal solution of the optimization problem in (2.17) is

$$R^*(z) = f_{\omega^*}(z)v_{\min}(z),$$

and the optimal value of the performance index is

$$J_{2/2}^* = \lambda_{\min}(\omega^*).$$

2.5.4 Norm based residual evaluation

As mentioned before, after the residual is generated it has to be evaluated (usually by comparing to a threshold) before a decision about fault occurrence can be made. In practice the instantaneous value of the residual is rarely used to produce an alarm signal. Instead, some norm of the residual is chosen as the residual evaluation function and based on that, the threshold is selected [13, 22]. The mostly used norm for this purpose is the $\mathcal{L}_2$ norm of the continuous-time residual $r(t)$ or the ℓ_2 norm of the discrete-time residual $r(k)$, for these norms indicate the energy level in a signal. Considering the continuous-time residual, the residual evaluation function is

$$\|r\|_2 = \left(\int_0^\infty r^T(t) \cdot r(t)\, dt\right)^{1/2}.$$

Since the evaluation over the whole time domain is unrealistic, the norm is often calculated over a limited window, i.e.,

$$\|r\|_2 = \left(\int_{t_1}^{t_2} r^T(t) \cdot r(t)\, dt\right)^{1/2}.$$

Now, based on this evaluation function, a threshold can be determined. In the most common logic for decision making, if the norm of the residual is

below threshold, then the system is fault free. Therefore, it is reasonable to select the threshold, denoted by J_{th}, as the maximum norm of the residual when no fault is present:

$$J_{\text{th}} = \sup_{\substack{d \\ f=0}} \|r\|_2.$$

Considering the general form of the residual generator in continuous-time, the threshold is then given by

$$J_{\text{th}} = \sup_{d} \|RM_u G_d d\|_2.$$

Now, assuming the disturbance is bounded by $\|d\|_2 \leq 1$, it follows that

$$J_{\text{th}} = \|R(s)M_u(s)G_d(s)\|_\infty.$$

2.6 Perfect disturbance decoupling

Perfect disturbance decoupling is the ideal case in FDI design. This happens when a residual can be made independent of the unknown input (namely, disturbance). If this is true then the residual is only sensitive to the fault, so there is no chance for false alarms. In this section, the necessary and sufficient conditions for perfect disturbance decoupling are discussed.

Consider the continuous-time process in (2.8). As seen earlier, perfect decoupling of the residual from the unknown inputs is possible if a stable post-filter $R(s)$ can be found such that

$$R(s)M_u(s)G_d(s) \equiv 0,$$
$$R(s)M_u(s)G_f(s) \not\equiv 0.$$

It is easy to check that such a post-filter exists if and only if (notice that $M_u(s)$ is full rank) [20]

$$\text{rank}\left[\begin{array}{cc} G_d(s) & G_f(s) \end{array}\right] > \text{rank}\left[\begin{array}{c} G_d(s) \end{array}\right]. \tag{2.18}$$

Here, rank $[\ G_d(s)\ ]$ denotes the normal rank or rank for almost all values of s. A necessary condition for (2.18) as shown in [20] is

$$\text{rank}\left[\begin{array}{c} G_d(s) \end{array}\right] < m,$$

which means that for perfect disturbance decoupling, the number of independent unknown inputs (rank [$G_d(s)$]) should be less than the number of measurements m [20, 22].

Similarly, for the discrete-time process in (2.14), perfect disturbance decoupling is possible if and only if

$$\text{rank}\left[\begin{array}{cc} G_d(z) & G_f(z) \end{array}\right] > \text{rank}\left[\begin{array}{c} G_d(z) \end{array}\right]. \tag{2.19}$$

In the formulation of the parity space approach (Section 2.4), perfect disturbance decoupling is possible if there exists a parity vector v_s such that

$$\begin{aligned} v_s H_{o,s} &= 0 \\ v_s H_{d,s} &= 0 \\ v_s H_{f,s} &\neq 0 \end{aligned}$$

Therefore, the necessary and sufficient condition for perfect disturbance decoupling is

$$\text{rank}\left[\begin{array}{ccc} H_{o,s} & H_{d,s} & H_{f,s} \end{array}\right] > \text{rank}\left[\begin{array}{cc} H_{o,s} & H_{d,s} \end{array}\right]. \tag{2.20}$$

It can be shown that conditions (2.19) and (2.20) are equivalent [22].

2.7 Summary

In this section, model based methods of fault detection were briefly reviewed. Two of the most common of these methods, namely parity space and factorization approaches, were discussed with more details. These methods are extensively used in this thesis. A fundamental step in robust residual generator design is the selection and optimization of a performance index. The performance index is a measure of robustness of the residual to disturbance and its sensitivity to fault. Analysis of the performance index in FDI design will be given in Chapter 6.

Chapter 3

Fault Detection in Sampled-data Systems

3.1 Introduction

In control systems, the signals of interest (reference input, error, control signal, actuator output, etc.) are usually continuous-time signals. The performance specifications (bandwidth, overshoot, settling time, steady state error, etc.) are also formulated in continuous time. Also the plants under control generally operate in continuous time and are modelled by differential equations. But since digital technology offers many benefits, modern control systems and fault detection algorithms are usually implemented by digital technology. Control systems with continuous-time plants and digitally implemented controllers are called *sampled-data* systems.

A sampled-data controller performs three functions:

- It samples and quantizes a continuous-time signal (measured output or tracking error) and produces a digital signal (A/D converter);
- it processes the digital signal using a digital computer and generates a digital control signal (digital controller);
- and it converts the digital control signal back into a continuous-time signal (D/A converter).

Some materials of this chapter has been published in:

I. Izadi, T. Chen and Q. Zhao, "Norm invariant discretization for sampled-data fault detection", *Automatica*, vol. 41, pp. 1633–1637, 2005.

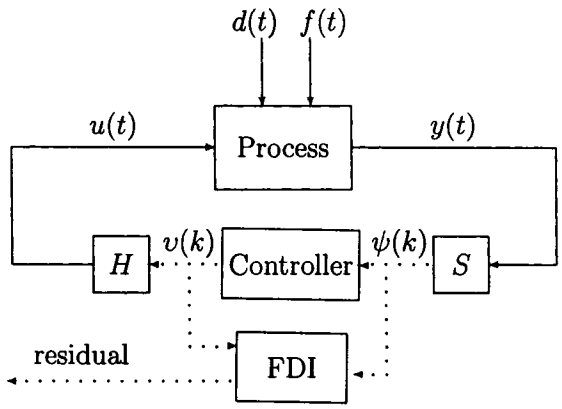

Figure 3.1: FDI in a sampled-data scheme

Similarly a sampled-data FDI processes the digital signals from A/D converter using a digital computer to produce the appropriate alarm signal. Sampled-data systems operate in continuous time, but they involve both continuous-time and discrete-time signals and systems and thus are hybrid systems [9]. Figure 3.1 illustrates a typical FDI in a sampled-data framework, where $u(t)$ is the control signal, $y(t)$ the plant output, $d(t)$ the unknown input (disturbance), and $f(t)$ the fault to be detected. A/D and D/A converters are modelled by ideal synchronized *sampling* (S) and *hold* (H) operators with sampling period h.

During the past decades, the topic of sampled-data systems has been intensively studied [9]. The achieved results show a significant improvement in control performance when the so-called direct design of digital controllers for continuous-time plants is adopted [9]. Consequently, because of the intimate relationship between control and FDI problems, research of FDI design in sampled-data systems has received increasing attention. Similar to the control problem [9], there are essentially two approaches to the FDI synthesis for sampled-data systems: indirect and direct. Many developed methods suggest the indirect design, which can be carried out using two approaches [9]:

Analog design and sampled-data implementation In this approach, a continuous-time FDI is first designed for the continuous-time plant. The

design can be performed using one of the numerous approaches available in the literature for continuous-time FDI design, some of which were introduced in Chapter 2. The continuous-time FDI is then digitally implemented. In other words, it is approximated by a discrete-time system using a method of continuous-to-discrete conversion (or discretization). For example one can use the bilinear or step invariant transformations.

Discrete-time design based on a discretized plant In this approach, the continuous-time process is first approximated by a discrete-time system (discretization). The discretization however, can only be done using the step invariant transformation. A discrete-time FDI is then designed for the discrete-time model of the process. This discrete-time FDI will be implemented on the actual continuous-time system.

Approximations exist in both approaches. They also ignore what is happening between the sampling instants (intersample behavior). Thus, the FDI may not work properly. In an example shown in [54], perfect disturbance decoupling is possible for both continuous-time and discretized processes. But, the FDI designed by neither of the indirect approaches can detect the fault when implemented in a sampled-data framework, let alone decoupling it from the disturbance. Motivated by the direct design approach in sampled-data control problem [9], recently a direct design approach was introduced for sampled-data FDI [53, 56, 58]. In [53, 56, 58] the parity space, $\mathcal{H}_\infty$ and $\mathcal{H}_2$ methods were adopted to design optimal residual generators for sampled-data systems. All the methods were based on introducing appropriate operators that capture the intersample behavior which is a well known technique in controller design for sampled-data systems [9].

All the above methods are successful extensions of the known design techniques to the sampled-data case. Unfortunately, introducing one individual operator for each approach makes those methods complicated and difficult to follow. In this chapter a unifying framework for sampled-data fault detection is developed which offers a convenient tool for both design and analysis. By clearly defining norms of sampled systems and the so-called norm invariant transformation, this framework allows us to easily extend any known ($\mathcal{H}_2$ or $\mathcal{H}_\infty$) norm based method of fault detection to sampled-data systems.

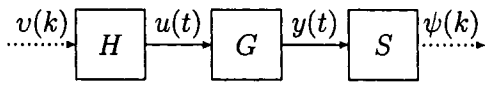

Figure 3.2: Step invariant transformation

3.2 Discretization of continuous-time systems

The process of converting a continuous-time system to a discrete-time system is called discretization. In this section three different methods of discretization are briefly reviewed: step invariant, impulse invariant, and bilinear transformations. Step invariant and bilinear transformations are the most common methods of discretization and are widely used in indirect controller/FDI design. The norm invariant transformation, a useful tool in solving sampled-data FDI problems, is also introduced.

3.2.1 Step invariant transformation

The step invariant transformation of a continuous-time system G is defined as $G_D = SGH$ (Figure 3.2). This method of discretization has the property that step responses of G and G_D have the same values at sampling instants, hence the term step invariant transformation [9]. In other words, $G_D 1_d(k) = SG1(t)$, where $1(t)$ and $1_d(k)$ are continuous-time and discrete-time unit step functions respectively. To show this, note that $1(t) = H1_d(k)$, then

$$G_D 1_d(k) = SGH1_d(k) = SG1(t).$$

Assume that the state space representation of the continuous-time system G is given as

$$G(s) = \left[\begin{array}{c|c} A & B \\ \hline C & D \end{array}\right],$$

then it is well known that [9]

$$G_D(z) = \left[\begin{array}{c|c} A_D & B_D \\ \hline C & D \end{array}\right],$$

where

$$A_D = e^{Ah}, \quad B_D = \int_0^h e^{A\tau} d\tau B.$$

3.2.2 Impulse invariant transformation

Consider a continuous-time strictly proper system G. The impulse invariant transformation of G, denoted by G_I, is a discrete-time system with the property that impulse responses of G and G_I have the same values at sampling instants. In other words $G_I\delta_d(k) = SG\delta(t)$, where $\delta(t)$ and $\delta_d(k)$ are continuous-time and discrete-time unit impulse functions respectively. Assuming G has the state space representation as

$$G(s) = \left[\begin{array}{c|c} A & B \\ \hline C & 0 \end{array}\right],$$

then it can be shown that [9]

$$G_I(z) = \left[\begin{array}{c|c} A_D & B_I \\ \hline C & D_I \end{array}\right], \tag{3.1}$$

where

$$A_D = e^{Ah}, \quad B_I = e^{Ah}B, \quad D_I = CB.$$

There is a relationship between the frequency responses of the continuous-time system G and its impulse invariant transformation G_I, known as the *Poisson Sampling Formula* [6]:

$$G_I(e^{j\omega h}) = \frac{1}{h}\sum_{k=-\infty}^{+\infty} G(j\omega + jk\omega_s), \tag{3.2}$$

where $\omega_s = \frac{2\pi}{h}$. This expression is also known as the *Impulse Modulation Formula.*

The following lemma states another property of the impulse invariant transformation:

Lemma 3.1 *A state space representation of $z^{-1}G_I(z)$ is given by*

$$z^{-1}G_I(z) = \left[\begin{array}{c|c} e^{Ah} & B \\ \hline C & 0 \end{array}\right].$$

Proof Using the state space representation of $G_I(z)$ in (3.1), the impulse response of G_I can be written as the following sequence

$$\begin{aligned} \text{impulse response of } G_I(z) &= \{D_I,\ CB_I,\ CA_DB_I,\ CA_D^2B_I\ \cdots\} \\ &= \{CB,\ Ce^{Ah}B,\ Ce^{2Ah}B,\ Ce^{3Ah}B,\ \cdots\}. \end{aligned}$$

Then,

$$\text{impulse response of } z^{-1}G_I(z) = \{0,\, CB,\, Ce^{Ah}B,\, Ce^{2Ah}B,\, \cdots\}.$$

Using this impulse response, the state space representation of $z^{-1}G_I(z)$ can be derived and the lemma is proved.

□

3.2.3 Norm invariant transformation

Another method of discretization, with extensive applications in sampled-data FDI design is the norm invariant transformation [32]. Consider the continuous-time strictly proper system G with the following state space model

$$G(s) = \left[\begin{array}{c|c} A & B \\ \hline C & 0 \end{array}\right]. \tag{3.3}$$

The norm invariant transformation of G, denoted by G_J, is defined as a discrete-time system with

$$G_J(z) = \left[\begin{array}{c|c} A_D & B_J \\ \hline C & 0 \end{array}\right], \tag{3.4}$$

where

$$A_D = e^{Ah}$$

and B_J is a full rank matrix satisfying

$$B_J B_J^T = \int_0^h e^{A\tau} B B^T e^{A^T\tau} d\tau.$$

The mathematical details on how to compute B_J are given in Appendix B.

An interesting and useful relationship involving the norm invariant transformation is given in the following lemma [27].

Lemma 3.2 *The following statement holds*

$$\big(G(s)G^T(-s)\big)_I(z) = G_J(z)G_J^T(z^{-1}),$$

where $\big(G(s)G^T(-s)\big)_I(z)$ *denotes the impulse invariant transformation of* $G(s)G^T(-s)$.

Proof Starting with the state space representation of G in (3.3), it easily follows that

$$G^T(-s) = \left[\begin{array}{c|c} -A^T & C^T \\ \hline -B^T & 0 \end{array}\right].$$

Using the formulas for the state space representation of the product of two transfer functions [9], it follows that

$$G(s)G^T(-s) = \left[\begin{array}{cc|c} -A^T & 0 & C^T \\ -BB^T & A & 0 \\ \hline 0 & C & 0 \end{array}\right].$$

Now, using Lemma 3.1, a state space representation of $z^{-1}\big(G(s)G^T(-s)\big)_I(z)$ can be constructed as

$$z^{-1}\big(G(s)G^T(-s)\big)_I(z) = \left[\begin{array}{cc|c} \exp\left(\left[\begin{array}{cc} -A^T & 0 \\ -BB^T & A \end{array}\right]\cdot h\right) & & C^T \\ \hline 0 & C & 0 \end{array}\right].$$

By using the matrix exponential formulas, the above equation is further simplified

$$z^{-1}\big(G(s)G^T(-s)\big)_I(z) = \left[\begin{array}{cc|c} e^{-A^Th} & 0 & C^T \\ -B_JB_J^Te^{-A^Th} & e^{Ah} & 0 \\ \hline 0 & C & 0 \end{array}\right]. \tag{3.5}$$

On the other hand, starting from the state space representation of G_J in (3.4),

$$G_J(z) = C(zI - A_D)^{-1}B_J$$

$$\begin{aligned} \Longrightarrow \qquad G_J^T(z^{-1}) &= B_J^T(z^{-1}I - A_D^T)^{-1}C^T \\ &= zB_J^T(I - zA_D^T)^{-1}C^T \\ &= zB_J^TA_D^{-T}(A_D^{-T} - zI)^{-1}C^T \end{aligned}$$

$$\begin{aligned} \Longrightarrow \qquad z^{-1}G_J^T(z^{-1}) &= -B_J^TA_D^{-T}(zI - A_D^{-T})^{-1}C^T \\ &= \left[\begin{array}{c|c} A_D^{-T} & C^T \\ \hline -B_J^TA_D^{-T} & 0 \end{array}\right]. \end{aligned}$$

Again, using the state space representation of the product of two transfer functions,

$$z^{-1}G_J(z)G_J^T(z^{-1}) = \left[\begin{array}{cc|c} A_D^{-T} & 0 & C^T \\ -B_JB_J^TA_D^{-T} & A_D & 0 \\ \hline 0 & C & 0 \end{array}\right]. \tag{3.6}$$

Comparing (3.5) and (3.6), the lemma will be proved:

$$\begin{aligned} & z^{-1}\big(G(s)G^T(-s)\big)_I(z) = z^{-1}G_J(z)G_J^T(z^{-1}) \\ \Longrightarrow \quad & \big(G(s)G^T(-s)\big)_I(z) = G_J(z)G_J^T(z^{-1}). \end{aligned}$$

□

The next lemma states an interesting relationship between the frequency responses of a continuous-time system and its norm invariant transformation.

Lemma 3.3 *The following statement holds*

$$G_J(e^{j\omega h})G_J^T(e^{-j\omega h}) = \frac{1}{h}\sum_{k=-\infty}^{+\infty} G(j\omega + jk\omega_s)G^T(-j\omega - jk\omega_s),$$

where $\omega_s = \frac{2\pi}{h}$.

Proof Evaluating the result of Lemma 3.2 at $z = e^{j\omega h}$ yields

$$\big(G(s)G^T(-s)\big)_I(e^{j\omega h}) = G_J(e^{j\omega h})G_J^T(e^{-j\omega h}). \tag{3.7}$$

On the other hand, using Poisson Sampling Formula (3.2), it follows that

$$\big(G(s)G^T(-s)\big)_I(e^{j\omega h}) = \frac{1}{h}\sum_{k=-\infty}^{+\infty} G(j\omega + jk\omega_s)G^T(-j\omega - jk\omega_s). \tag{3.8}$$

Comparing (3.7) and (3.8) proves the lemma.

□

Note that, unlike the step invariant and impulse invariant transformations, the inputs of the discrete-time system G_J are not related to the actual inputs of the original continuous-time system G.

Another important point to notice is the number of independent inputs of G_J. In the step invariant and impulse invariant cases, $\int_0^h e^{A\tau}d\tau$ and e^{Ah} are full rank square matrices (assuming h is non-pathological). Therefore B_D and B_I have the same dimension and rank as B. Thus the number of independent inputs of the original continuous-time system is equal to the number of independent inputs of its step invariant and impulse invariant transformations.

This, however, is not the case in the norm invariant transformation. The number of independent inputs of G_J can be generally greater than the number

of independent inputs of G [53, 58]. To show this, note that:

$$\begin{aligned}
\text{number of independent inputs of } G_J &= \text{number of independent columns of } B_J \\
&= \text{rank } (B_J B_J^T) \\
&= \text{rank } [\int_0^h e^{A\tau} B B^T e^{A^T \tau} d\tau] \\
&= \text{dimension of the controllable subspace of } (A, B) \\
&= \text{rank } [\ B \quad AB \quad \cdots\ ] \\
&\geq \text{number of independent columns of } B \\
&= \text{number of independent inputs of } G
\end{aligned}$$

As a matter of fact, the norm invariant transformation introduces some fictitious inputs which are used for design purposes only but carry no physical meaning.

3.2.4 Bilinear transformation

Another method of discretization is the bilinear transformation, also known as the Tustin's method [9]. The bilinear transformation of a continuous-time system is obtained by simply using the following bilinear relation between s and z (hence the term bilinear transformation)

$$s = \frac{2}{h} \frac{z-1}{z+1}.$$

Therefore, the continuous-time system G is transformed to the discrete-time system G_{BT}, where

$$G_{\text{BT}}(z) = G(s)\Big|_{s=\frac{2}{h}\frac{z-1}{z+1}}.$$

The inverse bilinear transformation from the discrete-time system G_{BT} into the continuous-time system G is given by

$$z = \frac{1+\frac{h}{2}s}{1-\frac{h}{2}s},$$

$$G(s) = G_{\text{BT}}(z)\Big|_{z=\frac{1+\frac{h}{2}s}{1-\frac{h}{2}s}}.$$

In this thesis, the fact that the bilinear transformation preserves the $\mathcal{H}_\infty$ norm of a system is used [9]:

$$\|G(s)\|_\infty = \|G_{\text{BT}}(z)\|_\infty.$$

3.2.5 Summary

In this section four methods of transforming a continuous-time system to a discrete-time one were briefly introduced. The step invariant and norm invariant transformations will be extensively used in this research to address the FDI problem in sampled-data systems. Throughout the thesis, the upper-case subscripts $_D$, $_I$, $_J$ and $_{BT}$ are used to denote the step invariant, impulse invariant, norm invariant and bilinear transformations of a continuous-time system respectively. Notice that the state space realizations of the step invariant and norm invariant transformations are the same except for the B term (i.e., they have the same A, C and D terms).

3.3 Norms of sampled systems

As seen in Chapter 2, in a variety of fault detection methods, a suitably chosen norm (e.g., $\mathcal{H}_\infty$ or $\mathcal{H}_2$ norm) is used to design and analyze residual generators. In sampled-data systems, we also require norms to extend the known design techniques. To define appropriate norms for sampled systems we generalize the concepts of $\mathcal{H}_\infty$ and $\mathcal{H}_2$ norms. Assume that $G : \mathcal{L}_2(\mathbb{R}) \rightarrow \mathcal{L}_2(\mathbb{R})$ is a stable and strictly proper continuous-time system with p inputs and m outputs, and the following state space realization

$$G(s) = \left[\begin{array}{c|c} A & B \\ \hline C & 0 \end{array}\right].$$

The operator $SG : \mathcal{L}_2(\mathbb{R}) \rightarrow \ell_2(\mathbb{Z})$ maps continuous-time signals to discrete-time signals and is called a sampled system.

3.3.1 $\mathcal{H}_\infty$ norm of SG

For continuous-time system G the $\mathcal{H}_\infty$ norm is

$$\|G(s)\|_\infty = \sup_{\|u\|_2 \leq 1} \|Gu\|_2.$$

Similarly, the $\mathcal{H}_\infty$ norm (also known as $\mathcal{L}_2$ induced norm or simply induced norm) of SG is defined as [9]

$$\|SG\|_\infty = \sup_{\|u\|_2 \leq 1} \|SGu\|_2.$$

Note that $\|\cdot\|_2$ in $\|u\|_2$ is defined for continuous-time signals in $\mathcal{L}_2(\mathbb{R})$, while $\|\cdot\|_2$ in $\|SGu\|_2$ is defined for discrete-time signals in $\ell_2(\mathbb{Z})$. To compute $\|SG\|_\infty$ the following lemma is useful:

Lemma 3.4 *[9, 58] The $\mathcal{H}_\infty$ norm of SG is given by*

$$\|SG\|_\infty = \|G_J(z)\|_\infty.$$

□

3.3.2 $\mathcal{H}_2$ norm of SG

For a continuous-time SISO system, the $\mathcal{H}_2$ norm is

$$\|G(s)\|_2^2 = \|G\delta(t)\|_2^2 = \int_{-\infty}^{\infty} g(t)^2 dt,$$

i.e., the $\mathcal{H}_2$ norm of the transfer function $G(s)$ equals the $\mathcal{L}_2$ norm (total energy) of its impulse response. In the multivariable case the $\mathcal{H}_2$ norm is

$$\|G(s)\|_2^2 = \sum_{i=1}^{p} \|G\delta(t)e_i\|_2^2,$$

where e_i, $i = 1, \ldots, p$, denote the standard basis vectors in $\mathbb{R}^p$ and $\delta(t)$ is the continuous-time unit impulse function. Thus, $\delta(t)e_i$ is an impulse applied to the i^{th} input channel.

To generalize the definition of $\mathcal{H}_2$ norm to sampled systems, notice that SG is a time-varying but h-periodic system. Hence, the $\mathcal{H}_2$ norm of SG is defined as the total energy of the outputs when impulses are applied in one period (sampling interval) to the input channels. Therefore, in the SISO case, the $\mathcal{H}_2$ norm of SG will be

$$\|SG\|_2^2 = \int_0^h \|SG\delta(t-\tau)\|_2^2 d\tau,$$

and in the multivariable case it is

$$\|SG\|_2^2 = \sum_{i=1}^{p} \left(\int_0^h \|SG\delta(t-\tau)e_i\|_2^2 \, d\tau \right). \tag{3.9}$$

Similar to the $\mathcal{H}_\infty$ norm, the $\mathcal{H}_2$ norm of SG is related to the $\mathcal{H}_2$ norm of discrete-time system G_J as shown in the following lemma:

Lemma 3.5 *The $\mathcal{H}_2$ norm of SG is given by*

$$\|SG\|_2 = \|G_J(z)\|_2.$$

Proof We know that

$$G\delta(t) = g(t) = Ce^{At}B\ 1(t),$$

where $1(t)$ is the continuous-time unit step function. Then,

$$\begin{aligned}
& G\delta(t-\tau) = Ce^{A(t-\tau)}B1(t-\tau), \\
\Longrightarrow\quad & SG\delta(t-\tau) = \left\{0, Ce^{A(h-\tau)}B, \cdots, Ce^{A(kh-\tau)}B, \cdots\right\}, \\
\Longrightarrow\quad & \sum_{i=1}^{p} \|SG\delta(t-\tau)e_i\|_2^2 = \text{trace}\left(\sum_{k=1}^{\infty} Ce^{A(kh-\tau)}BB^Te^{A^T(kh-\tau)}C^T\right), \\
\Longrightarrow\quad & \int_0^h \left(\sum_{i=1}^{p} \|SG\delta(t-\tau)e_i\|_2^2\right) d\tau = \\
& \qquad\qquad \text{trace}\left(\sum_{k=1}^{\infty} Ce^{Akh}\Big(\int_0^h e^{-A\tau}BB^Te^{-A^T\tau}d\tau\Big)e^{A^Tkh}C^T\right),
\end{aligned}$$

where trace$(\cdot)$ denotes the trace of a matrix. A change of variable $(k-1) \rightarrow k$ and $(h-\tau) \rightarrow \tau$ will yield

$$\begin{aligned}
& \sum_{i=1}^{p}\left(\int_0^h \|SG\delta(t-\tau)e_i\|_2^2\, d\tau\right) \\
& \quad = \text{trace}\left(\sum_{k=0}^{\infty} Ce^{Akh}\Big(\int_0^h e^{A\tau}BB^Te^{A^T\tau}d\tau\Big)e^{A^Tkh}C^T\right) \qquad (3.10) \\
& \quad = \text{trace}\left(\sum_{k=0}^{\infty} Ce^{Akh}B_JB_J^Te^{A^Tkh}C^T\right).
\end{aligned}$$

On the other hand [9]

$$\|G_J(z)\|_2^2 = \text{trace}\left(\sum_{k=0}^{\infty} CA_D^kB_JB_J^T(A_D^T)^kC^T\right). \qquad (3.11)$$

Comparing (3.10) and (3.11) and using definition (3.9) complete the proof. □

3.3.3 Norm of SG and norm invariant transformation

Lemmas 3.4 and 3.5 show that the $\mathcal{H}_\infty$ and $\mathcal{H}_2$ norms of sampled system SG are equal to the $\mathcal{H}_\infty$ and $\mathcal{H}_2$ norms of discrete-time system G_J, the norm invariant transformation of G. In other words, the norm invariant transformation preserves the $\mathcal{H}_\infty$ and $\mathcal{H}_2$ norms of sampled systems, hence the term norm invariant. Lemmas 3.4 and 3.5 play a significant role in developing norm based residual generators for sampled-data systems.

3.4 Residual generation in sampled-data systems

Consider the sampled-data system in Figure 3.1. The continuous-time system under consideration has the following input-output description

$$y(t) = G_u u(t) + G_d d(t) + G_f f(t), \tag{3.12}$$

where $y(t) \in \mathbb{R}^m$ is the vector of plant output, $u(t) \in \mathbb{R}^{n_u}$ the vector of control signal, $d(t) \in \mathbb{R}^{n_d}$ the vector of unknown input (disturbances) and $f(t) \in \mathbb{R}^{n_f}$ the vector of fault to be detected. G_u, G_d and G_f are LTI strictly proper systems. The assumption of strictly properness of G_u, G_d and G_f is standard in the sampled-data literature and necessary for boundedness of involved operators. In practice, because of antialiasing filters that are used before sampling, the systems are always strictly proper.

The output vector is sampled and discretized using an A/D converter modelled by

$$\psi(k) = y(kh),$$

and the control signal is generated by a computer and sent to the actuator using a zero-order hold D/A converter modelled by

$$u(t) = \upsilon(k), \quad kh \leq t < (k+1)h.$$

Hence,

$$\begin{aligned} \psi(k) &= Sy(t), \\ u(t) &= H\upsilon(k). \end{aligned} \tag{3.13}$$

3.4.1 General form of the residual generator

In the sampled-data scheme, the residual generator uses the discrete-time process input $\upsilon(k)$ and output $\psi(k)$ to generate the residual $\rho(k)$, which is also a discrete-time signal. So the residual generator is a (LTI and stable) discrete-time system. The general form of a sampled-data residual generator is

$$\rho(k) = R_1\psi(k) + R_2\upsilon(k), \tag{3.14}$$

where R_1 and R_2 are stable LTI discrete-time systems. Substituting $\psi(k) = Sy(t)$, $u(t) = H\upsilon(k)$ and using the system model in (3.12), it follows

$$\begin{aligned}
\rho(k) &= R_1Sy(t) + R_2\upsilon(k) \\
&= R_1S(G_uu(t) + G_dd(t) + G_ff(t)) + R_2\upsilon(k) \\
&= R_1SG_uu(t) + R_1SG_dd(t) + R_1SG_ff(t) + R_2\upsilon(k) \\
&= R_1SG_dd(t) + R_1SG_ff(t) + R_1SG_uH\upsilon(k) + R_2\upsilon(k).
\end{aligned}$$

Using the step invariant transformation $G_{uD} = SG_uH$, the residual generator can be further simplified

$$\rho(k) = R_1SG_dd(t) + R_1SG_ff(t) + (R_1G_{uD} + R_2)\upsilon(k). \tag{3.15}$$

Let $\big(M_u(z), N_u(z)\big)$ be a left coprime factorization of $G_{uD}(z)$, i.e.,

$$G_{uD}(z) = M_u^{-1}(z)N_u(z).$$

Using the factorization approach (similar to the continuous-time case in Section 2.5) and by choosing

$$\begin{aligned}
R_1(z) &= R(z)M_u(z), \\
R_2(z) &= -R(z)N_u(z),
\end{aligned}$$

the residual will be independent of the input. The design parameter $R(z) \in \mathcal{RH}_\infty^{1\times m}$ is a stable LTI discrete-time system. Substituting $R_1(z)$ and $R_2(z)$ in (3.14) yields

$$\rho(k) = R\big(M_u\psi(k) - N_u\upsilon(k)\big), \tag{3.16}$$

which is the general form of residual generator in sampled-data systems.

Also by substituting $R_1(z)$ and $R_2(z)$ in (3.15), the dynamics of the residual generator with respect to the continuous-time signals $d(t)$ and $f(t)$ is

$$\rho(k) = RM_uSG_dd(t) + RM_uSG_ff(t). \tag{3.17}$$

Here R and M_u are discrete-time systems while G_d and G_f are continuous-time ones. RM_uSG_d and RM_uSG_f are two operators that map continuous-time signals to discrete-time signals. Equation (3.17) shows how continuous-time signals $d(t)$ and $f(t)$ affect the discrete-time residual $\rho(k)$.

If a discrete-time post-filter $R(z)$ can be found such that

$$\begin{cases} RM_uSG_d \equiv 0, \\ RM_uSG_f \neq 0, \end{cases}$$

then perfect decoupling of the residual from the unknown input is achievable. The conditions of perfect disturbance decoupling will be discussed later in Section 2.6. If perfect disturbance decoupling is not possible, design of a robust residual generator is carried out by solving an optimization problem.

3.4.2 Robust residual generation

Consider the dynamics of the sampled-data residual generator in (3.17). If perfect decoupling of the residual from the unknown input is not possible (which is most of the times the case), then a robust residual generator is designed by solving an optimization problem. The idea is that the discrete-time residual $\rho(k)$ remains as sensitive as possible to the continuous-time fault $f(t)$, and as robust as possible to the continuous-time disturbance $d(t)$. In other words, RM_uSG_d should be made as small as possible while keeping RM_uSG_f reasonably large. From previous discussions, one method to quantify this requirement is to form the following optimization problem

$$\min_{R(z)\in\mathcal{RH}_\infty} J_\eta = \min_{R(z)\in\mathcal{RH}_\infty} \frac{\|RM_uSG_d\|_\eta}{\|RM_uSG_f\|_\eta}, \tag{3.18}$$

where $\eta = 2$ or $\eta = \infty$. The performance index in (3.18), is the generalization of similar performance indices introduced in Section 2.5 for continuous-time systems.

The norm preserving property of the norm invariant transformation makes it appropriate to approach the optimization problem given in (3.18). Lemmas

3.4 and 3.5 show that the ($\mathcal{H}_\infty$ and $\mathcal{H}_2$) norms of a sampled system are equal to the norms of its norm invariant transformation. Similarly, the following theorem can be stated and proved:

Theorem 3.1 *For the sampled-data residual generator given in (3.17), the following equations hold*

$$\|RM_uSG_d\|_\eta = \|R(z)M_u(z)G_{dJ}(z)\|_\eta$$
$$\|RM_uSG_f\|_\eta = \|R(z)M_u(z)G_{fJ}(z)\|_\eta$$

for $\eta = 2$ *and* $\eta = \infty$.

Using this theorem, the performance index in (3.18) is further simplified to

$$\min_{R(z)\in\mathcal{RH}_\infty} J_\eta = \min_{R(z)\in\mathcal{RH}_\infty} \frac{\|R(z)M_u(z)G_{dJ}(z)\|_\eta}{\|R(z)M_u(z)G_{fJ}(z)\|_\eta}, \quad \eta = 2 \text{ or } \eta = \infty. \tag{3.19}$$

This is a pure discrete-time optimization problem.

Now consider the following fictitious discrete-time system

$$\psi(k) = G_{uD}\upsilon(k) + G_{dJ}\bar{\gamma}(k) + G_{fJ}\bar{\phi}(k). \tag{3.20}$$

Note that this discrete-time system is obtained by discretizing the original continuous-time system in (3.12). The step invariant transformation is used to discretize G_u, as in indirect method. However, the norm invariant transformation is used instead to discretize G_d and G_f.

Suppose that we want to design a residual generator for the discrete-time system in (3.20). Then the general form of the residual generator is

$$\begin{aligned}\rho(k) &= R\big(M_u\psi(k) - N_u\upsilon(k)\big)\\ &= RM_uG_{dJ}\bar{\gamma}(k) + RM_uG_{fJ}\bar{\phi}(k).\end{aligned}$$

If perfect disturbance decoupling is not possible, for robust design the following optimization problem should be solved

$$\min_{R(z)\in\mathcal{RH}_\infty} J_\eta = \min_{R(z)\in\mathcal{RH}_\infty} \frac{\|R(z)M_u(z)G_{dJ}(z)\|_\eta}{\|R(z)M_u(z)G_{fJ}(z)\|_\eta}, \quad \eta = 2 \text{ or } \eta = \infty.$$

which is exactly the same as the one in (3.19) for sampled-data system.

This discussion suggests that to design a residual generator for the sampled-data system in (3.12) and (3.13), as far as the norms of the operators relating

the fault and disturbance signals to the residual are concerned, one can replace the sampled-data system with the discrete-time system in (3.20). Any optimal ($\mathcal{H}_2$ or $\mathcal{H}_\infty$) norm based residual generator designed for this discrete-time system will be optimal for the original sampled-data system as well. This will lead us to a unifying approach to (norm based) robust FDI design for sampled-data systems.

Considering the performance index in (3.18), for $\eta = \infty$ this result is the same as the one given in [58]. For $\eta = 2$, this approach provides an alternative solution to the optimal design given in [56]. The performance index considered in [56] for the sampled-data system is

$$J^2 = \frac{\int_0^{\omega_s} R(e^{j\omega h}) M_u(e^{j\omega h})}{\int_0^{\omega_s} R(e^{j\omega h}) M_u(e^{j\omega h})} \cdots$$
$$\cdots \frac{\sum_{k=-\infty}^{+\infty} \left(G_d(j\omega + jk\omega_s) G_d^T(-j\omega - jk\omega_s)\right) M_u^T(e^{-j\omega h}) R^T(e^{-j\omega h}) d\omega}{\sum_{k=-\infty}^{+\infty} \left(G_f(j\omega + jk\omega_s) G_f^T(-j\omega - jk\omega_s)\right) M_u^T(e^{-j\omega h}) R^T(e^{-j\omega h}) d\omega}$$

where $\omega_s = 2\pi/h$. It is easy to show that this performance index is equal to the $\mathcal{H}_2$ performance index (as in (3.19) for $\eta = 2$). Using Lemma 3.3,

$$G_{dJ}(e^{j\omega h}) G_{dJ}^T(e^{-j\omega h}) = \frac{1}{h} \sum_{k=-\infty}^{+\infty} G_d(j\omega + jk\omega_s) G_d^T(-j\omega - jk\omega_s),$$
$$G_{fJ}(e^{j\omega h}) G_{fJ}^T(e^{-j\omega h}) = \frac{1}{h} \sum_{k=-\infty}^{+\infty} G_f(j\omega + jk\omega_s) G_f^T(-j\omega - jk\omega_s).$$

Substituting these values in the expression of J^2 yields

$$J^2 = \frac{\int_0^{\omega_s} R(e^{j\omega h}) M_u(e^{j\omega h}) G_{dJ}(e^{j\omega h}) G_{dJ}^T(e^{-j\omega h}) M_u^T(e^{-j\omega h}) R^T(e^{-j\omega h}) d\omega}{\int_0^{\omega_s} R(e^{j\omega h}) M_u(e^{j\omega h}) G_{fJ}(e^{j\omega h}) G_{fJ}^T(e^{-j\omega h}) M_u^T(e^{-j\omega h}) R^T(e^{-j\omega h}) d\omega},$$

Now, by the definition of $\mathcal{H}_2$ norm for discrete-time systems, it follows that (notice that $R(z)$ is a row matrix)

$$J^2 = \frac{\|R(z) M_u(z) G_{dJ}(z)\|_2^2}{\|R(z) M_u(z) G_{fJ}(z)\|_2^2}.$$

This proves that the performance index in [56] is equal to J_2, the $\mathcal{H}_2$ performance indexed in (3.19). Nevertheless, this approach is simpler and requires less numerical computations.

3.4.3 Other methods

There are some other types of norm based performance index used in the literature to address the robustness problem in FDI design. For example in [13] the following norm based performance index is considered

$$\min_{R(z)\in\mathcal{RH}_\infty^{1\times m}} \left(\|RM_uSG_d\|_\infty - \|RM_uSG_f\|_\infty\right).$$

Now using the unifying approach, one can replace the original sampled-data system by the discrete-time system in (3.20). Then the following discrete-time optimization problem can be solved instead, whose solution is known [13]

$$\min_{R(z)\in\mathcal{RH}_\infty^{1\times m}} \left(\|R(z)M_u(z)G_{dJ}(z)\|_\infty - \|R(z)M_u(z)G_{fJ}(z)\|_\infty\right).$$

In the parity space approach, although the performance index does not involve norms of transfer functions, the unifying approach can still be used [53]. So, to design an optimal parity space based residual generator for a sampled-data system, one can apply the method to the equivalent discrete-time system in (3.20). The designed optimal residual generator is also optimal for the original sampled-data system.

3.4.4 Perfect disturbance decoupling

As seen in Section 2.6, for the original continuous-time system in (3.12), perfect decoupling of the residual from the unknown input is achievable if and only if

$$\text{rank}\left[\begin{array}{cc} G_d(s) & G_f(s) \end{array}\right] > \text{rank}\left[\begin{array}{c} G_d(s) \end{array}\right]. \tag{3.21}$$

A necessary condition for (3.21) is

$$\text{rank}\left[\begin{array}{c} G_d(s) \end{array}\right] < m,$$

which means that for perfect disturbance decoupling, the number of independent unknown inputs should be less than the number of measurements.

Using the norm invariant transformation, the necessary and sufficient condition for perfect disturbance decoupling in sampled-data system is obtained from the equivalent discrete-time model in (3.20) as

$$\text{rank}\left[\begin{array}{cc} G_{dJ}(z) & G_{fJ}(z) \end{array}\right] > \text{rank}\left[\begin{array}{c} G_{dJ}(z) \end{array}\right].$$

$G_{dJ}(z)$ and $G_d(s)$ have the same number of outputs m, but $G_{dJ}(z)$ has more inputs than $G_d(s)$. Therefore, the number of independent unknown inputs in the equivalent discrete-time system in (3.20) is greater than the number of independent unknown inputs in the original continuous-time system in (3.12). Hence, perfect disturbance decoupling is more difficult in the sampled-data case than in the continuous-time case [56, 58]. In other words, since in the equivalent discrete-time system, the number of independent unknown inputs has increased, the chances that this number is less than m decreases. Therefore, if perfect disturbance decoupling is possible for the original continuous-time system, it may not always be possible for the sampled-data system.

3.5 Indirect sampled-data design

In this section, the second method of indirect FDI design is briefly reviewed, for it is closely related to the direct design method. Again consider the sampled-data system in Figure 3.1, described in (3.12) and (3.13). In indirect approach, the original continuous-time system in (3.12) is discretized using the step invariant transformation

$$\psi(k) = G_{uD}\upsilon(k) + G_{dD}\gamma(k) + G_{fD}\phi(k), \tag{3.22}$$

where $\gamma(k) = Sd(t)$ and $\phi(k) = Sf(t)$. The discrete-time system obtained from step-invariant transformation is usually equivalent to the original continuous-time system at the sampling instants. Here because of the presence of an actual zero-order hold, the control signal $u(t)$ is constant over a sampling interval. Therefore, $\upsilon(k)$ carries all the information of $u(t)$. But unlike $u(t)$, the unknown input $d(t)$ and the fault $f(t)$ can arbitrarily take any value during the sampling interval. This means that $\gamma(k)$ and $\phi(k)$ are only approximations of $d(t)$ and $f(t)$ and carry only the information of $d(t)$ and $f(t)$ at $t = kh$. Therefore, the discretized model (3.22) is not accurate even at the sampling instants.

The indirect design procedure can be carried out for the discrete-time model in (3.22). As before, if $\big(M_u(z), N_u(z)\big)$ is a left coprime factorization of $G_{uD}(z)$, the general structure of a residual generator can be given as

$$\begin{aligned}\rho(k) &= R\big(M_u\psi(k) - N_u\upsilon(k)\big)\\ &= RM_uG_{dD}\gamma(k) + RM_uG_{fD}\phi(k).\end{aligned}$$

Notice that here the residual $\rho(k)$ is only affected by the values of the disturbance and fault at $t = kh$ (e.g., $\gamma(k)$ and $\phi(k)$). This is in contrast to the direct design, where the value of disturbance and fault during the whole sampling period affected the residual.

Another point worth mentioning is that in both indirect and direct designs, the original continuous-time system is replaced by a discrete-time model and the design is performed in discrete-time. The only difference is that in the indirect design the step invariant transformations G_{dD} and G_{fD} are used, while for the direct design, the norm invariant transformations G_{dJ} and G_{fJ} are used. So direct design does not involve more design steps or computation loads than the indirect design.

The necessary and sufficient condition for perfect disturbance decoupling in the discrete-time system in (3.22) is

$$\text{rank}\,\big[\; G_{dD}(z) \quad G_{fD}(z) \;\big] > \text{rank}\,\big[\; G_{dD}(z) \;\big]\,. \tag{3.23}$$

Notice that if $G_d(s)$ has no poles and (transmission) zeros at the origin and $G_{dD}(z)$ has no (transmission) zeros at $z = 1$ then

$$\text{rank}\,\big[\; G_d(s) \;\big] = \text{rank}\,\big[\; G_d(0) \;\big] = \text{rank}\big(CA^{-1}E_d\big),$$

and

$$\begin{aligned}\text{rank}\,\big[\; G_{dD}(z) \;\big] &= \text{rank}\,\big[\; G_{dD}(1) \;\big] = \text{rank}\big(C(I - A_D)^{-1}E_{dD}\big)\\ &= \text{rank}\big(C(I - e^{Ah})^{-1}(e^{Ah} - I)A^{-1}E_d\big) = \text{rank}\big(CA^{-1}E_d\big).\end{aligned}$$

Therefore, $\text{rank}\,\big[\; G_d(s) \;\big] = \text{rank}\,\big[\; G_{dD}(z) \;\big]$. This means that (3.21) implies (3.23) and vice-versa. In other words the perfect disturbance decoupling of the continuous-time system in (3.12) and the discrete-time system in (3.22) are equivalent. If the sampling is pathological or $G_d(s)$ has a zero at the origin or $G_{dD}(z)$ has a zero at $z = 1$, then perfect disturbance decoupling can be

achieved for one of the continuous or discrete-time systems but not for the other one. In fact $G_d(s)$ and $G_{dD}(z)$ can have different ranks even though they have the same dimensions.

Also note that

$$RM_uSG_d \equiv 0 \quad \Longrightarrow \quad RM_uSG_dH = RM_uG_{dD} \equiv 0,$$

which implies that if the sampled-data residual generator (direct design) can be perfectly decoupled from the disturbance, the same post-filter $R(z)$ can achieve perfect disturbance decoupling in indirect design.

3.6 Summary and conclusions

In this chapter, it was shown that in order to design a robust norm based residual generator for the following sampled-data system

$$\begin{aligned} y(t) &= G_u u(t) + G_d d(t) + G_f f(t) \\ \psi(k) &= Sy(t) \\ u(t) &= H\upsilon(k), \end{aligned}$$

it is enough to replace the system with the equivalent discrete-time system

$$\psi(k) = G_{uD}\upsilon(k) + G_{dJ}\bar{\gamma}(k) + G_{fJ}\bar{\phi}(k).$$

Any optimal norm based residual generator for the equivalent discrete-time system will be optimal for the original sampled-data system as well. The proposed framework unifies $\mathcal{H}_\infty$, $\mathcal{H}_2$, parity space and some other robust sampled-data FDI design methods. The results are consistent with the previous results in sampled-data FDI, but the framework developed here is simpler and more general.

Chapter 4

Fault Detection in Multirate Sampled-data Systems

4.1 Introduction

In most industrial process applications, the elements of the control system may be structured distributively, i.e., sensors, actuators and controller are connected via standard networks. In such applications D/A and A/D converters often work at different sampling periods, introducing the so-called multirate sampling [1, 9]. It is also well known that introducing multirate sampling can improve the performance of control systems [9]. Although there are many results available in the literature for multirate sampled-data systems [1, 9], there are very few pieces of work on fault detection for these systems.

One of the earliest results was reported in [49]. For the multirate sampled-data systems considered therein, all control inputs were updated at a single slow rate while the outputs were sampled at different fast rates. Three different fault detection schemes including parity space based, observer based and detection filter based were developed. In that approach it was assumed that no unknown disturbance would affect the system. Therefore, the robustness

---

The materials of this chapter has been published in:

I. Izadi, Q. Zhao and T. Chen, "An optimal scheme for fast-rate fault detection based on multirate sampled data", *Journal of Process Control*, vol. 15, pp. 307–319, 2005.

I. Izadi, Q. Zhao and T. Chen, "An $\mathcal{H}_\infty$ approach to fast-rate fault detection for multirate sampled-data systems", *Journal of Process Control*, vol. 16, pp. 651–658, 2006.

issue was not considered.

In [14, 16], the well-known lifting technique was used, and residual generators based on parity space and observers were proposed respectively. It was assumed that there is a single input sampling period and all of the output sampling periods are integer multiples of the input sampling period. In [55, 57, 59], the direct design approach was utilized to design parity space, $\mathcal{H}_\infty$ optimal and $\mathcal{H}_2$ optimal residual generators respectively. In all of these approaches the fault can only be detected at the end of the repetition period yielding a slow-rate fault detection scheme. In many cases this detection delay is unsatisfactory.

A technique to improve the detection speed was proposed in [15]. An observer was designed for each set of synchronous measurements resulting in a bank of observers that run simultaneously at different rates, which yields a fast-rate fault detection scheme. Another method to design a fast-rate residual generator was developed in [59]. An observer based residual generator with a static weighting matrix was constructed. The $\mathcal{H}_\infty$ performance index is used to design the optimal observer gain and weighting matrix.

In this chapter, the design of fast-rate residual generators for multirate sampled-data systems by adopting the norm invariant transformation and direct design is studied. The objective is to achieve fast-rate residual generation without losing performance. The lifting technique is used to convert the original multirate sampled-data system to an equivalent single-rate discrete-time one (but of higher dimension). Any available technique can be recruited here to design a residual generator for the equivalent discrete-time system. But regardless of the method used, the designed residual generator will be a slow-rate system for the equivalent discrete-time system works at slow rate. To overcome this, two methods are developed to generate a lifted (vector) residual rather than a scalar one. This lifted (vector) residual is also a slow-rate signal but applying the inverse lifting operation will render a scalar residual at the fast rate. The methods used here are parity space approach and factorization approach with $\mathcal{H}_\infty$ optimization. For both problems, the complete analytical solution of the optimization problem is given. Very large degrees of freedom in the solutions allow us to impose some constraints, amongst the most important of which are causality constraints.

As for the sampling periods, although the methods can be used for any

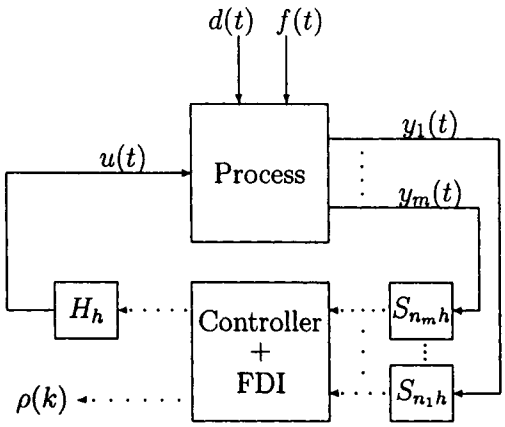

Figure 4.1: FDI in multirate sampled-data scheme

input sampling period, it is assumed that the inputs are available (but not necessarily updated) at the fast rate. This assumption may seem restrictive, but it is acceptable by the fact that input (control) signal is generated by the computer and so is known at any time instant. The output sampling periods are integer multiples of the single input sampling period.

4.1.1 System description

The continuous-time process under consideration (Figure 4.1) has the following state space description

$$\begin{cases} \dot{x}(t) = Ax(t) + Bu(t) + E_d d(t) + E_f f(t) \\ y_i(t) = C_i x(t), \quad i = 1, 2, \cdots, m \end{cases} \tag{4.1}$$

where $x(t) \in \mathbb{R}^n$ is the state vector, $u(t) \in \mathbb{R}^{n_u}$ the vector of control signals, $y_i(t) \in \mathbb{R}$ the i^{th} scalar plant output, $d(t) \in \mathbb{R}^{n_d}$ the vector of unknown inputs (disturbances), $f(t) \in \mathbb{R}^{n_f}$ the vector of faults to be detected. $A \in \mathbb{R}^{n \times n}$, $B \in \mathbb{R}^{n \times n_u}$, $E_d \in \mathbb{R}^{n \times n_d}$, $E_f \in \mathbb{R}^{n \times n_f}$ and $C_i \in \mathbb{R}^{1 \times n}$, $i = 1, 2, \cdots, m$, are known matrices. One may alternatively consider the transfer model form of the process

$$y(t) = G_u u(t) + G_d d(t) + G_f f(t),$$

where

$$[G_u(s) \quad G_d(s) \quad G_f(s)] = \left[\begin{array}{c|ccc} A & B & E_d & E_f \\ \hline C_1 & & & \\ \vdots & & 0 & \\ C_m & & & \end{array}\right].$$

As discussed in Chapter 2, the residual is independent of the control signal $u(t)$ if there is no uncertainty in the process model. Since this is the case in our research, the control signal and its sampling period has no effect on the residual. On the other hand, as mentioned earlier, although the control signal may be generated at any rate, it is known at any time instance. Therefore, for simplicity and without loss of generality, it is assumed that the control signal is available at the fast rate. So the D/A converter in the input channel can be described by

$$u(t) = v(k), \quad kh \leq t < (k+1)h. \tag{4.2}$$

Herein h corresponds to the fast-rate.

Each output channel is sampled at a different rate. The A/D converters in the output channels are then described by

$$\psi_i(k_i) = y_i(k_i T_i), \quad i = 1, 2, \cdots, m. \tag{4.3}$$

$T_i = n_i h$, $n_i \in \mathbb{N}$ is the sampling period of the scalar output $y_i(t)$. Hence,

$$\begin{aligned} u(t) &= H_h v(k), \\ \psi_i(k_i) &= S_{n_i h} y_i(t), \quad i = 1, 2, \cdots, m. \end{aligned}$$

Notice that since the sampled outputs are available at different rates, different time indices k_i, $i = 1, 2, \cdots, m$, were used.

Also let

$$\begin{aligned} N &= \text{l.c.m.}(n_1, n_2, \cdots, n_m) \\ q_i &= \frac{N}{n_i}, \quad i = 1, 2, \cdots, m \\ q &= q_1 + q_2 + \cdots + q_m \end{aligned} \tag{4.4}$$

where l.c.m. stands for the *least common multiple*. Nh is the repetition period, the length of one frame of data and is corresponding to the slow rate. q_i is the number of i^{th} output data in one frame. q is the total number of all output data in one frame.

4.1.2 Lifting

Let η be a discrete-time signal

$$\eta = \{\eta(0), \eta(1), \eta(2), ...\}.$$

The lifted signal $\underline{\eta}$ is defined as

$$\underline{\eta} = \left\{ \begin{bmatrix} \eta(0) \\ \eta(1) \\ .. \\ \eta(n-1) \end{bmatrix}, \begin{bmatrix} \eta(n) \\ \eta(n+1) \\ .. \\ \eta(2n-1) \end{bmatrix}, ... \right\}.$$

The (n-fold) lifting operator, L_n, is defined to be the map $\eta \mapsto \underline{\eta}$. Note that the dimension of the lifted signal $\underline{\eta} = L_n\eta$ is n times that of η, and the period of $\underline{\eta}$ again is n times that of η. The inverse lifting operator, L_n^{-1}, maps $\underline{\eta}$ back to η. A system with the lifted input and/or output is called a lifted system.

4.2 Slow-rate residual generator

A residual generator in multirate sampled-data systems uses the discrete-time input $v(k)$ and outputs $\psi_i(k_i)$, $i = 1, 2, \cdots, m$, to generate a residual. In this section it will be shown how to use the lifting technique to design a slow-rate residual generator for multirate sampled-data systems (i.e., it generates the residual at slow rate). In the following sections the methods will be improved to design a fast-rate residual generator.

The first step to design a residual generator is to convert the multirate sampled-data system to a single-rate (but of higher dimensions) system (called lifted system) using the lifting technique. To obtain a lifted model of the process, assume that $E_f = 0$ and $E_d = 0$ in (4.1). Only one output channel is considered first. Let G_1 denote the continuous-time system from input $u(t)$ to output $y_1(t)$:

$$y_1(t) = G_1u(t),$$
$$G_1(s) = \left[\begin{array}{c|c} A & B \\ \hline C_1 & 0 \end{array}\right].$$

Consider the discrete-time input $v(k)$ and the discrete-time output $\psi_1(k_1)$. Then,

$$\psi_1(k_1) = S_{n_1h}y_1(t) = S_{n_1h}G_1u(t) = S_{n_1h}G_1H_hv(k).$$

Therefore, the multirate system from $v(k)$ to $\psi_1(k_1)$ is $S_{n_1 h} G_1 H_h$. Define the slow-rate lifted model $\underline{G}_1$ as the discrete-time system from lifted input $\underline{v}(k_s)$ to the lifted output $\underline{\psi}_1(k_s)$, where

$$\underline{v}(k_s) = L_N v(k) \begin{bmatrix} v(Nk_s) \\ v(Nk_s+1) \\ \vdots \\ v(Nk_s+N-1) \end{bmatrix}_{N \cdot n_u \times 1},$$

$$\underline{\psi}_1(k_s) = L_{q_1} \psi_1(k_1) \begin{bmatrix} \psi_1(q_1 k_s) \\ \psi_1(q_1 k_s+1) \\ \vdots \\ \psi_1(q_1 k_s+q_1-1) \end{bmatrix}_{q_1 \times 1}.$$

Here, k_s is used for the time index of slow-rate signals. Then $\underline{G}_1$ will be

$$\begin{aligned} \underline{G}_1 &= L_{q_1} S_{n_1 h} G_1 H_h L_N^{-1} \\ &= D_{q_1} L_N S_h G_1 H_h L_N^{-1}. \end{aligned} \tag{4.5}$$

D_{q_1} is the operator of downsampling by q_1 described by

$$D_{q_1} = \left[\begin{array}{c|c|c|c} \overbrace{1\,0\,\cdots\,0}^{n_1} & \overbrace{0\,\cdots\,0}^{n_1} & \cdots\cdots & \overbrace{0\,\cdots\,0}^{n_1} \\ 0\,0\,\cdots\,0 & 1\,\cdots\,0 & \cdots\cdots & 0\,\cdots\,0 \\ \vdots\ \vdots\ \ \vdots & \vdots\ \ \vdots & \cdots\cdots & \vdots\ \ \vdots \\ 0\,0\,\cdots\,0 & 0\,\cdots\,0 & \cdots\cdots & 1\,\cdots\,0 \end{array}\right]_{q_1 \times N}.$$

As shown in [9]

$$(L_N S_h G_1 H_h L_N^{-1})(z) =$$

$$\left[\begin{array}{c|ccccc} A_D^N & A_D^{N-1}B_D & A_D^{N-2}B_D & \cdots & A_D B_D & B_D \\ \hline C_1 & 0 & 0 & \cdots & 0 & 0 \\ C_1 A_D & C_1 B_D & 0 & \cdots & 0 & 0 \\ \vdots & \vdots & \vdots & & \vdots & \vdots \\ C_1 A_D^{N-1} & C_1 A_D^{N-2} B_D & C_1 A_D^{N-3} B_D & \cdots & C_1 B_D & 0 \end{array}\right]_{N \times N \cdot n_u} \tag{4.6}$$

where A_D and B_D are as usual obtained from the step invariant transformation of $G_1(s)$

$$\begin{aligned} A_D &= e^{Ah}, \\ B_D &= \int_0^h e^{A\tau} d\tau B. \end{aligned} \tag{4.7}$$

Substituting (4.6) in (4.5), $\underline{G}_1$ becomes

$$\underline{G}_1(z) =$$

$$\left[\begin{array}{c|ccc} A_D^N & A_D^{N-1}B_D & A_D^{N-2}B_D & \cdots & B_D \\ \hline C_1 & 0 & 0 & \cdots & 0 \\ C_1A_D^{n_1} & C_1A_D^{n_1-1}B_D & C_1A_D^{n_1-2}B_D & \cdots & 0 \\ \vdots & \vdots & \vdots & & \vdots \\ C_1A_D^{(q_1-1)n_1} & C_1A_D^{(q_1-1)n_1-1}B_D & C_1A_D^{(q_1-1)n_1-2}B_D & \cdots & 0 \end{array}\right]_{q_1\times N\cdot n_u}.$$

For the other outputs ψ_i, $i = 1, 2, \cdots, m$, $\underline{G}_i$ can be derived similarly. Using the fact that

$$G_u(s) = \left[\begin{array}{c} G_1(s) \\ G_2(s) \\ \vdots \\ G_m(s) \end{array}\right],$$

define $\underline{G}_{uD}(z)$ as

$$\underline{G}_{uD}(z) = \left[\begin{array}{c} \underline{G}_1(z) \\ \underline{G}_2(z) \\ \vdots \\ \underline{G}_m(z) \end{array}\right].$$

The slow-rate lifted model $\underline{G}_{uD}$ is thus described by

$$\underline{G}_{uD}(z) = \tag{4.8}$$

$$\left[\begin{array}{c|ccc} A_D^N & A_D^{N-1}B_D & A_D^{N-2}B_D & \cdots & B_D \\ \hline C_1 & 0 & 0 & \cdots & 0 \\ C_1A_D^{n_1} & C_1A_D^{n_1-1}B_D & C_1A_D^{n_1-2}B_D & \cdots & 0 \\ \vdots & \vdots & \vdots & & \vdots \\ C_1A_D^{(q_1-1)n_1} & C_1A_D^{(q_1-1)n_1-1}B_D & C_1A_D^{(q_1-1)n_1-2}B_D & \cdots & 0 \\ \hline \vdots & \vdots & \vdots & & \vdots \\ \hline C_m & 0 & 0 & \cdots & 0 \\ C_mA_D^{n_m} & C_mA_D^{n_m-1}B_D & C_mA_D^{n_m-2}B_D & \cdots & 0 \\ \vdots & \vdots & \vdots & & \vdots \\ C_mA_D^{(q_m-1)n_m} & C_mA_D^{(q_m-1)n_m-1}B_D & C_mA_D^{(q_m-1)n_m-2}B_D & \cdots & 0 \end{array}\right]_{q\times N\cdot n_u}.$$

Define

$$\underline{G}_{uD}(z) = \left[\begin{array}{c|c} A_l & B_l \\ \hline C_l & D_l \end{array}\right].$$

$\underline{G}_{uD}$ is the slow-rate lifted system from the slow-rate lifted input $\underline{v}(k_s)$ to the slow-rate lifted output $\underline{\psi}(k_s)$ where

$$\underline{v}(k_s) = \begin{bmatrix} v(Nk_s) \\ v(Nk_s+1) \\ \vdots \\ v(Nk_s+N-1) \end{bmatrix}_{N\cdot n_u \times 1},$$

$$\underline{\psi}(k_s) = \begin{bmatrix} \underline{\psi}_1(k_s) \\ \underline{\psi}_2(k_s) \\ \vdots \\ \underline{\psi}_m(k_s) \end{bmatrix} = \begin{bmatrix} \psi_1(q_1k_s) \\ \psi_1(q_1k_s+1) \\ \vdots \\ \psi_1(q_1k_s+q_1-1) \\ \hdashline \vdots \\ \hdashline \psi_m(q_mk_s) \\ \psi_m(q_mk_s+1) \\ \vdots \\ \psi_m(q_mk_s+q_m-1) \end{bmatrix}_{q\times 1}.$$

The input and output of $\underline{G}_{uD}$ are slow-rate signals, thus $\underline{G}_{uD}$ represents a slow-rate LTI system.

It is known that the lifting does not change the ($\mathcal{H}_2$ or $\mathcal{H}_\infty$) norm of a signal or a system. Using the method of Chapter 3, the norm invariant transformation can be used to replace the original SISO/MIMO multirate sampled-data system with the following MIMO discrete-time system

$$\begin{cases} x_l(k_s+1) = A_l x_l(k_s) + B_l\underline{v}(k_s) + E_{dl}\bar{\underline{\gamma}}(k_s) + E_{fl}\bar{\underline{\gamma}}(k_s) \\ \underline{\psi}(k_s) = C_l x_l(k_s) + D_l\underline{v}(k_s) + D_{dl}\bar{\underline{\gamma}}(k_s) + D_{fl}\bar{\underline{\gamma}}(k_s) \end{cases} \tag{4.9}$$

Or alternatively the transfer function form

$$\underline{\psi}(k_s) = \underline{G}_{uD}\underline{v}(k_s) + \underline{G}_{dJ}\bar{\underline{\gamma}}(k_s) + \underline{G}_{fJ}\bar{\underline{\gamma}}(k_s). \tag{4.10}$$

(E_{dl}, D_{dl}) and (E_{fl}, D_{fl}) have the same structure as (B_l, D_l), replacing B_D with E_{dJ} and E_{fJ} respectively. E_{dl} and E_{fl} are as usual obtained from the norm invariant transformation

$$\begin{aligned} E_{dJ}E_{dJ}^T &= \int_0^h e^{A\tau}E_dE_d^Te^{A^T\tau}d\tau, \\ E_{fJ}E_{fJ}^T &= \int_0^h e^{A\tau}E_fE_f^Te^{A^T\tau}d\tau. \end{aligned} \tag{4.11}$$

$\underline{G}_{dJ}$ and $\underline{G}_{fJ}$ are defined as

$$\underline{G}_{dJ} = \left[\begin{array}{c|c} A_l & E_{dl} \\ \hline C_l & D_{dl} \end{array}\right], \quad \underline{G}_{fJ} = \left[\begin{array}{c|c} A_l & E_{fl} \\ \hline C_l & D_{fl} \end{array}\right].$$

Now, any norm based optimal residual generator designed for the discrete-time system in (4.9) or (4.10), is also optimal for the original sampled-data system. But because the discrete-time system in (4.9) or (4.10) is essentially a slow-rate system (updated every Nh sec), any residual generated by this model will be slow rate. In other words, the slow-rate residual generator waits for one complete frame of data before proceeding with any calculations. So, the updated residual is available every Nh sec, even though the information from the system is received by the computer more often. This can cause a substantial delay in the process of fault detection. In the next two sections two methods are developed to generate a fast-rate residual for the multirate sampled-data system to eliminate any unnecessary delays.

4.3 Fast-rate residual generator: Parity space

Consider the equivalent slow-rate discrete-time model in (4.9). Following the discussions in Chapter 3, an optimal parity space based residual generator for the discrete-time lifted model in (4.9) is also optimal for the original multirate system. Applying the parity space approach (Section 2.4) to the lifted model (4.9), the residual generator is

$$\rho(k_s) = v_s\big(\underline{\psi}_s(k_s) - \underline{H}_{u,s}\underline{v}_s(k_s)\big),$$

where

$$\underline{v}_s(k_s) = \left[\begin{array}{c} \underline{v}(k_s - s) \\ \vdots \\ \underline{v}(k_s) \end{array}\right] = \left[\begin{array}{l} v(Nk_s - Ns) \\ v(Nk_s - Ns + 1) \\ \vdots \\ v(Nk_s - Ns + N - 1) \\ \hdashline \vdots \\ \hdashline v(Nk_s) \\ v(Nk_s + 1) \\ \vdots \\ v(Nk_s + N - 1) \end{array}\right]_{N \cdot n_u(s+1) \times 1}, \qquad (4.12)$$

$$\underline{\psi}_s(k_s) = \begin{bmatrix} \underline{\psi}(k_s - s) \\ \vdots \\ \underline{\psi}(k_s) \end{bmatrix} = \left[\begin{array}{l} \psi_1(q_1k_s - q_1s) \\ \vdots \\ \psi_1(q_1k_s - q_1s + q_1 - 1) \\ \hdashline \vdots \\ \hdashline \psi_m(q_mk_s - q_ms) \\ \vdots \\ \psi_m(q_mk_s - q_ms + q_m - 1) \\ \hline \vdots \\ \hline \psi_1(q_1k_s) \\ \vdots \\ \psi_1(q_1k_s + q_1 - 1) \\ \hdashline \vdots \\ \hdashline \psi_m(q_mk_s) \\ \vdots \\ \psi_m(q_mk_s + q_m - 1) \end{array}\right]_{q(s+1)\times 1}, \quad (4.13)$$

$$\underline{H}_{u,s} = \begin{bmatrix} D_l & 0 & \cdots & 0 & 0 \\ C_lB_l & D_l & \cdots & 0 & 0 \\ \vdots & \vdots & & \vdots & \vdots \\ C_lA_l^{s-1}B_l & C_lA_l^{s-2}B_l & \cdots & C_lB_l & D_l \end{bmatrix}. \quad (4.14)$$

$s+1$ is the number of data frames used to generate the residual. In this residual generator, v_s is a $1 \times q(s+1)$ vector. Therefore, the residual is a scalar (slow-rate) signal. It can be shown that this slow-rate residual generator is equivalent to the one that was developed in [55] by properly choosing s.

To make sure that a residual is generated as soon as new information from the system is received, a fast-rate residual generator has to be designed. Let us consider v_s to be a $N \times q(s+1)$ matrix, denoted by V_s. This will result in a vector (or lifted) residual $\underline{\rho}(k_s)$ which is still a slow-rate signal. But after applying the inverse lifting operator to this vector signal (during the implementation of the residual generator), a scalar fast-rate residual will be obtained. This scheme is illustrated in Figure 4.2. So the residual generator becomes

$$\underline{\rho}(k_s) = V_s\big(\underline{\psi}_s(k_s) - \underline{H}_{u,s}\underline{v}_s(k_s)\big), \quad (4.15)$$

and the fast-rate residual is

$$\rho(k) = L_N^{-1}\underline{\rho}(k_s). \quad (4.16)$$

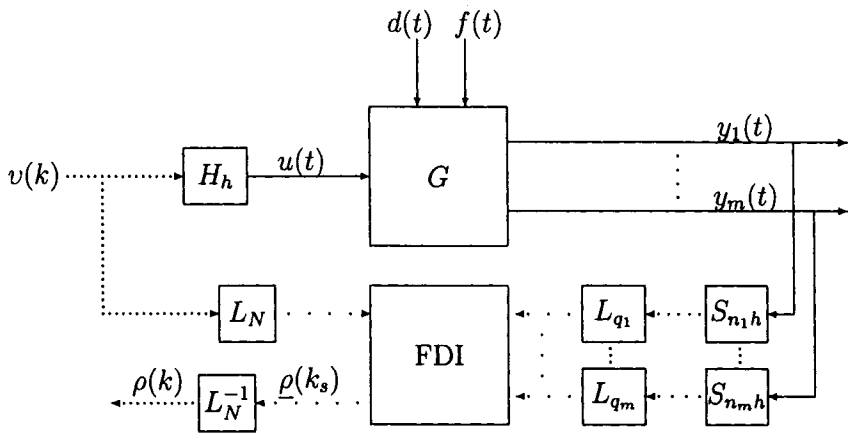

Figure 4.2: Proposed fault detection scheme for multirate systems

Assuming perfect disturbance decoupling is not possible, to make a trade-off between sensitivity of the residual to faults and its robustness to unknown inputs, a performance index is defined as

$$J_{\text{ps}} = \frac{\|V_s \underline{H}_{d,s}\|_2^2}{\|V_s \underline{H}_{f,s}\|_2^2} = \frac{\lambda_{\max}(V_s \underline{H}_{d,s} \underline{H}_{d,s}^T V_s^T)}{\lambda_{\max}(V_s \underline{H}_{f,s} \underline{H}_{f,s}^T V_s^T)}.$$

Thus V_s is a solution of the following constrained optimization problem

$$\begin{aligned} &\min_{V_s:\ N \times q(s+1)} J_{\text{ps}} \\ &\text{s.t. } V_s \underline{H}_{o,s} = 0. \end{aligned} \tag{4.17}$$

In the definition of J_{ps},

$$\begin{aligned} \underline{H}_{d,s} &= \begin{bmatrix} D_{dl} & 0 & \cdots & 0 & 0 \\ C_l E_{dl} & D_{dl} & \cdots & 0 & 0 \\ \vdots & \vdots & & \vdots & \vdots \\ C_l A_l^{s-1} E_{dl} & C_l A_l^{s-2} E_{dl} & \cdots & C_l E_{dl} & D_{dl} \end{bmatrix}, \\ \underline{H}_{f,s} &= \begin{bmatrix} D_{fl} & 0 & \cdots & 0 & 0 \\ C_l E_{fl} & D_{fl} & \cdots & 0 & 0 \\ \vdots & \vdots & & \vdots & \vdots \\ C_l A_l^{s-1} E_{fl} & C_l A_l^{s-2} E_{fl} & \cdots & C_l E_{fl} & D_{fl} \end{bmatrix}, \\ \underline{H}_{o,s} &= \begin{bmatrix} C_l \\ C_l A_l \\ \vdots \\ C_l A_l^s \end{bmatrix}, \end{aligned} \tag{4.18}$$

and $\lambda_{\max}(\cdot)$ represents maximum eigenvalue. Unlike the single-rate case, here $V_s\underline{H}_{d,s}\underline{H}_{d,s}^T V_s^T$ and $V_s\underline{H}_{f,s}\underline{H}_{f,s}^T V_s^T$ are two $N\times N$ positive semi-definite matrices. Note that the design parameter V_s is a matrix instead of a vector, so standard methods can not apply directly. In the next section the analytical solution to the problem in (4.17) will be proposed.

4.3.1 Analytical solution

If N_B is the basis matrix of parity space (i.e., N_B is the basis of Null($\underline{H}_{o,s}$)) then V_s can be expressed in this basis as

$$V_s = U_s N_B. \tag{4.19}$$

The optimization problem (4.17) will then be simplified to

$$\begin{aligned} &\min_{U_s:\ N\times q'} J_{\text{ps}} \\ &J_{\text{ps}} = \frac{\|U_s N_B \underline{H}_{d,s}\|_2^2}{\|U_s N_B \underline{H}_{f,s}\|_2^2} = \frac{\lambda_{\max}(U_s N_B \underline{H}_{d,s}\underline{H}_{d,s}^T N_B^T U_s^T)}{\lambda_{\max}(U_s N_B \underline{H}_{f,s}\underline{H}_{f,s}^T N_B^T U_s^T)}, \end{aligned} \tag{4.20}$$

where $q' = \dim\left(\text{Null}(\underline{H}_{o,s})\right)$ and U_s is the new design parameter. If $N_B\underline{H}_{d,s}$ is singular then there exists a nonzero matrix U_s^* such that

$$U_s^* N_B \underline{H}_{d,s} = 0.$$

In this case perfect disturbance decoupling is achievable and

$$J_{\text{ps}}^* = 0.$$

The solution is trivial. Since it is assumed that perfect disturbance decoupling is not possible, then $N_B\underline{H}_{d,s}$ is nonsingular. First several steps of singular value decompositions (SVD) are performed

$$N_B\underline{H}_{d,s}\underline{H}_{d,s}^T N_B^T = U_a\Sigma_a U_a^T \qquad \begin{cases} U_a^T U_a = U_a U_a^T = I \\ \Sigma_a = \text{diag}\{\sigma_{a_1}, \cdots, \sigma_{a_{q'}}\} \\ \sigma_{a_1} \geq \sigma_{a_2} \geq \cdots \geq \sigma_{a_{q'}} > 0 \end{cases}$$

$$\Sigma_a^{-\frac{1}{2}} U_a^T N_B \underline{H}_{f,s}\underline{H}_{f,s}^T N_B^T U_a^T \Sigma_a^{-\frac{1}{2}} = U_b\Sigma_b U_b^T \qquad \begin{cases} U_b^T U_b = U_b U_b^T = I \\ \Sigma_b = \text{diag}\{\sigma_{b_1}, \cdots, \sigma_{b_{q'}}\} \\ \sigma_{b_1} \geq \sigma_{b_2} \geq \cdots \geq \sigma_{b_{q'}} \geq 0 \end{cases} \tag{4.21}$$

Consider a change of variable from U_s to W_s defined by

$$U_s = W_s U_b^T \Sigma_a^{-\frac{1}{2}} U_a^T, \tag{4.22}$$

which always exists since $U_b^T \Sigma_a^{-\frac{1}{2}} U_a^T$ is nonsingular. Then the optimization problem in (4.20) is further simplified to

$$\begin{aligned} &\min_{W_s:\ N\times q'} J_{\text{ps}} \\ &J_{\text{ps}} = \frac{\|W_s\|_2^2}{\|W_s \Sigma_b^{\frac{1}{2}}\|_2^2} = \frac{\lambda_{\max}(W_s W_s^T)}{\lambda_{\max}(W_s \Sigma_b W_s^T)}. \end{aligned} \tag{4.23}$$

This problem is easier to solve. The following two lemmas are useful in finding the solution.

Lemma 4.1 *The minimal value of J_{ps} defined in (4.23) is*

$$J_{ps}^* = \frac{1}{\sigma_{b1}}.$$

Proof Submultiplicative property of the induced 2-norm states that for any matrices A and B of appropriate dimensions [5]

$$\|AB\|_2 \leq \|B\|_2 \|A\|_2.$$

Using this property, it follows that

$$J_{\text{ps}} = \frac{\|W_s\|_2^2}{\|W_s \Sigma_b^{\frac{1}{2}}\|_2^2} \geq \frac{\|W_s\|_2^2}{\|W_s\|_2^2 \|\Sigma_b^{\frac{1}{2}}\|_2^2} = \frac{1}{\|\Sigma_b^{\frac{1}{2}}\|_2^2} = \frac{1}{\sigma_{b1}}.$$

The above lower bound can be achieved by appropriate choice of W_s (see Lemma 4.2 later). This completes the proof.

□

The optimal performance index J_{ps}^*, does not actually depend on the size of W_s. Whether a parity matrix V_s or a parity vector v_s (as in the slow-rate case) is used, the optimal performance index does not change. Therefore, using a lifted residual instead of a scalar one does not degrade the performance of the residual generator. In other words, the slow-rate and fast-rate residual generators have the same performance.

The next lemma parameterizes a class of optimal solutions of J_{ps}.

Lemma 4.2 *Any matrix W_s^* of appropriate dimensions with a SVD of the form*

$$W_s^* = U_w \Sigma_w$$

is an optimal solution of (4.23), where

$$\begin{cases} U_w^T U_w = U_w U_w^T = I \\ \Sigma_w = \text{diag}\{\sigma_{w1}, \sigma_{w2}, \cdots, \sigma_{wn}\}, \quad \sigma_{w1} \geq \sigma_{w2} \geq \cdots \geq \sigma_{wn}. \end{cases}$$

Proof It follows easily from the fact that a unitary transformation preserves the induced 2-norm of a matrix:

$$J_{\text{ps}} = \frac{\|W_s^*\|_2^2}{\|W_s^* \Sigma_b^{\frac{1}{2}}\|_2^2} = \frac{\|U_w \Sigma_w\|_2^2}{\|U_w \Sigma_w \Sigma_b^{\frac{1}{2}}\|_2^2} = \frac{\|\Sigma_w\|_2^2}{\|\Sigma_w \Sigma_b^{\frac{1}{2}}\|_2^2} = \frac{\sigma_{w1}^2}{\sigma_{w1}^2 \sigma_{b1}} = \frac{1}{\sigma_{b1}} = J_{\text{ps}}^*.$$

□

This lemma states that every matrix with a SVD of the form $U_w \Sigma_w V_w^T$ (which is the general form of SVD) for which $V_w = I$ is an optimal solution of (4.23). The optimization problem in (4.23) has an infinite number of optimal solutions. The available degree of freedom is later used to impose additional constraints (e.g., causality constraints) on the solution. The class of solutions introduced herein does not encompass the whole optimal solutions as can be shown by a counter example, though it is enough for considering causality constraints.

4.3.2 Causality constraints

Recall the fast-rate residual generator in (4.15)

$$\underline{\rho}(k_s) = \begin{bmatrix} \rho(Nk_s) \\ \rho(Nk_s + 1) \\ \vdots \\ \rho(Nk_s + N - 1) \end{bmatrix} = V_s \Big(\underline{\psi}_s(k_s) - \underline{H}_{u,s} \underline{v}_s(k_s) \Big),$$

where

$$\underline{\psi}_s(k_s) = \left[\begin{array}{l} \psi_1(q_1k_s - q_1s) \\ \vdots \\ \psi_1(q_1k_s - q_1s + q_1 - 1) \\ \hdashline \vdots \\ \hdashline \psi_m(q_mk_s - q_ms) \\ \vdots \\ \psi_m(q_mk_s - q_ms + q_m - 1) \\ \hline \vdots \\ \hline \psi_1(q_1k_s) \\ \vdots \\ \psi_1(q_1k_s + q_1 - 1) \\ \hdashline \vdots \\ \hdashline \psi_m(q_mk_s) \\ \vdots \\ \psi_m(q_mk_s + q_m - 1) \end{array}\right]_{q(s+1)\times 1}.$$

This residual generator is generally noncausal (and hence can not be implemented), for some elements of $\underline{\rho}(k_s)$ can depend on the future values in $\underline{\psi}_s(k_s)$. This noncausality is caused by the lifting operation. To make $\underline{\rho}(k_s)$ causal the dependency of $\rho(Nk_s + i - 1)$(the i^{th} entry of $\underline{\rho}(k_s)$), $i = 1, 2, \cdots, N$, on the future values in $\underline{\psi}_s(k_s)$ should be removed. Note that because of the lower triangular structure of $\underline{H}_{u,s}$, $\underline{\rho}(k_s)$ is already independent of the future values in $\underline{v}_s(k_s)$. This causality issue enforces some of the entries of V_s to be zero. If $\rho(Nk_s + i - 1)$ depends on $\psi_j(q_jk_s + m_j)$ for some $i = 1, 2, \cdots, N$, $j = 1, 2, \cdots, m$, and

$$(Nk_s + i - 1)h < (q_jk_s + m_j)n_jh \quad \Longrightarrow \quad n_jm_j > i - 1$$

(which implies noncausality), then the corresponding entry of V_s should be zero. Since only the last q entries (the last block) of $\underline{\psi}_s(k_s)$ contain future values, zeros only appear in the last q columns of V_s.

Let us first consider causality constraints caused by the future values of the first output ψ_1 only. The entries of $\underline{\psi}_s(k_s)$ containing the future values of ψ_1 are only the first q_1 elements of the last block. Therefore, a necessary condition for $V_{s,ij}$ to be zero due to ψ_1 is:

$$qs + 1 \leq j \leq qs + q_1. \tag{4.24}$$

Now, the j^{th} entry of $\underline{\psi}_s(k_s)$ for $j = qs+1, qs+2, \cdots, qs+q_1$, is $\psi_1(q_1k_s + j - qs - 1)$. Following the above discussion $V_{s,ij} = 0$ if $\rho(Nk_s + i - 1)$, the i^{th} entry of $\underline{\rho}(k_s)$, depends on $\psi_1(q_1k_s + j - qs - 1)$ and

$$n_1(j - qs - 1) > i - 1,$$

or

$$i \leq (j - qs - 1)n_1. \tag{4.25}$$

Combining (4.24) and (4.25), in order for $\underline{\rho}(k_s)$ to be causal in regards of the output ψ_1, $V_{s,ij}$ should be zero if

$$i \leq (j - qs - 1)n_1 \quad \text{and} \quad qs + 1 \leq j \leq qs + q_1.$$

Similar results can be derived for other outputs. Furthermore, since the latest future value in $\underline{\psi}_s(k_s)$ corresponds to $t = Nk_sh + \max_k(q_k - 1)n_kh$, the search on i can be done only in the interval

$$1 \leq i \leq \max_k(q_k - 1)n_k.$$

In summary causality constraints can be formulated as: The entry $V_{s,ij}$ of V_s is zero if the pair (i, j) satisfy

$$1 \leq i \leq \max_k(q_k - 1)n_k \quad \text{and}$$

$$\begin{cases} & \Big(i \leq (j - qs - 1)n_1 \\ & \qquad \text{and} \quad qs + 1 \leq j \leq qs + q_1\Big), \\ \text{or} & \Big(i \leq (j - qs - q_1 - 1)n_2 \\ & \qquad \text{and} \quad qs + q_1 + 1 \leq j \leq qs + q_1 + q_2\Big), \\ \text{or} & \cdots \\ \text{or} & \Big(i \leq (j - qs - q_1 - \cdots - q_{m-1} - 1)n_m \\ & \qquad \text{and} \quad qs + q_1 + \cdots + q_{m-1} + 1 \leq j \leq q(s+1)\Big). \end{cases} \tag{4.26}$$

Let $\mathcal{M}$ denote the set of all (i, j)-pairs satisfying (4.26). The causality constraints are

$$V_{s,ij} = 0, \quad (i, j) \in \mathcal{M}.$$

And the original optimization problem (4.17) with the causality constraints will be

$$\begin{aligned} &\min_{V_s:\ N\times q(s+1)} J_{\text{ps}} \\ &\text{s.t. } V_s \underline{H}_{o,s} = 0, \\ &\text{s.t. } V_{s,ij} = 0, \quad (i,j) \in \mathcal{M}. \end{aligned} \tag{4.27}$$

In the next section, a method is developed to find an optimal solution of this problem.

4.3.3 Optimal solution with causality constraints

In Section 4.3.1, a class of solutions to the optimization problem were proposed. Now, it is enough to find an optimal solution within the proposed class that satisfies the causality constraints as well. To do so, constraints on V_s are first translated to constraints on W_s. Combining (4.19) and (4.22) yields

$$V_s = W_s U_b^T \Sigma_a^{-\frac{1}{2}} U_a^T N_B. \tag{4.28}$$

Assume that w_i is the i^{th} row of W_s and γ_j is the j^{th} column of $U_b^T \Sigma_a^{-\frac{1}{2}} U_a^T N_B$. $V_{s,ij} = 0$ implies that $w_i \gamma_j = 0$. Thus, causality constraints on W_s are

$$w_i \gamma_j = 0, \quad (i,j) \in \mathcal{M}. \tag{4.29}$$

The optimization problem to be solved now is

$$\begin{aligned} &\min_{W_s:\ N\times q'} J_{\text{ps}} \\ &\text{s.t. } w_i \gamma_j = 0, \quad (i,j) \in \mathcal{M}, \end{aligned}$$

$$J_{\text{ps}} = \frac{\|W_s\|_2^2}{\|W_s \Sigma_b^{\frac{1}{2}}\|_2^2} = \frac{\lambda_{\max}(W_s W_s^T)}{\lambda_{\max}(W_s \Sigma_b W_s^T)}.$$

To find a solution for this problem, the idea is to apply the causality constraints to the general solution given by Lemma 4.2. For simplicity assume that $N < q'$ (i.e., W_s is a fat matrix). The procedure for a tall matrix is similar. Recall from Lemma 4.2 that a general solution can be given as

$$W_s = U_w \Sigma_w.$$

Let

$$\Sigma_w = \left[\begin{array}{c:c} I & 0 \end{array} \right],$$

$$U_w = \left[\begin{array}{c} U_{w_1} \\ \vdots \\ U_{w_N} \end{array} \right].$$

Then,

$$W_s = \left[\begin{array}{cc} U_w & 0 \end{array} \right] = \left[\begin{array}{cc} U_{w_1} & 0 \\ \vdots & \vdots \\ U_{w_N} & 0 \end{array} \right]. \tag{4.30}$$

Partition γ_j as

$$\gamma_j = \left[\begin{array}{c} \gamma_{j1} \\ \gamma_{j2} \end{array} \right]$$

according to (4.3.3). Then the causality constraints in (4.29) could be simplified to

$$U_{w_i}\gamma_{j1} = 0, \quad (i,j) \in \mathcal{M}. \tag{4.31}$$

Since U_w is a unitary matrix, it satisfies

$$U_{w_i}U_{w_j}^T = \begin{cases} 0 & i \neq j \\ 1 & i = j \end{cases} \tag{4.32}$$

To find vectors $U_{w_1},...,U_{w_N}$ that satisfy (4.31) and (4.32) is a standard algorithm in linear algebra. When $U_{w_1},...,U_{w_N}$ are selected, W_s will be known, and using (4.28) V_s can be calculated. This V_s minimizes the performance index and satisfies causality constraints. This is summarized in the following theorem:

Theorem 4.1 *A parity matrix V_s calculated in (4.28), where W_s is obtained from (4.30) and solving (4.31) and (4.32) for U_w, is an optimal solution of (4.27).*

Proof The proof is clear from previous discussions.

□

From the above theorem, an optimal residual generator with practical causality constraints is designed that generates the lifted residual vector $\underline{\rho}(k_s)$ at a slow rate as in (4.15). By applying the inverse lifting operation when implementing the residual generator, a fast-rate residual (scalar-valued) is obtained as in (4.16).

4.3.4 Design procedure and implementation

The procedure of designing an optimal fast-rate parity space based residual generator for multirate sampled-data systems is summarized in the following steps:

Consider the multirate sampled-data system in (4.1), (4.2) and (4.3):

1. Compute N, q_i, $i = 1, 2, \cdots, m$, and q according to (4.4).
2. Compute A_D, B_D, E_{dJ} and E_{fJ} according to (4.7) and (4.11).
3. Construct the discrete-time lifted model in (4.9).
4. Compute the matrices $\underline{H}_{u,s}$, $\underline{H}_{d,s}$, $\underline{H}_{f,s}$ and $\underline{H}_{o,s}$as in (4.14) and (4.18).
5. Compute N_B and SVDs in (4.21) and construct γ_j.
6. Determine the set $\mathcal{M}$ for causality constraints from (4.26).
7. Find vectors U_{w_1},...,U_{w_N} from (4.31) and (4.32) and compute W_s according to (4.30) and subsequently V_s from (4.28).
8. Implement the lifted fast-rate residual generator in (4.15) with $\underline{v}_s(k_s)$ and $\underline{\psi}_s(k_s)$ as in (4.12) and (4.13). Each entry of the residual $\underline{\rho}(k_s)$ is calculated and implemented at one time instant: The first entry $\rho(Nk_s)$ is calculated at $t = Nk_sh$, the second entry $\rho(Nk_s + 1)$ at $t = Nk_sh + h$, ..., and the N^{th} entry $\rho(Nk_s + N - 1)$ at $t = Nk_sh + Nh - h$. Hence, the residual can be calculated in real-time at each time instant.

4.4 Fast-rate residual generator: $\mathcal{H}_\infty$ optimization

In Section 4.2, it was shown that designing an optimal residual generator for the multirate sampled-data system in (4.1), (4.2) and (4.3) is equivalent to designing an optimal residual generator for the following discrete-time system

$$\underline{\psi}(k_s) = \underline{G}_{uD}\underline{v}(k_s) + \underline{G}_{dJ}\underline{\bar{\gamma}}(k_s) + \underline{G}_{fJ}\underline{\bar{\gamma}}(k_s), \tag{4.33}$$

where

$$\left[\begin{array}{ccc} \underline{G}_{uD}(z) & \underline{G}_{dJ}(z) & \underline{G}_{fJ}(z) \end{array}\right] = \left[\begin{array}{c|ccc} A_l & B_l & E_{dl} & E_{fl} \\ \hline C_l & D_l & D_{dl} & D_{fl} \end{array}\right]. \tag{4.34}$$

A_l, B_l, E_{dl}, E_{fl}, C_l, D_l, D_{dl} and D_{fl} are defined in Section 4.2. In this section, a fast-rate residual generator is designed based on the equivalent discrete-time model and $\mathcal{H}_\infty$ optimization technique.

4.4.1 Residual generator

Applying the factorization approach in Section 2.5 to the equivalent discrete-time system given in (4.33) yields the general form of the residual generator as

$$\rho(k_s) = R\big(\underline{M}_u\underline{\psi}(k_s) - \underline{N}_u\underline{v}(k_s)\big), \tag{4.35}$$

where

$$\underline{\psi}(k_s) = \left[\begin{array}{l} \psi_1(q_1k_s) \\ \psi_1(q_1k_s+1) \\ \vdots \\ \psi_1(q_1k_s+q_1-1) \\ \hdashline \vdots \\ \hdashline \psi_m(q_mk_s) \\ \psi_m(q_mk_s+1) \\ \vdots \\ \psi_m(q_mk_s+q_m-1) \end{array}\right], \quad \underline{v}(k_s) = \left[\begin{array}{l} v(Nk_s) \\ v(Nk_s+1) \\ \vdots \\ v(Nk_s+N-1) \end{array}\right]. \tag{4.36}$$

Here $R(z) \in \mathcal{RH}_\infty$ is a designable post-filter and $(\underline{M}_u(z), \underline{N}_u(z))$ is a left coprime factorization of $\underline{G}_{uD}(z)$ satisfying

$$\underline{G}_{uD}(z) = \underline{M}_u^{-1}(z)\underline{N}_u(z).$$

$\underline{M}_u(z)$ and $\underline{N}_u(z)$ can be parameterized as

$$\begin{aligned} \underline{M}_u(z) &= \left[\begin{array}{c|c} A_l - LC_l & L \\ \hline -C_l & I \end{array}\right], \\ \underline{N}_u(z) &= \left[\begin{array}{c|c} A_l - LC_l & B_l - LD_l \\ \hline C_l & D_l \end{array}\right]. \end{aligned} \tag{4.37}$$

Assume that perfect disturbance decoupling is not possible. Therefore, in order to compromise between the sensitivity of the residual to the faults and

its robustness to the unknown inputs, the following $\mathcal{H}_\infty$ optimization problem is considered

$$\begin{aligned} &\min_{R(z)\in\mathcal{RH}_\infty} J_{\infty/\infty}, \\ &J_{\infty/\infty} = \frac{\|R(z)\underline{M}_u(z)\underline{G}_{dJ}(z)\|_\infty}{\|R(z)\underline{M}_u(z)\underline{G}_{fJ}(z)\|_\infty}. \end{aligned} \tag{4.38}$$

Assuming that $\underline{M}_u(z)\underline{G}_{dJ}(z)$ has no transmission zeros on the unit circle, it has a co-inner-outer factorization as

$$\underline{M}_u(z)\underline{G}_{dJ}(z) = \underline{G}_{do}(z)\underline{G}_{di}(z).$$

For details of computing the co-inner-outer factorization see Appendix A. The general solution of the optimization problem in (4.38) can then be parameterized as (Section 2.5.1)

$$R^*(z) = Q(z)\underline{G}_{do}^{-1}(z),$$

where the parameter $Q(z) \in \mathcal{RH}_\infty$ satisfies

$$\|Q(z)\underline{G}_{do}^{-1}(z)\underline{M}_u(z)\underline{G}_{fJ}(z)\|_\infty = \|Q(z)\|_\infty \|\underline{G}_{do}^{-1}(z)\underline{M}_u(z)\underline{G}_{fJ}(z)\|_\infty.$$

Conventionally $Q(z) = I$ is chosen, but here the general form of $Q(z)$ is considered. The degree of freedom available in $Q(z)$ is used later to satisfy the causality constraints. The optimal value of the performance index J is

$$J^*_{\infty/\infty} = \frac{1}{\|\underline{G}_{do}^{-1}(z)\underline{M}_u(z)\underline{G}_{fJ}(z)\|_\infty}.$$

The residual generator in (4.35) is a slow-rate system resulting in a slow-rate residual. It means that the residual is updated at the end of each repetition period. This may cause substantial delay in detection of the faults, for new information is also available during the repetition period. To update the residual whenever new information arrives (no matter during the repetition period or at the end of it), a fast-rate residual generator has to be designed. This can be achieved by introducing a set of N slow-rate residual generators as

$$\begin{aligned} \rho(Nk_s) &= R_1\big(\underline{M}_u\underline{\psi}(k_s) - \underline{N}_u\underline{\upsilon}(k_s)\big), \\ \rho(Nk_s+1) &= R_2\big(\underline{M}_u\underline{\psi}(k_s) - \underline{N}_u\underline{\upsilon}(k_s)\big), \\ &\vdots \\ \rho(Nk_s+N-1) &= R_N\big(\underline{M}_u\underline{\psi}(k_s) - \underline{N}_u\underline{\upsilon}(k_s)\big). \end{aligned} \tag{4.39}$$

To calculate the residual at the fast rate, each of the residual generators in (4.39) is used at one time instant during the repetition period. Notice that all the post-filters $R_i(z)$, $i = 1, \cdots, N$, in (4.39) optimize the same performance index in (4.38). Also all the residual generators in (4.39) use the same lifted input and output vectors in (4.36). But since these lifted vectors carry the future values too, some of the information needed for the earlier residual generators in (4.39) may not be available at the calculation time. In other words all the N residual generators in (4.39) may not be causal. So to accommodate these causality constraints, appropriate post-filter $R_i(z)$ should be chosen for each residual generator. Fortunately the degree of freedom available in the optimal post-filter $R_i(z)$ (notably the free-to-choose $Q(z)$) allows us to satisfy the causality constraints.

Suggested by the general solution, the optimal post-filters $R_i(z)$ are given as

$$R_i(z) = Q_i(z)\underline{G}_{do}^{-1}(z), \quad i = 1, \cdots, N.$$

$Q_i(z)$, $i = 1, \cdots, N$, are stable transfer function matrices satisfying

$$\|Q(z)\underline{G}_{do}^{-1}(z)\underline{M}_u(z)\underline{G}_{fJ}(z)\|_\infty = \|Q(z)\|_\infty \|\underline{G}_{do}^{-1}(z)\underline{M}_u(z)\underline{G}_{fJ}(z)\|_\infty. \quad (4.40)$$

4.4.2 Causality constraints

To discuss the causality constraints of the residual generators in (4.39), let us focus on the i^{th} residual generator

$$\rho(Nk_s + i - 1) = Q_i\underline{G}_{do}^{-1}\big(\underline{M}_u\underline{\psi}(k_s) - \underline{N}_u\underline{v}(k_s)\big). \quad (4.41)$$

Observing the lifted input and output vectors in (4.36), future values of $\psi(k)$ and $v(k)$ only appear in the current values of $\underline{\psi}(k_s)$ and $\underline{v}(k_s)$. In other words, $\underline{\psi}(k_s - 1)$ and $\underline{v}(k_s - 1)$ do not contain any future values. Therefore, the causality problem in the residual generator in (4.41) is caused only by the current values of $\underline{\psi}(k_s)$ and $\underline{v}(k_s)$. This means that the causality constraints only affect the direct feed-through term of the residual generator. Let $D_{i\psi}$ and D_{iv} denote the direct feed-through terms from $\underline{\psi}(k_s)$ and $\underline{v}(k_s)$ to $\rho(Nk_s+i-1)$, respectively. Then,

$$\begin{aligned} D_{i\psi} &= D_{Q_i}D_{G_{do}}D_{M_u}, \\ D_{iv} &= -D_{Q_i}D_{G_{do}}D_{N_u}, \end{aligned} \quad (4.42)$$

where D_{Q_i}, $D_{G_{do}}$, D_{M_u} and D_{N_u} are the direct feed-through terms (D-term in a realization) of $Q_i(z)$, $\underline{G}_{do}^{-1}(z)$, $\underline{M}_u(z)$ and $\underline{N}_u(z)$ respectively. It follows from (4.37) that $D_{M_u} = I$ and $D_{N_u} = D_l$. Then, (4.42) can be simplified to

$$D_{i\psi} = D_{Q_i} D_{G_{do}},$$
$$D_{iv} = -D_{Q_i} D_{G_{do}} D_l.$$

Because of the lower triangular structure of D_l, the future values of $v(k)$ in $\underline{v}(k_s)$, does not appear in the calculation of the residual. So causality of the residual generator in (4.41) depends on $D_{i\psi}$ only. Define

$$D_{i\psi} = D_{Q_i} D_{G_{do}} = \begin{bmatrix} d_{i1} & d_{i2} & \cdots & d_{iq} \end{bmatrix}.$$

To calculate the residual $\rho(Nk_s + i - 1)$ in (4.41), if the j^{th} entry of $\underline{\psi}(k_s)$ is a future value then the corresponding column in $D_{i\psi}$ (i.e., d_{ij}) should be zero. This guarantees that $\rho(Nk_s + i - 1)$ is independent of any unavailable information.

Corresponding to the i^{th} residual generator in (4.41), define $\mathcal{M}_i$ as the set of all indices j for which $d_{ij} = 0$. Similar to the steps in Section 4.3, it can be shown that

$$\begin{aligned} \mathcal{M}_i = &\Big\{ j : \ 1 \le j \le q_1 \quad \text{and} \quad i \le (j-1)n_1 \Big\} \cup \\ &\Big\{ j : \ q_1 + 1 \le j \le q_1 + q_2 \quad \text{and} \quad i \le (j - q_1 - 1)n_2 \Big\} \cup \\ &\quad \vdots \\ &\Big\{ j : \ q - q_m + 1 \le j \le q \quad \text{and} \quad i \le (j - q + q_m - 1)n_m \Big\}. \end{aligned} \tag{4.43}$$

For the residual generator in (4.41), the causality constraints on $D_{i\psi}$ are

$$d_{ij} = 0, \quad j \in \mathcal{M}_i.$$

Now, the causality constraints on $D_{i\psi} = D_{Q_i} D_{G_{do}}$ are translated to constraints on D_{Q_i} ($D_{G_{do}}$ is a known matrix). Let $D_{\mathcal{M}_i}$ be a matrix constructed from the corresponding columns of $D_{G_{do}}$ determined by $\mathcal{M}_i$ (e.g., if $\mathcal{M}_i = \{1, 3\}$ then D_{Q_i} contains the first and third column of $D_{G_{do}}$). Then the causality constraint on D_{Q_i} is

$$D_{Q_i} D_{\mathcal{M}_i} = 0.$$

If $N_{\mathcal{M}_i}$ denotes the orthonormal basis of $\text{Null}(D_{\mathcal{M}_i})$, then D_{Q_i} can be written as $D_{Q_i} = X_i N_{\mathcal{M}_i}$ where X_i is arbitrarily chosen. Therefore, the problem is

simplified to finding stable transfer function matrix $Q_i(z)$ that satisfies (4.40) and $Q_i(\infty) = D_{Q_i} = X_i N_{\mathcal{M}_i}$ for some X_i. One method to find such $Q_i(z)$ is presented in Appendix C. Notice that $Q_i(z)$ has q columns, but the number of its rows can be chosen freely. Once $Q_i(z)$ is calculated, the residual generators in (4.39) can be implemented.

4.4.3 Design procedure and implementation

The procedure of designing an $\mathcal{H}_\infty$ optimal fast-rate residual generation scheme for multirate sampled-data systems is summarized in the following steps:

Consider the multirate sampled-data system in (4.1), (4.2) and (4.3):

1. Compute N, q_i, $i = 1, 2, \cdots, m$, and q according to (4.4).

   item Compute A_D, B_D, E_{dJ} and E_{fJ} according to (4.7) and (4.11).

2. Construct the lifted models $\underline{G}_{uD}$, $\underline{G}_{dJ}$ and $\underline{G}_{fJ}$ as in (4.34).

3. Find the left coprime factorization $\underline{G}_{uD}(z) = \underline{M}_u^{-1}(z)\underline{N}_u(z)$ and the co-inner-outer factorization $\underline{M}_u(z)\underline{G}_{dJ}(z) = \underline{G}_{do}(z)\underline{G}_{di}(z)$ and calculate $\underline{G}_{do}^{-1}(z)$.

4. Determine the sets $\mathcal{M}_i$, $i = 1, \cdots, N$, for causality constraints as in (4.43) and find $D_{\mathcal{M}_i}$ and $N_{\mathcal{M}_i}$.

5. Compute the transfer function matrices $Q_i(z)$, $i = 1, \cdots, N$, according to Appendix C.

6. Construct the N residual generators in (4.39) with $\underline{\psi}(k_s)$ and $\underline{v}(k_s)$ as in (4.36) and $R_i(z) = Q_i(z)\underline{G}_{do}^{-1}(z)$, $i = 1, \cdots, N$.

Each residual is sequentially calculated and implemented at one time instant to render a residual signal at the fast rate:

$$\begin{aligned}
\rho(Nk_s) &= Q_1\underline{G}_{do}^{-1}\big(\underline{M}_u\underline{\psi}(k_s) - \underline{N}_u\underline{v}(k_s)\big), \quad \text{at } t = Nk_sh, \\
\rho(Nk_s+1) &= Q_2\underline{G}_{do}^{-1}\big(\underline{M}_u\underline{\psi}(k_s) - \underline{N}_u\underline{v}(k_s)\big), \quad \text{at } t = Nk_sh + h, \\
&\vdots \\
\rho(Nk_s+N-1) &= Q_N\underline{G}_{do}^{-1}\big(\underline{M}_u\underline{\psi}(k_s) - \underline{N}_u\underline{v}(k_s)\big), \quad \text{at } t = Nk_sh + Nh - h.
\end{aligned} \tag{4.44}$$

Implementing this residual generation framework will result in a sequence of residuals as

$$\{\cdots,\rho(Nk_s),\rho(Nk_s+1),\cdots,\rho(Nk_s+N-1)$$
$$,\rho(N(k_s+1)),\rho(N(k_s+1)+1),\cdots\}.$$

Different evaluation algorithms may be used, the simplest of which is

$$\|\rho(k)\|=\begin{cases}\text{zero or very small} & f(t)\equiv 0,\\ \text{nonzero or large} & f(t)\neq 0.\end{cases}$$

4.5 Example

To illustrate the proposed methods an example is given. The system is adopted from [55]. The continuous-time process model is:

$$\begin{cases}\dot{x}(t)=Ax(t)+Bu(t)+E_d d(t)+E_f f(t)\\ y_1(t)=C_1x(t)\\ y_2(t)=C_2x(t)\end{cases}$$

where

$$A=\begin{bmatrix}-1 & 5\\ 0 & -2\end{bmatrix},\quad B=\begin{bmatrix}0\\ 1\end{bmatrix},\quad E_d=\begin{bmatrix}0.1\\ 1\end{bmatrix},\quad E_f=\begin{bmatrix}0\\ 1\end{bmatrix},$$
$$C_1=\begin{bmatrix}1 & 0\end{bmatrix},\quad C_2=\begin{bmatrix}0 & 1\end{bmatrix}.$$

Define

$$[G_u(s)\quad G_d(s)\quad G_f(s)]=\left[\begin{array}{c|ccc}A & B & E_d & E_f\\ \hline C_1 & 0 & 0 & 0\\ C_2 & 0 & 0 & 0\end{array}\right].$$

The sampling period of the D/A converter is h sec and the sampling periods of the A/D converters are $T_{y_1}=2h$ sec and $T_{y_2}=3h$ sec (Figure 4.3).

Matrices A_D, B_D, E_{dJ} and E_{fJ} are computed according to (4.7) and (4.11), respectively. For $h=1$ sec,

$$A_D=\begin{bmatrix}0.368 & 1.163\\ 0 & 1.135\end{bmatrix},\quad B_D=\begin{bmatrix}0.999\\ 0.432\end{bmatrix},$$
$$E_{dJ}=\begin{bmatrix}1.108 & 0\\ 0.351 & 0.350\end{bmatrix},\quad E_{fJ}=\begin{bmatrix}1.052 & 0\\ 0.339 & 0.361\end{bmatrix}.$$

Let

$$[G_{uD}(z)\quad G_{dJ}(z)\quad G_{fJ}(z)]=\left[\begin{array}{c|ccc}A_D & B_D & E_{dJ} & E_{fJ}\\ \hline C_1 & 0 & 0 & 0\\ C_2 & 0 & 0 & 0\end{array}\right].$$

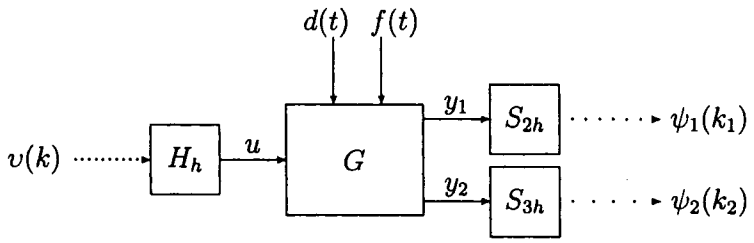

Figure 4.3: Multirate sampled-data system

As it can be seen, B_D has the same dimensions as B. Hence, $G(s)$ and $G_{uD}(z)$ have the same number of inputs, which is expected because the step invariant transformation does not change the number of inputs. In contrast, dimensions of E_d and E_{dJ} are different. Consecutively $G_d(s)$ has only one input while $G_{dJ}(z)$ has two inputs. So, the norm invariant transformation has introduced an extra disturbance input (also an extra fault input).

Using the following values

$$\begin{aligned} n_1 = 2, \quad n_2 = 3, \quad N = 6, \\ q_1 = 3, \quad q_2 = 2, \quad q = 5, \end{aligned}$$

the lifted model in (4.8) can be calculated as

$$\underline{G}_{uD}(z) = \left[\begin{array}{c|c} A_l & B_l \\ \hline C_l & D_l \end{array}\right]$$

$$= \left[\begin{array}{c|cccccc} A_D^6 & A_D^5 B_D & A_D^4 B_D & A_D^3 B_D & A_D^2 B_D & A_D B_D & B_D \\ \hline C_1 & 0 & 0 & 0 & 0 & 0 & 0 \\ C_1 A_D^2 & C_1 A_D B_D & C_1 B_D & 0 & 0 & 0 & 0 \\ C_1 A_D^4 & C_1 A_D^3 B_D & C_1 A_D^2 B_D & C_1 A_D B_D & C_1 B_D & 0 & 0 \\ C_2 & 0 & 0 & 0 & 0 & 0 & 0 \\ C_2 A_D^3 & C_2 A_D^2 B_D & C_2 A_D B_D & C_2 B_D & 0 & 0 & 0 \end{array}\right].$$

$\underline{G}_{dJ}(z)$ and $\underline{G}_{fJ}(z)$ have the same structure as $\underline{G}_{uD}(z)$, replacing B_D with E_{dJ} and E_{fJ} respectively. The input and output of $\underline{G}_{uD}$ are

$$\underline{v}(k_s) = \begin{bmatrix} v(6k_s) \\ v(6k_s+1) \\ v(6k_s+2) \\ v(6k_s+3) \\ v(6k_s+4) \\ v(6k_s+5) \end{bmatrix}, \quad \underline{\psi}(k_s) = \begin{bmatrix} \psi_1(3k_s) \\ \psi_1(3k_s+1) \\ \psi_1(3k_s+2) \\ \psi_2(2k_s) \\ \psi_2(2k_s+1) \end{bmatrix}.$$

Notice that $\underline{G}_{uD}$ has 6 inputs and 5 inputs, while $\underline{G}_{dJ}$ and $\underline{G}_{fJ}$ have 12 inputs and 5 outputs. This is because G_{dJ} and G_{fJ} have twice the number of inputs as G_{uD}.

4.5.1 Slow-rate residual generator

For a slow-rate residual generator, the parity space method can be applied to the lifted model. As mentioned before, this slow-rate residual generator is the same as the one developed in [55] with appropriate choice of s. In fact by setting $s = 1$ (which uses two frames of data to generate the residual), the obtained residual generator is identical to the one designed in [55] for $s = 11$. Using the approach in [55] the slow-rate residual generator is given by

$$\rho(k_s) = \hat{v}_s\Big(\hat{\psi}_s(k_s) - \hat{H}_{u,s}\hat{v}_s(k_s)\Big),$$

where

$$\hat{v}_s(k_s) = \begin{bmatrix} v(6k_s - 11) \\ \vdots \\ v(6k_s) \end{bmatrix}_{12\times 1}, \quad \hat{\psi}_s(k_s) = \begin{bmatrix} \psi_1(3k_s - 5) \\ \psi_2(2k_s - 3) \\ \psi_1(3k_s - 4) \\ \psi_2(2k_s - 2) \\ \psi_1(3k_s - 3) \\ \psi_1(3k_s - 2) \\ \psi_2(2k_s - 1) \\ \psi_1(3k_s - 1) \\ \psi_2(2k_s) \\ \psi_1(3k_s) \end{bmatrix}_{10\times 1},$$

$$\hat{H}_{u,s} = \begin{bmatrix} 0 & 0 & 0 & 0 & \cdots & 0 & 0 & 0 \\ 0 & 0 & 0 & 0 & \cdots & 0 & 0 & 0 \\ C_1A_DB_D & C_1B_D & 0 & 0 & \cdots & 0 & 0 & 0 \\ C_2A_D^2B_D & C_2A_DB_D & C_2B_D & 0 & \cdots & 0 & 0 & 0 \\ \vdots & \vdots & \vdots & \vdots & & \vdots & \vdots & \vdots \\ C_2A_D^8B_D & C_2A_D^7B_D & C_2A_D^6B_D & C_2A_D^5B_D & \cdots & 0 & 0 & 0 \\ C_1A_D^9B_D & C_1A_D^8B_D & C_1A_D^7B_D & C_1A_D^6B_D & \cdots & C_1B_D & 0 & 0 \end{bmatrix}.$$

The performance index is defined as

$$J_{\text{ps}} = \frac{\hat{v}_s\hat{H}_{d,s}\hat{H}_{d,s}^T\hat{v}_s^T}{\hat{v}_s\hat{H}_{f,s}\hat{H}_{f,s}^T\hat{v}_s^T}.$$

The optimal parity vector $\hat{v}_s$ is a 1×10 vector and is the solution of the following optimization problem

$$\min_{\hat{v}_s:\ 1\times 10} J_{\text{ps}}$$
$$\text{s.t. } \hat{v}_s \hat{H}_{o,s} = 0,$$

where

$$\hat{H}_{o,s} = \begin{bmatrix} C_1 \\ C_2 \\ C_1 A_D^2 \\ C_2 A_D^3 \\ C_1 A_D^4 \\ C_1 A_D^6 \\ C_2 A_D^6 \\ C_1 A_D^8 \\ C_2 A_D^9 \\ C_1 A_D^{10} \end{bmatrix}.$$

$\hat{H}_{d,s}$ and $\hat{H}_{f,s}$ have the same structure as $\hat{H}_{u,s}$ replacing B by E_{dJ} and E_{fJ} respectively. The optimal solution for $\hat{v}_s$ is:

$$v_s^* = \begin{bmatrix} 0 & 0 & 0.01 & 0.07 & -0.06 & 0.21 & -1 & 0 & 0 & 0 \end{bmatrix},$$

and the optimal performance index is:

$$J_{\text{ps}}^* = 0.9575 \tag{4.45}$$

4.5.2 Fast-rate residual generator: Parity space

Again choosing $s = 1$ (i.e., two frames of data are used) and applying the method in Section 4.3, the fast-rate residual generator is

$$\underline{\rho}(k_s) = \begin{bmatrix} \rho(6k_s) \\ \rho(6k_s+1) \\ \rho(6k_s+2) \\ \rho(6k_s+3) \\ \rho(6k_s+4) \\ \rho(6k_s+5) \end{bmatrix} = V_s \left(\begin{bmatrix} \psi_1(3k_s-3) \\ \psi_1(3k_s-2) \\ \psi_1(3k_s-1) \\ \psi_2(2k_s-2) \\ \psi_2(2k_s-1) \\ \psi_1(3k_s) \\ \psi_1(3k_s+1) \\ \psi_1(3k_s+2) \\ \psi_2(2k_s) \\ \psi_2(2k_s+1) \end{bmatrix} - \underline{H}_{u,s} \underline{\upsilon}_s(k_s) \right), \tag{4.46}$$

where $\underline{\upsilon}_s(k_s)$ and $\underline{H}_{u,s}$ are given in (4.12) and (4.14). It is now obvious that some entries of V_s can cause dependence on the future values of outputs. For

instance $r(6k_s)$ depends on $\psi_1(3k_s+1)$, $\psi_1(3k_s+2)$ and $\psi_2(2k_s+1)$ which are not available at $t = 6k_s$. Therefore, causality constraints enforces V_s to have the following structure

$$V_s = \begin{bmatrix} * & * & * & * & * & * & 0 & 0 & * & 0 \\ * & * & * & * & * & * & 0 & 0 & * & 0 \\ * & * & * & * & * & * & * & 0 & * & 0 \\ * & * & * & * & * & * & * & 0 & * & * \\ * & * & * & * & * & * & * & * & * & * \\ * & * & * & * & * & * & * & * & * & * \end{bmatrix},$$

where $*$ means a designable value. Hence

$$\mathcal{M} = \Big\{(1,7),(1,8),(1,10),(2,7),(2,8),(2,10),(3,8),(3,10),(4,8)\Big\}.$$

To calculate an optimal V_s, one should find a unitary matrix U_w satisfying (4.31) and (4.32). In other words, orthonormal vectors $U_{w_1}, \cdots, U_{w_6}$ should be found such that:

$$\begin{aligned} &U_{w_1}\gamma_{7,1} = 0, && U_{w_1}\gamma_{8,1} = 0, && U_{w_1}\gamma_{10,1} = 0, \\ &U_{w_2}\gamma_{7,1} = 0, && U_{w_2}\gamma_{8,1} = 0, && U_{w_2}\gamma_{10,1} = 0, \\ &U_{w_3}\gamma_{8,1} = 0, && U_{w_3}\gamma_{10,1} = 0, && U_{w_4}\gamma_{8,1} = 0. \end{aligned}$$

Combining these equations with (4.32), normal vectors U_{w_1},...,U_{w_6} can be computed as follows:

$$\begin{aligned} U_{w_1} &\in \text{Null}\Big(\begin{bmatrix} \gamma_{7,1} & \gamma_{8,1} & \gamma_{10,1} \end{bmatrix}\Big), \\ U_{w_2} &\in \text{Null}\Big(\begin{bmatrix} \gamma_{7,1} & \gamma_{8,1} & \gamma_{10,1} & U_{w_1}^T \end{bmatrix}\Big), \\ U_{w_3} &\in \text{Null}\Big(\begin{bmatrix} \gamma_{8,1} & \gamma_{10,1} & U_{w_1}^T & U_{w_2}^T \end{bmatrix}\Big), \\ U_{w_4} &\in \text{Null}\Big(\begin{bmatrix} \gamma_{8,1} & U_{w_1}^T & U_{w_2}^T & U_{w_3}^T \end{bmatrix}\Big), \\ U_{w_5} &\in \text{Null}\Big(\begin{bmatrix} U_{w_1}^T & U_{w_2}^T & U_{w_3}^T & U_{w_4}^T \end{bmatrix}\Big), \\ U_{w_6} &\in \text{Null}\Big(\begin{bmatrix} U_{w_1}^T & U_{w_2}^T & U_{w_3}^T & U_{w_4}^T & U_{w_5}^T \end{bmatrix}\Big). \end{aligned}$$

One optimal solution for V_s is

$$V_s^* = \begin{bmatrix} 0.01 & 0.01 & 0.01 & 0 & 0.01 & 0 \\ -0.05 & -0.06 & -0.08 & 0.09 & -0.08 & -0.04 \\ 0.02 & -0.01 & 0.23 & 0.04 & 0.07 & 0.21 \\ 0.02 & 0.04 & 0.03 & -0.06 & 0.04 & 0.01 \\ -0.32 & -0.35 & -0.63 & -0.21 & 0.37 & -0.57 \\ 0.14 & 0.15 & -0.37 & 0.27 & 0.07 & -0.14 \\ 0 & 0 & 0.04 & -0.15 & 0.19 & -0.08 \\ 0 & 0 & 0 & 0 & -0.20 & -0.10 \\ -0.99 & -1.03 & 0.66 & -0.88 & -0.57 & 1.05 \\ 0 & 0 & 0 & -0.31 & 0.35 & -0.12 \end{bmatrix}^T,$$

and the optimal performance index is

$$J_{\text{ps}}^* = 0.9575$$

Note that this performance index is equal to the optimal performance of the slow-rate residual generator in (4.45).

To generate the residual one should use the calculated V_s^* and evaluate the residual generator in (4.46) one row at a time. For example the first row of (4.46) will be

$$\begin{aligned} \rho(6k_s) &= 0.01\ \psi_1(3k_s-3) - 0.05\ \psi_1(3k_s-2) + 0.02\ \psi_1(3k_s-1) \\ &+ 0.02\ \psi_2(2k_s-2) - 0.32\ \psi_2(2k_s-1) + 0.14\ \psi_1(3k_s) \\ &- 0.99\ \psi_2(2k_s) - v_1 \underline{H}_{u,s} \underline{v}_s(k_s), \end{aligned}$$

where v_1 is the first row of V_s^*. As it can be seen, no future data is needed to compute $\rho(6k_s)$.

4.5.3 Fast-rate residual generator: $\mathcal{H}_\infty$ optimization

Since $G_u(s)$ (and subsequently $\underline{G}_{uD}(z)$) is stable, $\underline{M}_u(z) = I$ and $\underline{N}_u(z) = \underline{G}_{uD}(z)$ can be selected as a left coprime factorization of $\underline{G}_{uD}(z)$. The co-inner-outer factorization $\underline{M}_u(z)\underline{G}_{dJ}(z) = \underline{G}_{dJ}(z) = \underline{G}_{do}(z)\underline{G}_{di}(z)$ can then be

calculated as

$$\underline{G}_{do}(z) = \left[\begin{array}{cc|ccccc} 0.003 & 0.012 & 0.007 & 0.054 & 0.377 & 0.003 & -0.089 \\ 0 & 0 & 0 & 0 & 0.006 & 0 & -0.003 \\ \hline 1 & 0 & 1.450 & 0 & 0 & 0 & 0 \\ 0.135 & 0.585 & 0.377 & 1.453 & 0 & 0 & 0 \\ 0.018 & 0.090 & 0.054 & 0.377 & 1.453 & 0 & 0 \\ 0 & 1 & 0.309 & 0.062 & -0.007 & 0.388 & 0 \\ 0 & 0.003 & 0.001 & 0.042 & 0.303 & -0.001 & 0.395 \end{array}\right],$$

$$\underline{G}_{do}^{-1}(z) = \left[\begin{array}{cc|ccccc} -0.824 & -0.174 & -0.002 & 0.036 & -0.306 & -0.006 & 0.224 \\ -0.014 & 0.027 & 0 & 0.001 & -0.005 & 0 & 0.007 \\ \hline 0.690 & 0 & 0.690 & 0 & 0 & 0 & 0 \\ -0.086 & 0.403 & -0.179 & 0.689 & 0 & 0 & 0 \\ 0.009 & -0.043 & 0.021 & -0.179 & 0.688 & 0 & 0 \\ -0.535 & 2.511 & -0.520 & -0.114 & 0.012 & 2.576 & 0 \\ 0 & 0 & 0.001 & 0.064 & -0.528 & 0.004 & 2.529 \end{array}\right].$$

Now the slow-rate residual generator can be obtained by simply applying the $\mathcal{H}_\infty$ optimization method to the slow-rate lifted system. The slow-rate residual generator is

$$\rho(k_s) = \underline{G}_{do}^{-1}\big(\underline{\psi}(k_s) - \underline{G}_{uD}(z)\underline{v}(k_s)\big).$$

The optimal performance achieved by the slow-rate residual generator is

$$J_{\infty/\infty}^* = \frac{1}{\|\underline{G}_{do}^{-1}(z)\underline{G}_{fJ}(z)\|_\infty} = 0.978.$$

For a fast-rate residual generator, the causality constraints has to be considered first. The sets $\mathcal{M}_i$, $i = 1, \cdots, 6$, for causality constraints can be determined as in (4.26)

$$\mathcal{M}_1 = \mathcal{M}_2 = \Big\{2,3,5\Big\}, \quad \mathcal{M}_3 = \Big\{3,5\Big\},$$
$$\mathcal{M}_4 = \Big\{3\Big\}, \quad \mathcal{M}_5 = \mathcal{M}_6 = \Big\{\Big\}.$$

The direct feed-through term (D-term in a realization) of $\underline{G}_{do}^{-1}(z)$ is

$$D_R = \left[\begin{array}{ccccc} 0.690 & 0 & 0 & 0 & 0 \\ -0.179 & 0.689 & 0 & 0 & 0 \\ 0.021 & -0.179 & 0.688 & 0 & 0 \\ -0.520 & -0.114 & 0.012 & 2.576 & 0 \\ 0.001 & 0.064 & -0.528 & 0.004 & 2.529 \end{array}\right].$$

Corresponding to the sets $\mathcal{M}_i$, $i = 1, \cdots, 6$, matrices $D_{\mathcal{M}_i}$, $i = 1, \cdots, 6$, can be constructed as

$$D_{\mathcal{M}_1} = D_{\mathcal{M}_2} = \begin{bmatrix} 0 & 0 & 0 \\ 0.689 & 0 & 0 \\ -0.179 & 0.688 & 0 \\ -0.114 & 0.012 & 0 \\ 0.064 & -0.528 & 2.529 \end{bmatrix},$$

$$D_{\mathcal{M}_3} = \begin{bmatrix} 0 & 0 \\ 0 & 0 \\ 0.688 & 0 \\ 0.012 & 0 \\ -0.528 & 2.529 \end{bmatrix}, \quad D_{\mathcal{M}_4} = \begin{bmatrix} 0 \\ 0 \\ 0.688 \\ 0.012 \\ -0.528 \end{bmatrix}.$$

The basis matrices of the null spaces of $D_{\mathcal{M}_i}$, $i = 1, \cdots, 6$, are

$$N_{\mathcal{M}_1} = N_{\mathcal{M}_2} = \begin{bmatrix} -0.137 & 0.157 & -0.017 & 0.978 & 0 \\ 0.991 & 0.022 & -0.002 & 0.135 & 0 \end{bmatrix},$$

$$N_{\mathcal{M}_3} = \begin{bmatrix} -0.793 & -0.608 & 0 & -0.017 & 0 \\ -0.013 & -0.010 & -0.017 & 1 & 0 \\ 0.609 & -0.794 & 0 & 0 & 0 \end{bmatrix},$$

$$N_{\mathcal{M}_4} = \begin{bmatrix} 0 & 1 & 0 & 0 & 0 \\ -0.793 & 0 & 0.370 & -0.011 & 0.483 \\ -0.013 & 0 & -0.011 & 1 & 0.008 \\ 0.609 & 0 & 0.483 & 0.008 & 0.630 \end{bmatrix},$$

$$N_{\mathcal{M}_5} = N_{\mathcal{M}_6} = I.$$

$Q_i(z)$, $i = 1, \cdots, 6$, can now be calculated. For example by choosing $X_1 = [0.6166 \quad 0.1133]$, $\psi = 100$ and $P_1(s) = (s + 0.1)^3$, $Q_1(z)$ is obtained as (ω_o is determined to be 0.1)

$$Q_1(z) = \frac{1}{z^3 - 1.6\,z^2 + 0.87\,z - 0.16} \times \begin{bmatrix} 0.028\,z^3 - 0.87\,z^2 + 1.5\,z - 0.54 \\ 0.099\,z^3 - 9.6\,z^2 + 16.0\,z - 6.1 \\ -0.011\,z^3 + 2.6\,z^2 - 3.8\,z + 1.2 \\ 0.62\,z^3 - 60.0\,z^2 + 100.0\,z - 38.0 \\ 2.2\,z^2 - 3.1\,z + 1.0 \end{bmatrix}^T.$$

The residual generators in (4.44) can now be implemented. The optimal performance index is $J^*_{\infty/\infty} = 0.978$ which is the same performance achieved by the slow-rate residual generator.

4.5.4 Simulation

For simulation let $h = 1$ sec, and since the input signal $u(t)$ has no effect on the residual, it is assumed that $u(t) \equiv 0$. $d(t)$ is white noise with variance 1 and $f(t)$ is a step function with amplitude 10 and step time at 20 sec. The results of simulation for slow-rate, parity space based fast-rate and $\mathcal{H}_\infty$ based fast-rate residual generators are illustrated in Figures 4.4, 4.5 and 4.6 respectively. The figures show that the fast-rate residual is actually updated 6 times faster than the slow-rate residual, which significantly improves the detection speed. For the slow-rate residual in Figure 4.4, the effect of the fault appears in the residual after 4 sec. But for the fast-rate residual generators in Figures 4.5 and 4.6, the fault can be detected after 1 sec.

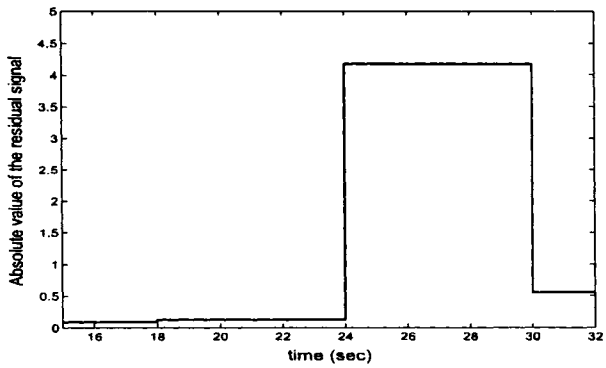

Figure 4.4: Parity space based slow-rate residual

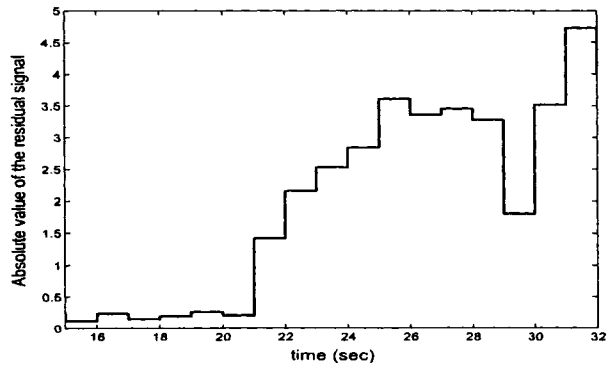

Figure 4.5: Parity space based fast-rate residual

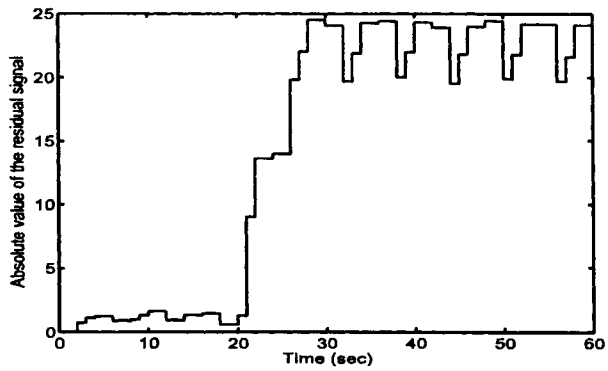

Figure 4.6: $\mathcal{H}_\infty$ based fast-rate residual

4.6 Discussions and conclusions

In this section two design approaches to optimal fast-rate residual generation for multirate sampled-data systems were developed. The fast-rate residual generation schemes ensure the detection of a fault at the earliest time possible preventing the system from any undesirable operation caused by the fault. Furthermore, using the norm invariant transformation and direct design ensures that the intersample behavior of the faults and unknown inputs is captured. So no approximation was made during the derivations.

Of course the fact that the residual generator operates at the fast rate does not necessarily mean that the fault is always detected at the fast rate. The reason is that the new information (from the outputs) does not necessarily become available at the fast rate. However, the proposed fast-rate residual generators can guarantee the detection of a fault at the earliest time possible. Let T_d denote the detection delay which is the difference between the time the fault occurs and the time its effect appears in the residual, then

$$0 \leq T_d \leq n_{\min} h,$$

where

$$n_{\min} = \min_i n_i$$

and $n_i h$ is the sampling period of the i^{th} output. $n_{\min} h$ is the maximum gap between the sampled outputs. So the new information from outputs will be available no later than $n_{\min} h$ sec, and as soon as the residual generator receives the new information the residual can be updated.

It is also notable that introducing the multirate sampling will improve the detection speed. For example if all the outputs are sampled synchronously with $T = n_{\min}h$ sec, again the maximum delay in fault detection would be $n_{\min}h$ sec. But the multirate sampled-data scheme would probably detect the fault earlier because of the inherently redundant information available at different sampling rates. This improves the chance of early detection of the fault which means that the multirate scheme is usually better than the (synchronous) single-rate scheme in terms of detection speed.

As an example, consider a system with two outputs. If both of the outputs are sampled at a single rate with $T = 2$ sec, then the maximum delay in fault detection is 2 sec. Now for the same system if the two outputs are sampled at two different rates, e.g., $T_1 = 2$ sec and $T_2 = 3$ sec, again the maximum delay in fault detection is 2 sec. But in the latter case, there are some periods of time (for example $6k+2 < t < 6k+3$) that if a fault occurs during this period, it can be detected within 1 sec, while the same fault will be detected between 1 sec and 2 sec in the single-rate scheme. So the probability of early detection of the fault is improved in the multirate fault detection. In case of asynchronous sampling, the same methods can be applied with minor modifications.

Two different methods were used for fast-rate residual generation: parity space approach and factorization approach with $\mathcal{H}_\infty$ optimization. For both methods, the design is carried out by converting the original multirate sampled-data system to an equivalent discrete-time system. This discrete-time system is a slow-rate model, thus the residual generator designed for this method will also work at the slow rate. The idea used to yield a fast-rate residual generator was to generate a lifted (vector) residual rather than a scalar one. Applying the inverse lifting operator to the lifted slow-rate residual will result in a fast-rate residual. In the parity space approach, this is achieved by introducing a *parity matrix* rather than the known *parity vector*. For the $\mathcal{H}_\infty$ approach, a bank of optimal residual generators was introduces, each working at one time instant.

To deal with multirate sampling, the lifting technique is used. It enables us to replace the multirate system with a MIMO single-rate one. Using lifting also helps in developing a more general and systematic formulation. In both approaches, to compromise between the sensitivity of residual to the fault and its robustness to other unknown inputs, a performance index was defined.

Analytical solutions were proposed to minimize the performance indices for both cases. The analytical solutions, involve many degrees of freedom, which help us consider more constraints on the solution. The use of lifting operator arises the issue of causality. This issue is dealt with properly using the degrees of freedom available in the optimal solution. The degrees of freedom might also be used to involve more useful constraints, optimize other performance criteria or accommodate issues of evaluation and isolation of faults.

Chapter 5

Performance Analysis in Sampled-data Systems

5.1 Introduction

As discussed in previous chapters, sampled-data systems are widely used and accepted in industry because of the numerous advantages of digital technology. In these types of systems the actual process is continuous-time while the controller is digitally implemented by computer (Figure 5.1). Thus a sampled-data system is a hybrid system involving both continuous and discrete-time signals. Multirate sampled-data systems, in which digital-to-analog and analog-to-digital converters work at different sampling rates, are also abundant in industry. In a variety of industrial process applications, the elements of the control system may be structured distributively, i.e., sensors, actuators and controller are connected via standard networks. Moreover, in many chemical engineering systems, measurements are not available at the same rate and practical constraints may exist on the sampling rates of several physical variables. Extensive research on development and analysis of single-rate and

---

The materials of this chapter has been submitted for publication in:

> I. Izadi, T. Chen and Q. Zhao, "Performance analysis in multirate sampled-data control systems", submitted to *IEEE Transactions on Automatic Control*, November 2005.

Some materials of this chapter has also been published in:

> I. Izadi, T. Chen and Q. Zhao, "$\mathcal{H}_\infty$ performance comparison of single-rate and multirate sampled-data systems", *Proceedings of the American Control Conference*, Minneapolis, MN, pp. 183–187, 2006.

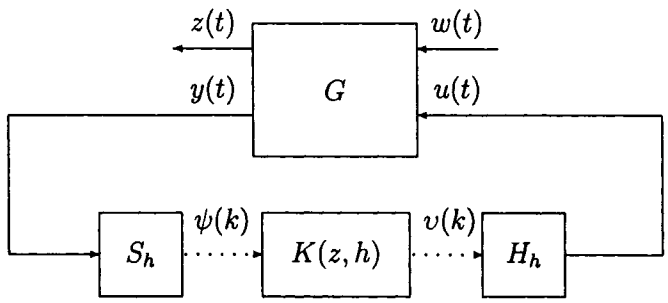

Figure 5.1: The standard single-rate sampled-data system.

multirate sampled-data control systems has been carried out during the past decades [1, 9].

Most of the existing sampled-data control techniques are based on the availability of all the measurements at a single rate. These techniques can not be directly used to design controllers for multirate systems. To resolve this drawback, one approach is to downsample the multirate measurements to a lower sampling rate. In other words the multirate system is replaced with a single-rate system whose sampling period is the least common multiple of all the sampling periods of the multirate system. This particular single-rate system is known as the slow single-rate or simply slow-rate system. One expects that the single-rate controller designed based on the slow-rate system would not necessarily be an appropriate controller for the original multirate system. The reason is that the slow-rate controller does not use all the information that is available through feedback. To use all the information present in the multirate data one would need to design a multirate controller. A well known approach for treating a multirate system is to convert it into a single-rate system (with slower sampling rate and higher dimension) using the lifting operator. The concept of lifting involves stacking of fast-rate measurements of a signal during one repetition period to form a slow-rate signal. An intuitive reason for changing to multirate controller from slow-rate controller is that, hopefully the former gives better performance than the latter. However, there has been very few theoretical results to support this intuition.

On the other hand, it is intuitive too, that if all the signals were available at a faster rate than that in the multirate system, one could expect better

performance. For this purpose, another single-rate system, known as the fast single-rate or simply fast-rate system is introduced. The sampling period of the fast-rate system is the greatest common divisor of all the sampling periods of the multirate system. In the fast-rate system, control signals are generated at the fast rate assuming that all the signals are available at that rate. There have also been very few theoretical results to support the intuition that the fast-rate controller offers better performance than the multirate controller.

A theoretical comparison of multirate and single-rate systems was reported in [48]. The lifting method was adopted to transform a multirate system into an LTI single-rate system. The performance index used was the continuous-time LQR cost function. It was shown that multirate control performs no worse than slow single-rate control. It was also shown that the fast-rate controller yields the same LQR performance as the multirate controller. However, it was assumed that all measurements are sampled at one rate and all the control signals are generated at another rate (i.e., a dual-rate concept). In addition, it was assumed that the input is generated at a faster rate than the measured output. These assumptions limit the application of the results.

Another result was recently presented in [50]. The performance index used in this paper was the variance of the fast sampled output. It was shown that the optimal dual-rate controller (in the sense of minimum variance) performs better than the optimal slow-rate controller but worse than the optimal fast-rate controller. The lifting technique was used and a linear matrix inequity (LMI) approach was developed to calculate the optimal controller. The system under investigation was single-input single-output and the controller was dual-rate. In addition, only the case when the sampling frequency of the controller output is an integer multiple of the sampling frequency of the controller input was considered. These assumptions are restrictive.

In this section, the following questions are studied:

- Do multirate controllers give better performance than slow-rate controllers?
- Do fast-rate controllers give better performance than multirate controllers?

For a fair comparison, the choice of the performance index is very important. A discrete-time performance index is not suitable because of the differ-

ent sampling periods involved. Since the input and output of the closed-loop system are continuous-time signals (Figure 5.1), a performance index defined in continuous-time is more appropriate. Here the $\mathcal{H}_\infty$ and $\mathcal{H}_2$ norms of the closed-loop system are considered as measures for quality of control. However, the approach presented in this chapter is general and with little modification can be used for a variety of performance indices including the $\mathcal{L}_p$ induced norm of the closed-loop system and the LQR performance.

The approach followed in this chapter is different from the previous ones in [48, 50]: Firstly, the lifting technique is not used to prove the theorems. This makes the proofs fairly simple and easy to follow. Secondly, no assumption is made on sampling periods of inputs and outputs. The results hold for general multirate systems and are not limited to dual-rate systems or systems with fast output sampling. Furthermore, no assumptions are made on the systems except that the optimal controller exists. Finally, as stated before, the approach is general and paves a way for further analysis using a wide range of performance indices. As a byproduct, an analysis of $\mathcal{H}_2$ performance of sampled-data systems with linear periodically time-varying (LPTV) controllers is presented in this chapter. It is shown how to convert a sampled-data system with LPTV controller to a pure discrete-time system with the same controller. It is also proved that for sampled-data systems, the optimal LTI controller performs better than any LPTV controller.

In the rest of this section, descriptions of the single-rate and multirate sampled-data systems under consideration are given. Some useful lemmas are also introduced.

5.1.1 Single-rate sampled-data system

A standard single-rate sampled-data control system is shown in Figure 5.1. Here G is a continuous-time causal finite order linear time-invariant (LTI) plant, $w(t)$ the exogenous input, $z(t)$ the controlled output, $y(t)$ the measured output of the plant and $u(t)$ the control signal. Since G has two inputs and two outputs, it can be partitioned into four components

$$G = \begin{bmatrix} G_{11} & G_{12} \\ G_{21} & G_{22} \end{bmatrix}.$$

The plant output is sampled and discretized using an A/D converter mod-

elled by

$$\psi(k) = y(kh),$$

where h is the sampling period. The control signal is generated by a computer and sent to the actuator using a zero-order hold D/A converter modelled by

$$u(t) = v(k), \quad kh \leq t < (k+1)h.$$

Hence,

$$\psi(k) = S_h y(t),$$
$$u(t) = H_h v(k).$$

$K(z,h)$ is the discrete-time controller with sampling period h (since different sampling periods are used in this section, the dependency of the discrete-time transfer functions on the sampling period is explicitly indicated). Consecutively, the sampled-data control rule is

$$u(t) = H_h K(z,h) S_h \; y(t).$$

It is assumed that $K(z,h)$ belongs to the set of all admissible (i.e., discrete-time, causal, finite order and LTI) controllers.

The closed-loop system from $w(t)$ to $z(t)$ is denoted by $\mathcal{F}\big(G(s), K(z,h)\big)$; thus

$$z(t) = \mathcal{F}\big(G(s), K(z,h)\big)\, w(t).$$

$\mathcal{F}\big(G(s), K(z,h)\big)$ is a linear and periodic operator with period h. It can be derived that [9]

$$\mathcal{F}\big(G(s), K(z,h)\big) =$$
$$G_{11}(s) + G_{12}(s) H_h K(z,h) S_h \Big(I - G_{22}(s) H_h K(z,h) S_h\Big)^{-1} G_{21}(s).$$

In this chapter, LPTV controllers are considered as well. Let q^{-1} be the standard delay operator for discrete-time signals, i.e.,

$$q^{-1}\alpha(k) = \alpha(k-1).$$

A discrete-time system $K(z,h,N)$ is linear periodically time-varying (LPTV) with period N if it is linear and

$$\begin{cases} K = q^N K q^{-N}, \\ K \neq q^i K q^{-i}, \quad 0 < i \leq N-1. \end{cases}$$

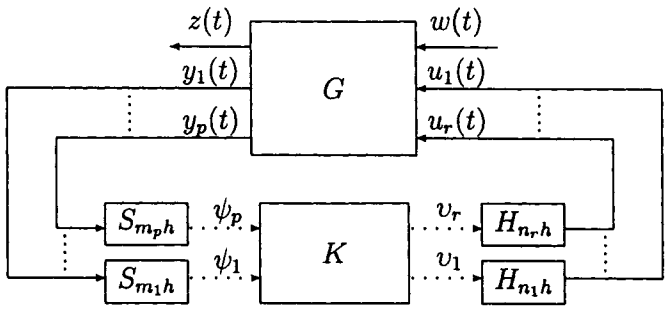

Figure 5.2: The general multirate sampled-data system.

Notice that the dependency of an LPTV transfer function to its period is explicitly denoted. For a discrete-time LPTV controller $K(z,h,N)$, the closed-loop system $\mathcal{F}\big(G(s),K(z,h,N)\big)$ is a linear and Nh-periodic operator. The LPTV controller $K(z,h,N)$ belongs to the set of all admissible LPTV (i.e., discrete-time, causal, finite order, linear and N-periodic) controllers.

5.1.2 Multirate sampled-data system

A general multirate sampled-data control system is shown in Figure 5.2. Here each output channel is sampled at a different rate. The first output $y_1(t)$ is sampled every m_1h seconds, the second output $y_2(t)$ is sampled every m_2h seconds and so on. If p is the number of plant outputs then,

$$\begin{aligned}
\psi_1(k_{m_1}) &= S_{m_1h}y_1(t),\\
\psi_2(k_{m_2}) &= S_{m_2h}y_2(t),\\
&\vdots\\
\psi_p(k_{m_p}) &= S_{m_ph}y_p(t).
\end{aligned}$$

Note that since the discrete-time signals ψ_i, $i=1,\cdots,p$, are available at different time instants, they have different time indices k_{m_i}, $i=1,\cdots,p$.

Different control signals are also generated at different rates; the first control signal is generated every n_1h seconds and so on. If r is the number of

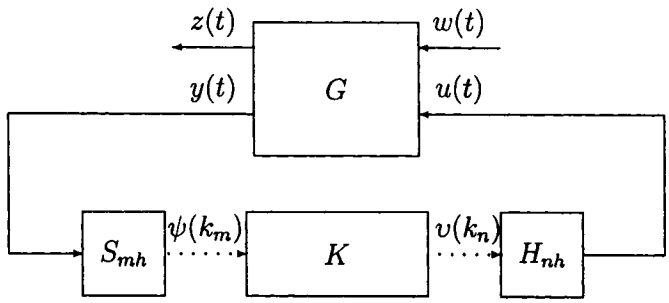

Figure 5.3: The standard dual-data sampled-data system.

control signals then,

$$\begin{aligned} u_1(t) &= H_{n_1 h}\upsilon_1(k_{n_1}), \\ u_2(t) &= H_{n_2 h}\upsilon_2(k_{n_2}), \\ &\vdots \\ u_r(t) &= H_{n_r h}\upsilon_r(k_{n_r}). \end{aligned}$$

Discrete-time signals υ_i, $i = 1, \cdots, r$, also have different time indices k_{n_i}, $i = 1, \cdots, r$. Assume that the greatest common divisor and the least common multiple of m_i, $i = 1, \cdots, p$, and n_i, $i = 1, \cdots, r$, are 1 and l respectively

$$\begin{aligned} \text{g.c.d.}(m_1, \cdots, m_p, n_1, \cdots, n_r) &= 1, \\ \text{l.c.m.}(m_1, \cdots, m_p, n_1, \cdots, n_r) &= l. \end{aligned}$$

Then the sampling periods of the corresponding fast-rate and slow-rate controllers are h and lh respectively.

The multirate controller is generally an l-periodic time-varying discrete-time system. But if considered in one repetition period (lh seconds) with lifted input and output, the multirate controller can be regarded as a (higher dimension) discrete-time LTI system with sampling period lh. Let $K(z, lh)$ denote this LTI multirate controller with lifted input and output, which belongs to the set of all admissible (i.e., discrete-time, causal, finite order and LTI) multirate controllers. For definitions of periodicity and causality of multirate systems see [10]. In Figure 5.2, $\mathcal{F}\big(G(s), K(z, lh)\big)$ denotes the closed-loop system from $w(t)$ to $z(t)$ which is a linear lh-periodic operator.

Dual-rate systems, a common subcategory of multirate systems, are defined when $m_1 = \cdots = m_p = m$ and $n_1 = \cdots = n_r = n$. In a dual-rate sampled-data

control system (Figure 5.3), all the plant output channels are sampled every mh seconds while all the control signals are generated every nh seconds (hence the term dual-rate). So,

$$\psi(k_m) = S_{mh}y(t),$$
$$u(t) = H_{nh}v(k_n).$$

With the assumption that m and n are coprime, the sampling period of the fast-rate and slow-rate controllers are h and mnh respectively. $K(z, mnh)$ denotes the dual-rate controller with lifted input and output. Therefore, the dual-rate control rule is

$$u(t) = H_{nh}L_m^{-1}K(z, mnh)L_nS_{mh}\ y(t).$$

Let $\mathcal{F}\big(G(s), K(z, mnh)\big)$ denote the closed-loop system from $w(t)$ to $z(t)$, which is a linear mnh-periodic operator.

For every multirate (dual-rate) system, corresponding slow single-rate and fast single-rate systems can be defined. When confusion may arise, subscripts MR (DR), SR and FR are used to distinguish amongst the signals in multirate (dual-rate) and corresponding slow-rate and fast-rate systems. For instance u_{MR} and u_{SR} denote the control signals in the multirate and its corresponding slow-rate systems respectively.

5.1.3 Two lemmas

Two lemmas involving sampling, hold and lifting operators, which will be used later in this chapter, are stated here.

Lemma 5.1 [9] *The following statements hold:*

i. $H_hS_hH_{nh} = H_{nh}$,

ii. $S_{nh}H_hS_h = S_{nh}$,

iii. $S_hH_{nh} = L_n^{-1}\left\{\begin{bmatrix} I \\ \vdots \\ I \end{bmatrix}\right\} n$,

iv. $S_{nh}H_h = \overbrace{\begin{bmatrix} I & 0 & \cdots & 0 \end{bmatrix}}^{n} L_n$.

□

Lemma 5.2 *For any discrete-time system $G(z, nh)$, the following identity holds:*

$$H_{nh}G(z, nh)S_{nh}H_h = H_{nh}G(z^n, h).$$

Proof For simplicity, the proof is given for $n = 2$. The proof for general n follows the same steps. Let η be a discrete-time signal:

$$\eta = \{\eta(0), \eta(1), \eta(2), ...\}$$

and define

$$\varphi = \{\varphi(0), \varphi(1), \varphi(2), ...\} = \{\eta(0), \eta(2), \eta(4), ...\},$$

hence $\varphi(k_s) = \eta(2k_s) = S_{2h}H_h\eta(k)$. Assume that $G(z, 2h) = a_0 + a_1z^{-1} + a_2z^{-2} + \cdots$. Then,

$$\begin{aligned} G(q, 2h)S_{2h}H_h\eta(k) &= G(q, 2h)\varphi(k_s) \\ &= a_0\varphi(k_s) + a_1\varphi(k_s - 1) + a_2\varphi(k_s - 2) + \cdots \end{aligned}$$

On the other hand

$$\begin{aligned} G(q^2, h)\eta(k) &= (a_0 + a_1q^{-2} + a_2q^{-4} + \cdots)\eta(k) \\ &= a_0\eta(k) + a_1\eta(k - 2) + a_2\eta(k - 4) + \cdots \end{aligned}$$

The former and the latter equations are evaluated every $2h$ and h seconds respectively, but they are equivalent at $t = 2kh$. Therefore $H_{2h}G(z, 2h)S_{2h}H_h = H_{2h}G(z^2, h)$.

□

5.2 Performance of sampled-data systems

To compare the performance of sampled-data systems with different controllers (e.g., single-rate with different sampling periods or multirate), the performance index should be defined in continuous-time. In this section, two well-known performance indices for single-rate sampled-data systems are defined and then a generalization to the multirate case is given. An appropriate performance index also has the property that if two systems (continuous-time, sampled-data, multirate, etc.) have the same input-output relation (i.e., for any input they generate the same output) they have the same performance. This is an intuitive property and essential for the theorems given later. All the performance indices used throughout this chapter satisfy this property.

5.2.1 $\mathcal{H}_\infty$ performance of sampled-data systems

In Section 2.5.1, the definition of $\mathcal{H}_\infty$ norm was generalized to sampled-systems. Here the same concept is used to define the $\mathcal{H}_\infty$ norm of sampled-data systems. Recall that for a continuous-time LTI system G, the $\mathcal{H}_\infty$ norm is defined as

$$\|G\|_\infty = \sup_{\|w\|_2 \le 1} \|Gw\|_2,$$

i.e., the $\mathcal{H}_\infty$ norm (also known as the $\mathcal{L}_2$ induced norm) is related to the maximum $\mathcal{L}_2$ norm of the output over all bounded inputs. For sampled-data systems, because of the sampling and hold operators which are time-varying, no transfer function can be defined in the normal sense. But the above definition is still valid. Thus, the $\mathcal{H}_\infty$ norm of a sampled-data system is defined as the $\mathcal{L}_2$ induced norm of the related operator. The $\mathcal{H}_\infty$ norm of $\mathcal{F}\big(G(s), K(z,h)\big)$ in Figure 5.1 is defined as

$$\|\mathcal{F}\big(G(s), K(z,h)\big)\|_\infty = \sup_{\|w\|_2 \le 1} \|\mathcal{F}\big(G(s), K(z,h)\big)\, w\|_2.$$

Similarly, for the multirate sampled-data system in Figure 5.2, the $\mathcal{H}_\infty$ norm of the closed-loop operator $\mathcal{F}\big(G(s), K(z,lh)\big)$ is then defined as

$$\|\mathcal{F}\big(G(s), K(z,lh)\big)\|_\infty = \sup_{\|w\|_2 \le 1} \|\mathcal{F}\big(G(s), K(z,lh)\big)\, w\|_2.$$

The $\mathcal{H}_\infty$ control problem is to find the admissible stabilizing controller that minimizes the $\mathcal{H}_\infty$ norm of the closed-loop system. Solution of the $\mathcal{H}_\infty$ control problem for sampled-data systems is well established in the literature [2, 9]. Let $K^*_\infty(z,h)$ be the optimal $\mathcal{H}_\infty$ discrete-time controller for single-rate sampled-data system in Figure 5.1. Therefore, for any admissible controller $K(z,h)$,

$$\|\mathcal{F}\big(G(s), K^*_\infty(z,h)\big)\|_\infty \le \|\mathcal{F}\big(G(s), K(z,h)\big)\|_\infty.$$

Solution of multirate $\mathcal{H}_\infty$ control problem is also known [10]. If $K^*_\infty(z,lh)$ denotes the optimal $\mathcal{H}_\infty$ controller for multirate sampled-data system in Figure 5.2, then for any admissible multirate controller $K(z,lh)$,

$$\|\mathcal{F}\big(G(s), K^*_\infty(z,lh)\big)\|_\infty \le \|\mathcal{F}\big(G(s), K(z,lh)\big)\|_\infty.$$

Similar to the $\mathcal{H}_\infty$ norm, the $\mathcal{L}_p$ induced norm of the sampled-data system in Figure 5.2 is defined as

$$\|\mathcal{F}\big(G(s),K(z,h)\big)\|_{\mathcal{L}_p}= \sup_{\|w\|_p\leq 1} \|\mathcal{F}\big(G(s),K(z,h)\big)\,w\|_p.$$

It is obvious that if for any input, two systems generate the same output, their $\mathcal{L}_p$ induced norms (including the $\mathcal{H}_\infty$ norm) are equal. Another important fact that is extensively used in this chapter states that: for any given LPTV controller, an LTI controller can be constructed to give better $\mathcal{L}_p$ induced norm of the closed-loop system [51]. An instant result is that the optimal LTI controller is better than any admissible LPTV controller in the $\mathcal{H}_\infty$ norm sense. So if $K(z,h,N)$ is an admissible LPTV controller then,

$$\|\mathcal{F}\big(G(s),K^*_\infty(z,h)\big)\|_\infty\leq \|\mathcal{F}\big(G(s),K(z,h,N)\big)\|_\infty.$$

5.2.2 $\mathcal{H}_2$ performance of sampled-data systems

In Section 2.5.2, the $\mathcal{H}_2$ norm of a sampled system was defined. Here the sam concept is generalized for single-rate and multirate sampled-data systems. Recall that for a continuous-time SISO LTI system G, the $\mathcal{H}_2$ norm is

$$\|G\|_2^2= \|G\delta(t)\|_2^2= \int_{-\infty}^{\infty} g(t)^2dt,$$

where $\delta(t)$ is the continuous-time unit impulse function. In other words, the $\mathcal{H}_2$ norm of G equals the $\mathcal{L}_2$ norm of its impulse response. In the multivariable case the $\mathcal{H}_2$ norm is

$$\|G\|_2^2= \sum_{i=1}^{n_w}\|G\delta(t)e_i\|_2^2,$$

where e_i, $i=1,\ldots,n_w$, are the standard basis vectors in $\mathbb{R}^{n_w}$ and n_w is the number of inputs of G. Thus, $\delta(t)e_i$ is an impulse applied to the i^{th} input channel.

To generalize the definition of $\mathcal{H}_2$ norm to sampled-data systems (Figure 5.1), notice that $\mathcal{F}\big(G(s),K(z,h)\big)$ is an h-periodic time-varying system. Therefore, the $\mathcal{H}_2$ norm of $\mathcal{F}\big(G(s),K(z,h)\big)$ is defined as the average norm of the outputs when impulses are applied in one sampling period to the input channels, i.e.,

$$\|\mathcal{F}\big(G(s),K(z,h)\big)\|_2^2= \frac{1}{h}\int_0^h \left(\sum_{i=1}^{n_w}\|\mathcal{F}\big(G(s),K(z,h)\big)\delta(t-\tau)e_i\|_2^2\right)d\tau.$$

If a N-periodic LPTV controller is used for the single-rate sampled-data system in Figure 5.1, the closed-loop system will be Nh-periodic and the averaging is over a period of Nh seconds. Therefore, the $\mathcal{H}_2$ norm of the closed-loop system with the LPTV controller $K(z,h,N)$ is

$$\|\mathcal{F}\big(G(s),K(z,h,N)\big)\|_2^2= \frac{1}{Nh}\int_0^{Nh}\left(\sum_{i=1}^{n_w}\|\mathcal{F}\big(G(s),K(z,h,N)\big)\delta(t-\tau)e_i\|_2^2\right)d\tau.$$

Similarly, for the multirate sampled-data system in Figure 5.2, the averaging is over a period of lh seconds and the $\mathcal{H}_2$ norm is defined as

$$\|\mathcal{F}\big(G(s),K(z,lh)\big)\|_2^2= \frac{1}{lh}\int_0^{lh}\left(\sum_{i=1}^{n_w}\|\mathcal{F}\big(G(s),K(z,lh)\big)\delta(t-\tau)e_i\|_2^2\right)d\tau.$$

The solution of $\mathcal{H}_2$ control problem (namely, finding the admissible stabilizing controller that minimizes the $\mathcal{H}_2$ norm of the closed-loop system) is known for sampled-data systems [3, 9, 39] and multirate systems [45, 46]. Let $K_2^*(z,h)$ and $K_2^*(z,lh)$ be the $\mathcal{H}_2$ optimal controllers for single-rate and multirate sampled-data systems respectively. Then for any admissible sampled-data controller $K(z,h)$ and for any admissible multirate controller $K(z,lh)$,

$$\|\mathcal{F}\big(G(s),K_2^*(z,h)\big)\|_2 \le \|\mathcal{F}\big(G(s),K(z,h)\big)\|_2.$$
$$\|\mathcal{F}\big(G(s),K_2^*(z,lh)\big)\|_2 \le \|\mathcal{F}\big(G(s),K(z,lh)\big)\|_2.$$

It is easy to verify that if two sampled-data systems (single-rate or multirate) generate equal outputs for the same input, their $\mathcal{H}_2$ performances are equal.

As mentioned before, for the $\mathcal{H}_\infty$ norm, the optimal LTI controller performs better than any admissible LPTV controller. In the rest of this section the proof of the same property for the $\mathcal{H}_2$ norm is given. Consider the single-rate sampled-data system in Figure 5.1. Let G have the following state-space model

$$G(s)=\left[\begin{array}{c|cc} A & B_1 & B_2 \\ \hline C_1 & 0 & D_{12} \\ C_2 & 0 & 0 \end{array}\right].$$

Assume that

(A1) (A,B_2) is stabilizable and (C_2,A) is detectable;

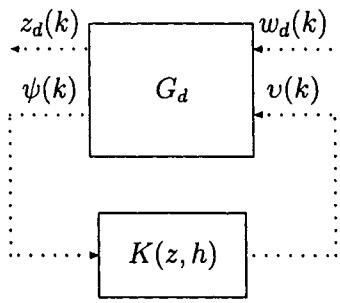

Figure 5.4: The associated discrete-time system.

(A2) the sampling period h is non-pathological with respect to G [9].

Now bring in an associated pure discrete-time feedback system (Figure 5.4) with the same controller $K(z,h)$ and generalized discrete-time transfer function $G_d(z,h)$, where

$$G_d(z,h) = \left[\begin{array}{c|cc} A_D & B_{1J} & B_{2D} \\ \hline C_{1d} & 0 & D_{12d} \\ C_2 & 0 & 0 \end{array}\right].$$

A_D, B_{1J}, B_{2D}, C_{1d} and D_{12d} are obtained from

$$A_D = e^{Ah},$$

$$B_{1J}B_{1J}^T = \int_0^h e^{A\tau}B_1B_1^Te^{A^T\tau}d\tau,$$

$$B_{2D} = \int_0^h e^{A\tau}d\tau B_2,$$

$$\left[\begin{array}{cc} C_{1d} & D_{12d} \end{array}\right]^T \left[\begin{array}{cc} C_{1d} & D_{12d} \end{array}\right] = \int_0^h e^{\underline{A}^T\tau}\left[\begin{array}{cc} C_1 & D_{12} \end{array}\right]^T \left[\begin{array}{cc} C_1 & D_{12} \end{array}\right] e^{\underline{A}\tau}d\tau,$$

with

$$\underline{A} = \left[\begin{array}{cc} A & B_2 \\ 0 & 0 \end{array}\right].$$

It is a well known result that under assumptions (A1)–(A2), for any LTI controller $K(z,h)$ [3, 9, 39],

$$\|\mathcal{F}\big(G(s),K(z,h)\big)\|_2^2 = \frac{1}{h}\,\|\mathcal{F}\big(G_d(z,h),K(z,h)\big)\|_2^2 + \frac{1}{h}\,L,$$

where $\mathcal{F}\big(G_d(z,h),K(z,h)\big)$ denotes the closed-loop transfer function of the associated discrete-time system in Figure 5.4 and

$$L = \text{trace}\left(C_1\int_0^h\int_0^{h-t} e^{A\tau}B_1B_1^Te^{A^T\tau}d\tau dt\,C_1^T\right).$$

The following theorem generalizes this result for LPTV controllers.

Theorem 5.1 *Under assumptions (A1)-(A2) and for any admissible LPTV controller $K(z,h,N)$,*

$$\|\mathcal{F}\big(G(s),K(z,h,N)\big)\|_2^2 = \frac{1}{h}\,\|\mathcal{F}\big(G_d(z,h),K(z,h,N)\big)\|_2^2 + \frac{1}{h}\,L.$$

Proof By the definition of the $\mathcal{H}_2$ norm

$$\begin{aligned}
&\|\mathcal{F}\big(G(s),K(z,h,N)\big)\|_2^2 \\
&\quad= \frac{1}{Nh}\int_0^{Nh}\left(\sum_{i=1}^{n_w}\|\mathcal{F}\big(G(s),K(z,h,N)\big)\delta(t-\tau)e_i\|_2^2\right)d\tau \\
&\quad= \frac{1}{N}\sum_{j=0}^{N-1}\left(\frac{1}{h}\int_{jh}^{(j+1)h}\left(\sum_{i=1}^{n_w}\|\mathcal{F}\big(G(s),K(z,h,N)\big)\delta(t-\tau)e_i\|_2^2\right)d\tau\right).
\end{aligned}$$

Following the same steps as in the proof for LTI controllers in [8],

$$\int_{jh}^{(j+1)h}\left(\sum_{i=1}^{n_w}\|\mathcal{F}\big(G(s),K(z,h,N)\big)\delta(t-\tau)e_i\|_2^2\right)d\tau = \sum_{i=1}^{n_w}\|\mathcal{F}\big(G_d(z,h),K(z,h,N)\big)\delta(k-j)e_i\|_2^2 + L.$$

Therefore

$$\begin{aligned}
&\mathcal{F}\big(G(s),K(z,h,N)\big) \\
&\quad= \frac{1}{N}\sum_{j=0}^{N-1}\left(\frac{1}{h}\sum_{i=1}^{n_w}\|\mathcal{F}\big(G_d(z,h),K(z,h,N)\big)\delta(k-j)e_i\|_2^2 + \frac{1}{h}\,L\right) \\
&\quad= \frac{1}{h}\left(\frac{1}{N}\sum_{j=0}^{N-1}\sum_{i=1}^{n_w}\|\mathcal{F}\big(G_d(z,h),K(z,h,N)\big)\delta(k-j)e_i\|_2^2\right) + \frac{1}{h}\,L \\
&\quad= \frac{1}{h}\,\|\mathcal{F}\big(G_d(z,h),K(z,h,N)\big)\|_2^2 + \frac{1}{h}\,L.
\end{aligned}$$

□

Theorem 5.2 *Under assumptions (A1)-(A2) and for any admissible LPTV controller $K(z,h,N)$,*

$$\|\mathcal{F}\big(G(s),K_2^*(z,h)\big)\|_2 \le \|\mathcal{F}\big(G(s),K(z,h,N)\big)\|_2.$$

Proof

$$\begin{aligned}\|\mathcal{F}\big(G(s), K_2^*(z,h)\big)\|_2^2 &= \frac{1}{h}\,\|\mathcal{F}\big(G_d(z,h), K_2^*(z,h)\big)\|_2^2 + \frac{1}{h}\,L \\ &\le \frac{1}{h}\,\|\mathcal{F}\big(G_d(z,h), K(z,h,N)\big)\|_2^2 + \frac{1}{h}\,L \\ &= \|\mathcal{F}\big(G(s), K(z,h,N)\big)\|_2^2.\end{aligned}$$

The inequality used here is based on the fact that in pure discrete-time systems, the optimal LTI controller performs better than any LPTV controller [52].

□

5.3 Performance comparison

In this section a comparison of the performance of sampled-data systems with different controllers (slow-rate, fast-rate and multirate) will be given. The performance measures used are $\mathcal{H}_2$ or $\mathcal{H}_\infty$ norm of the closed-loop system as well as any other $\mathcal{L}_p$ induced norm. Let $J(K(z,h),h)$, $J(K(z,h,N),h,N)$ and $J(K(z,lh),m_1h,\cdots,m_ph,n_1h,\cdots,n_rh)$ be the performances of single-rate sampled-data system (Figure 5.1), single-rate sampled-data system with LPTV controller, and multirate system (Figure 5.2) respectively. Also let $K^*(z,h)$ and $K^*(z,lh)$ be the optimal sampled-data and multirate controllers respectively and $J^*(h)$ and $J^*(m_1h,\cdots,m_ph,n_1h,\cdots,n_rh)$ their corresponding optimal performances. Hence,

$J^*(h) = J(K^*(z,h),h)$,

$J^*(m_1h,\cdots,m_ph,n_1h,\cdots,n_rh) = J(K^*(z,lh),m_1h,\cdots,m_ph,n_1h,\cdots,n_rh)$.

Throughout this section, it is assumed that for the related sampled-data problem an optimal controller exists.

5.3.1 Slow-rate vs. fast-rate performance

Here it is shown that the optimal performance of a sampled-data system with a fast-rate controller is better than the optimal performance with a slow-rate controller. This fact is not only theoretically important but also introduces the method that is used to prove the theorems. Note that the sampling period of the slow-rate controller is always an integer multiple of the sampling period of the fast-rate controller.

First the following lemma is proved:

Lemma 5.3 *In the standard sampled-data system in Figure 5.1, for any admissible slow-rate controller, there exists an admissible LPTV fast-rate controller with the same performance.*

Proof Assume that $K(z, Nh)$ is an admissible slow-rate controller. Using Lemmas 5.1 and 5.2 yields

$$\begin{aligned} H_{Nh}K(z,Nh)S_{Nh} &= H_{Nh}K(z,Nh)S_{Nh}H_hS_h \\ &= H_{Nh}K(z^N,h)S_h \\ &= H_hS_hH_{Nh}K(z^N,h)S_h \\ &= H_hL_N^{-1}\begin{bmatrix} I \\ \vdots \\ I \end{bmatrix} K(z^N,h)S_h. \end{aligned}$$

Now define the LPTV fast-rate controller

$$\hat{K}(z,h,N) = L_N^{-1}\begin{bmatrix} I \\ \vdots \\ I \end{bmatrix} K(z^N,h).$$

Based on the above result, for any input $w(t)$,

$$\left.\begin{aligned} u_{\rm SR}(t) &= H_{Nh}K(z,Nh)S_{Nh}\, y(t) \\ u_{\rm FR}(t) &= H_h\hat{K}(z,h,N)S_h\, y(t) \end{aligned}\right\} \quad \Longrightarrow \quad u_{\rm SR}(t) = u_{\rm FR}(t),$$

i.e., the slow-rate LTI controller $K(z, Nh)$ and the fast-rate LPTV controller $\hat{K}(z, h, N)$ generate the same control signal $u(t)$ for all time. This implies that $z_{\rm SR}(t) = z_{\rm FR}(t)$. Therefore, the closed-loop systems with the slow-rate controller $K(z, Nh)$ and the fast-rate controller $\hat{K}(z, h, N)$ are equivalent

$$\mathcal{F}\big(G(s), K(z,Nh)\big) \equiv \mathcal{F}\big(G(s), \hat{K}(z,h,N)\big)$$

and subsequently

$$J(\hat{K}(z,h,N),h,N) = J(K(z,Nh),Nh).$$

□

To understand the idea behind the proof of this lemma, notice that the slow-rate controller updates the control signal every kNh seconds. Therefore, if one can find a fast-rate controller that generates the same control signal

at $t = kNh$ and then maintains it for a period of Nh seconds (i.e., does not update the control signal at $t = kNh+h, \ldots,$ and $t = (k+1)Nh-h$), then the two systems are equivalent. That is the reason why the fast-rate controller has to be time-varying. Lemma 5.3 shows how to construct a satisfying fast-rate LPTV controller. For $n = 2$, the fast-rate controller is

$$\hat{K}(z,h,2) = \begin{cases} K(z^2,h) & k \text{ even}, \\ z^{-1}K(z^2,h) & k \text{ odd}. \end{cases}$$

Theorem 5.3 *For the standard sampled-data system in Figure 5.1 and for any* $N \in \mathbb{N}$,

$$J^*(h) \leq J^*(Nh).$$

Proof Assume that $K^*(z,Nh)$ is the optimal slow-rate controller. Using Lemma 5.3 there exist an LPTV fast-rate controller $\hat{K}(z,h,N)$ such that

$$J^*(Nh) = J(K^*(z,Nh),Nh) = J(\hat{K}(z,Nh),h,N).$$

Now, using the fact that the optimal LTI controller performs better than any LPTV controller (this is proved for the $\mathcal{L}_p$ induced norm in [51] and for the $\mathcal{H}_2$ norm in Theorem 5.2) yields

$$J^*(h) \leq J(\hat{K}(z,h,N),h,N) = J^*(Nh).$$

□

5.3.2 Multirate vs. single-rate performance

In this section, the main theorem is presented and the proof is given: the optimal performance of a system with a fast-rate controller is better than the optimal performance with a multirate controller; and the latter is better than the optimal performance with a slow-rate controller. At first two useful lemmas are given. Consider the multirate sampled-data control system in Figure 5.2 and the corresponding slow-rate and fast-rate systems.

Lemma 5.4 *For any admissible slow-rate controller* $K(z,lh)$ *there exists an admissible multirate controller* $\hat{K}(z,lh)$ *that yields the same performance*

$$J(K(z,lh),lh) = J(\hat{K}(z,lh),m_1h,\cdots,m_ph,n_1h,\cdots,n_rh).$$

Proof For simplicity, the proof is given for the dual-rate case (it is similar for general multirate systems). Consider the dual-rate sampled-data system in Figure 5.3 and let $K(z, mnh)$ be a slow-rate controller. The objective is to construct an admissible dual-rate controller $\hat{K}(z, mnh)$ that satisfies

$$J(K(z, mnh), mnh) = J(\hat{K}(z, mnh), mh, nh).$$

Using Lemma 5.1

$$\begin{aligned} H_{mnh}K(z, mnh)S_{mnh} &= H_{mnh}K(z, mnh)S_{mnh}H_{mh}S_{mh} \\ &= H_{mnh}K(z, mnh)\begin{bmatrix} I & 0 & \cdots & 0 \end{bmatrix}L_nS_{mh} \\ &= H_{nh}S_{nh}H_{mnh}K(z, mnh)\begin{bmatrix} I & 0 & \cdots & 0 \end{bmatrix}L_nS_{mh} \\ &= H_{nh}L_m^{-1}\begin{bmatrix} I \\ \vdots \\ I \end{bmatrix}K(z, mnh)\begin{bmatrix} I & 0 & \cdots & 0 \end{bmatrix}L_nS_{mh}. \end{aligned}$$

Now define the dual-rate controller

$$\hat{K}(z, mnh) = \begin{bmatrix} I \\ \vdots \\ I \end{bmatrix}K(z, mnh)\begin{bmatrix} I & 0 & \cdots & 0 \end{bmatrix}.$$

For any input $w(t)$,

$$\left.\begin{aligned} u_{\mathrm{SR}}(t) &= H_{mnh}K(z, mnh)S_{mnh}\, y(t) \\ u_{\mathrm{DR}}(t) &= H_{nh}L_m^{-1}\hat{K}(z, mnh)L_nS_{mh}\, y(t) \end{aligned}\right\} \quad \Longrightarrow \quad u_{\mathrm{SR}}(t) = u_{\mathrm{DR}}(t).$$

This means that the slow-rate controller $K(z, mnh)$ and the dual-rate controller $\hat{K}(z, mnh)$ generate the same control signal $u(t)$ for all time. Thus $z_{\mathrm{SR}}(t) = z_{\mathrm{DR}}(t)$. Therefore, the closed-loop systems with the slow-rate controller $K(z, mnh)$ and the dual-rate controller $\hat{K}(z, mnh)$ are equivalent

$$\mathcal{F}\big(G(s), K(z, mnh)\big) \equiv \mathcal{F}\big(G(s), \hat{K}(z, mnh)\big)$$

and thus they have the same performance

$$J(K(z, mnh), mnh) = J(\hat{K}(z, mnh), mh, nh).$$

□

The slow-rate controller $K(z, mnh)$ receives the information every mnh seconds and also updates the control signal every mnh seconds. On the other

hand, the dual-rate controller receives the information every nh seconds, but updates the control signal every mh seconds. So for a dual-rate controller to be equivalent to a given slow-rate controller it should: First, uses only the information that it receives at $t = kmnh$ and ignores the other information (those at $t = kmnh + nh, \ldots, t = (k+1)mnh - nh$), hence the term $[I \quad 0 \quad \cdots \quad 0]$. Second, maintains the control signal that is generated at $t = kmnh$ for a period of mnh seconds, hence the term $[I \quad \cdots \quad I]^T$. Lemma 5.4, illustrates the method of construction of the equivalent dual-rate controller. For $m = 3$, $n = 2$ and the slow-rate controller $K(z, 6h)$, the equivalent dual-rate controller is

$$\hat{K}(z,6h) = \begin{bmatrix} I \\ I \\ I \end{bmatrix} K(z,6h) \begin{bmatrix} I & 0 \end{bmatrix} = \begin{bmatrix} K(z,6h) & 0 \\ K(z,6h) & 0 \\ K(z,6h) & 0 \end{bmatrix}.$$

Lemma 5.5 *For any admissible multirate controller $K(z, lh)$ there exists an admissible LPTV fast-rate controller $\hat{K}(z, h, l)$ that yields the same performance*

$$J(K(z,lh), m_1 h, \cdots, m_p h, n_1 h, \cdots, n_r h) = J(\hat{K}(z,h,l), h, l).$$

Proof Again for simplicity, the proof is given for the dual-rate case with the assumption that $n = 1$. In the dual-rate system in Figure 5.3, consider the dual-rate controller $K(z, mh)$. The goal is to construct an admissible LPTV fast-rate controller $\hat{K}(z, h, m)$ such that

$$J(K(z,mh), mh, h) = J(\hat{K}(z,h,m), h, m).$$

Using Lemmas 5.1 and 5.2 and the fact that $S_{mh}H_{mh} = I$ yield

$$\begin{aligned} H_h L_m^{-1} K(z,mh) S_{mh} &= H_h L_m^{-1} K(z,mh) S_{mh} H_h S_h \\ &= H_h L_m^{-1} S_{mh} H_{mh} K(z,mh) S_{mh} H_h S_h \\ &= H_h L_m^{-1} S_{mh} H_{mh} K(z^m, h) S_h \\ &= H_h L_m^{-1} K(z^m, h) S_h. \end{aligned}$$

Now define the LPTV fast-rate controller

$$\hat{K}(z,h,m) = L_m^{-1} K(z^m, h).$$

For any input $w(t)$,

$$\left.\begin{aligned} u_{\mathrm{DR}}(t) &= H_h L_m^{-1} K(z,mh) S_{mh}\, y(t) \\ u_{\mathrm{FR}}(t) &= H_h \hat{K}(z,h,m) S_h\, y(t) \end{aligned}\right\} \quad \Longrightarrow \quad u_{\mathrm{DR}}(t) = u_{\mathrm{FR}}(t).$$

In other words, the control signals generated by the dual-rate LTI controller $K(z, mh)$ and the LPTV fast-rate controller $\hat{K}(z, h, m)$ are equal at all time. Which in turn implies that $z_{\mathrm{DR}}(t) = z_{\mathrm{FR}}(t)$. Therefore, the two closed-loop systems are equivalent

$$\mathcal{F}\big(G(s), K(z, mh)\big) \equiv \mathcal{F}\big(G(s), \hat{K}(z, h, m)\big)$$

and thus they have the same performance

$$J(K(z, mh), mh, h) = J(\hat{K}(z, h, m), h, m).$$

□

For $m = 3$ and $n = 2$ assume that $K(z, 6h)$ is an admissible dual-rate controller, i.e.,

$$\underline{v} = K(z, 6h)\,\underline{\psi} = \begin{bmatrix} K_1(z, 6h) & K_2(z, 6h) \\ K_3(z, 6h) & K_4(z, 6h) \\ K_5(z, 6h) & K_6(z, 6h) \end{bmatrix} \underline{\psi},$$

where

$$\underline{v} = \left\{ \begin{bmatrix} v(0) \\ v(2h) \\ v(4h) \end{bmatrix}, \begin{bmatrix} v(6h) \\ v(8h) \\ v(10h) \end{bmatrix}, \cdots \right\},$$
$$\underline{\psi} = \left\{ \begin{bmatrix} \psi(0) \\ \psi(3h) \end{bmatrix}, \begin{bmatrix} \psi(6h) \\ \psi(9h) \end{bmatrix}, \cdots \right\}.$$

Then the equivalent LPTV fast-rate controller is

$$K_{\mathrm{FR}}(z, h, 6) = \begin{cases} K_1(z^6, h) + z^3 K_2(z^6, h) & k = 6i, \\ z^{-1}(K_1(z^6, h) + z^3 K_2(z^6, h)) & k = 6i + 1, \\ z^{-2}(K_3(z^6, h) + z^3 K_4(z^6, h)) & k = 6i + 2, \\ z^{-3}(K_3(z^6, h) + z^3 K_4(z^6, h)) & k = 6i + 3, \\ z^{-4}(K_5(z^6, h) + z^3 K_6(z^6, h)) & k = 6i + 4, \\ z^{-5}(K_5(z^6, h) + z^3 K_6(z^6, h)) & k = 6i + 5. \end{cases}$$

Now the main theorem that compares the performances of multirate, slow-rate and fast-rate controls can be stated:

Theorem 5.4 *For the multirate sampled-data system in Figure 5.2, the following inequalities hold:*

$$J^*(h) \leq J^*(m_1 h, \cdots, m_p h, n_1 h, \cdots, n_r h) \leq J^*(lh).$$

Proof

Part 1: $J^*(m_1h, \cdots, m_ph, n_1h, \cdots, n_rh) \leq J^*(lh)$.

Assume that $K^*(z, lh)$ is the optimal slow-rate controller. By Lemma 5.4 there exists a multirate controller $\hat{K}(z, lh)$ such that

$$\begin{aligned} J^*(lh) &= J(K^*(z, lh), lh) \\ &= J(\hat{K}(z, lh), m_1h, \cdots, m_ph, n_1h, \cdots, n_rh). \end{aligned}$$

Since the optimal multirate controller is better than any admissible multirate controller it follows that

$$\begin{aligned} J^*(lh) &= J(\hat{K}(z, lh), m_1h, \cdots, m_ph, n_1h, \cdots, n_rh) \\ &\geq J^*(m_1h, \cdots, m_ph, n_1h, \cdots, n_rh). \end{aligned}$$

Part 2: $J^*(h) \leq J^*(m_1h, \cdots, m_ph, n_1h, \cdots, n_rh)$

Assume that $C^*(z, lh)$ is the optimal multirate controller, and $\hat{C}(z, h, l)$ is the corresponding LPTV fast-rate controller from Lemma 5.5. Thus,

$$\begin{aligned} J^*(m_1h, \cdots, m_ph, n_1h, \cdots, n_rh) &= J(C^*(z, lh), m_1h, \cdots, m_ph, n_1h, \cdots, n_rh) \\ &= J(\hat{C}(z, h, l), h, l). \end{aligned}$$

Using the fact that the optimal LTI controller performs better than any LPTV controller

$$J^*(m_1h, \cdots, m_ph, n_1h, \cdots, n_rh) = J(\hat{C}(z, h, l), h, l) \geq J^*(h).$$

□

5.4 Conclusions and remarks

In this section it was theoretically proved that the optimal performance of a system controlled by a multirate controller is better than the optimal performance achieved by a slow-rate controller, and worse than the optimal performance achieved by a fast-rate controller. To prove this, it was shown that for any admissible slow-rate (alternatively multirate) controller, one can find a multirate (alternatively LPTV fast-rate) controller with the same performance.

The performance measures used here are the $\mathcal{H}_\infty$ and $\mathcal{H}_2$ norms of the closed-loop system. The proofs are based on the fact that for these performance measures, the optimal LTI controller is better than any LPTV controller. In other words, the optimal LTI controller is the optimal controller over the set of LTI and LPTV controllers. As a matter of fact, the results given in this chapter hold true for any performance index that satisfies this property (optimal LTI controller is better than any LPTV controller), e.g., $\mathcal{L}_p$ induced norm of closed-loop system and LQR performance.

Throughout this chapter no regularity assumption is made on the matrices defining the state space form of G or on the sampling period. The only assumption made is the existence of the optimal controller.

Chapter 6

Fault Detection in Sampled-data Systems: Revisited

6.1 Introduction

As mentioned before, among the most important properties of an FDI system is that, it has to be sensitive with respect to faults in order to detect incipient faults, but robust with respect to unknown inputs, such as noise and disturbance, in order to avoid false alarms. This objective is usually achieved by defining a performance index and optimizing it. In Chapter 3, it was shown how to define different performance indices for a residual generator in sampled-data systems. A method was also developed to optimize those performance indices by converting the sampled-data problem to a discrete-time one with the same performance. Intuitively one expects that the performance will be improved by increasing the sampling frequency (a special case of this conjecture was proved in Theorem 5.3 for standard sampled-data control problem). The reason is that by faster sampling more information can be provided to the FDI or control algorithm. In this chapter, it is shown that this property is not true for the performance indices defined in Chapter 3 for sampled-data systems (e.g., in (3.18)).

In Chapter 4, two well known methods of FDI design (parity space and $\mathcal{H}_\infty$ optimization) were generalized to multirate sampled-data systems. Two

The materials of this chapter has been submitted for publication in:

I. Izadi, Q. Zhao and T. Chen, "Analysis of performance criteria in sampled-data fault detection", submitted to *Systems & Control Letters*, February 2006.

performance indices, similar to the ones used in sampled-data FDI design, were defined and optimized. Recall that to study the performance of a multirate system, the following single-rate systems are defined:

- slow single-rate or simply slow-rate system whose sampling period is the least common multiple of all the sampling periods of the multirate system;
- fast single-rate or simply fast-rate system whose sampling period is the greatest common divisor of all the sampling periods of the multirate system.

Another intuitive conjecture is that the slow-rate system with a slow-rate residual generator would not necessarily achieve the level of performance that can be achieved in the multirate systems with a multirate residual generator. The reason is that the slow-rate residual generator does not have access to all the information that is available to the multirate residual generator. On the other hand, it is expected that a fast-rate residual generator designed for the fast-rate system can yield better performance than one designed for the multirate system. Again the reason is the excess information available from the fast-rate system. However, it will be shown that these two properties do not hold for most of the performance indices defined for residual generator design.

Nonetheless, it was shown in Chapter 5 that the aforementioned properties are in fact true for the performance indices used in controller design, i.e., the $\mathcal{H}_\infty$ and $\mathcal{H}_2$ norm of the closed-loop system in the standard framework (Theorem 5.4). In order to take advantage of this, the sampled-data FDI problem is converted to a standard sampled-data control problem. This allows us to use the $\mathcal{H}_\infty$ and $\mathcal{H}_2$ norms of the closed-loop system as measures of performance of the FDI and hopefully achieve the properties that were missing in the conventional sampled-data FDI. The idea of using the standard control problem to design an FDI system is not new and has been introduced in the literature (e.g., see [7] and the references therein). In this chapter however, the extension to the sampled-data and multirate cases is developed.

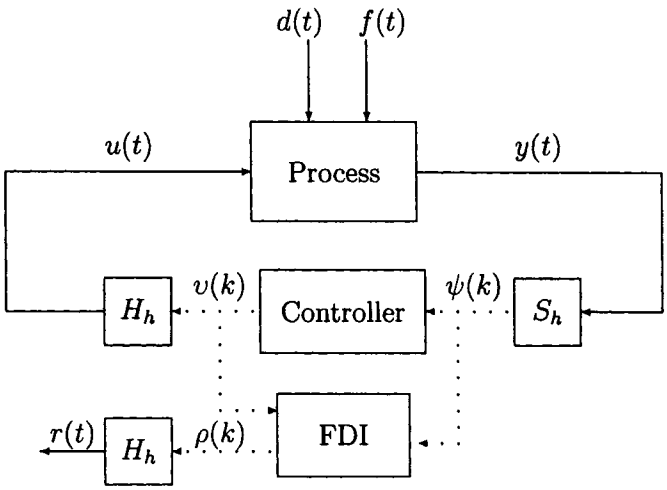

Figure 6.1: FDI in a sampled-data scheme

6.1.1 System description

Consider the sampled-data system in Figure 6.1. As usual, the continuous-time process has the following input-output description

$$y(t) = G_u u(t) + G_d d(t) + G_f f(t), \tag{6.1}$$

where $y(t) \in \mathbb{R}^m$ is the vector of plant outputs, $u(t) \in \mathbb{R}^{n_u}$ the vector of control signals, $d(t) \in \mathbb{R}^{n_d}$ the vector of unknown inputs or disturbances and $f(t) \in \mathbb{R}^{n_f}$ the vector of faults to be detected. G_u, G_d and G_f are linear time-invariant strictly proper systems of appropriate dimensions. In this chapter, for simplicity it is assumed that G_u is stable.

The output vector is sampled and discretized using an A/D converter modelled by

$$\psi(k) = y(kh), \tag{6.2}$$

where h is the sampling period. The control signal is generated by a computer and sent to the actuator using a (zero-order hold) D/A converter modelled by

$$u(t) = v(k), \quad kh \leq t < (k+1)h. \tag{6.3}$$

Hence, $\psi(k) = S_h y(t)$ and $u(t) = H_h v(k)$.

6.1.2 Residual generation

In the sampled-data scheme, the residual generator uses discrete-time process input $v(k)$ and output $\psi(k)$ to generate a discrete-time residual $\rho(k)$. As seen in Chapter 3 (equation (3.16)), by applying the factorization approach, the general form of residual generator for the sampled-data system described above is

$$\rho(k) = R\big(\psi(k) - G_{uD}v(k)\big), \tag{6.4}$$

where $R(z) \in \mathcal{RH}_\infty$ is a designable post-filter and $G_{uD}(z)$ is the step invariant transformation of $G_u(s)$. Note that since $G_u(s)$ (and subsequently $G_{uD}(z)$) is stable, the coprime factorization of $G_{uD}(z)$ would be $(I, G_{uD}(z))$. Substituting $\psi(k) = S_h y(t)$, $u(t) = H_h v(k)$ and the system model (6.1) in (6.4), the dynamics of the discrete-time residual with respect to continuous-time signals $d(t)$ and $f(t)$ is

$$\rho(k) = RS_hG_d d(t) + RS_hG_f f(t).$$

RS_hG_d and RS_hG_f are two operators that map continuous-time signals to discrete-time signals. Assuming that perfect disturbance decoupling is not possible (which is almost always the case), the goal is set to make RS_hG_d as small as possible (in some sense) while keeping RS_hG_f reasonably large. This is done by designing $R(z)$ to optimize a certain performance index.

In this chapter the objective is to compare the performance of different sampled-data FDI designs (e.g., single-rate with different sampling periods or multirate). Similar to the control problem, for a fair comparison, the performance index is preferred to be defined in continuous time. So let $r(t)$ be the continuous-time residual obtained by holding the discrete-time residual (Figure 6.1)

$$r(t) = H_h\rho(k).$$

It is easy to check that $r(t) \in \mathcal{L}_2(\mathbb{R})$ if and only if $\rho(k) \in \ell_2(\mathbb{Z})$. Moreover

$$\|r\|_2^2 = h\,\|\rho\|_2^2. \tag{6.5}$$

The dynamics of the continuous-time residual is then given by

$$r(t) = H_hRS_hG_d d(t) + H_hRS_hG_f f(t). \tag{6.6}$$

Let Γ_{rd} and Γ_{rf} denote the operators from continuous-time signals $d(t)$ and $f(t)$ to $r(t)$ respectively

$$\Gamma_{rd} = H_h R S_h G_d,$$
$$\Gamma_{rf} = H_h R S_h G_f.$$

The design objective in terms of the new operators is to make $\|\Gamma_{rd}\|$ as small as possible while keeping $\|\Gamma_{rf}\|$ large, for some definition of operator norm. The $\mathcal{H}_\infty$ and $\mathcal{H}_2$ norms of the operators are defined in Section 3.3.1 and Section 3.3.2 respectively. As a matter of fact, using the relationship between the norms of $\rho(k)$ and $r(t)$ in (6.5), it is easy to see that

$$\begin{aligned}
\|\Gamma_{rd}\|_\infty &= \sup_{\|d\|_2 \le 1} \|\Gamma_{rd} d\|_2 \\
&= \sup_{\|d\|_2 \le 1} \|H_h R S_h G_d d\|_2 \\
&= \sqrt{h} \sup_{\|d\|_2 \le 1} \|R S_h G_d d\|_2 \\
&= \sqrt{h}\, \|R S_h G_d\|_\infty
\end{aligned}$$

and

$$\begin{aligned}
\|\Gamma_{rd}\|_2 &= \left(\sum_{i=1}^{n_d} \left(\int_0^h \|\Gamma_{rd} \delta(t-\tau) e_i\|_2^2 \, d\tau \right) \right)^{1/2} \\
&= \left(\sum_{i=1}^{n_d} \left(\int_0^h \|H_h R S_h G_d \delta(t-\tau) e_i\|_2^2 \, d\tau \right) \right)^{1/2} \\
&= \sqrt{h} \left(\sum_{i=1}^{n_d} \left(\int_0^h \|R S_h G_d \delta(t-\tau) e_i\|_2^2 \, d\tau \right) \right)^{1/2} \\
&= \sqrt{h}\, \|R S_h G_d\|_2.
\end{aligned}$$

As usual, the following performance indices are defined

$$J_{\infty/\infty} = \frac{\|\Gamma_{rd}\|_\infty}{\|\Gamma_{rf}\|_\infty} = \frac{\|R S_h G_d\|_\infty}{\|R S_h G_d\|_\infty}, \tag{6.7}$$

$$J_{2/2} = \frac{\|\Gamma_{rd}\|_2}{\|\Gamma_{rf}\|_2} = \frac{\|R S_h G_d\|_2}{\|R S_h G_d\|_2}. \tag{6.8}$$

In Chapter 3, these performance indices were optimized by using the norm invariant transformation and equivalent discrete-time model.

A similar performance index can also been defined based on the parity space approach (Section 2.4)

$$J_{\text{ps}} = \frac{v_s H_{d,s} H_{d,s}^T v_s^T}{v_s H_{f,s} H_{f,s}^T v_s^T}. \tag{6.9}$$

where the parity vector v_s belongs to the parity space P_s. $H_{d,s}$, $H_{f,s}$ and P_s are defined in Section 2.4, for the equivalent discrete-time system.

Later in this chapter, it is shown through some examples that the above performance indices are not appropriate choices for comparison and analysis of performance in sampled-data FDI design. This study, however, focuses on the most common performance indices, i.e., (6.7) and (6.9). Let $J^*_{\infty/\infty}(h)$ and $J^*_{\text{ps}}(h)$ denote the optimal values of the performance indices in (6.7) and (6.9) which are functions of the sampling period h. As shown in Chapter 3

$$J^*_{\infty/\infty}(h) = \frac{1}{\|G_{do}^{-1}(z) G_{fJ}(z)\|_\infty},$$

where $G_{dJ}(z)$ and $G_{fJ}(z)$ are the norm invariant transformations of $G_d(s)$ and $G_f(s)$ respectively, and $G_{do}(z)$ is the co-outer of $G_{dJ}(z)$. Also for the parity space performance,

$$J^*_{\text{ps}}(h) = \lambda_{\min},$$

where $\lambda_{\min}$ is the minimal generalized eigenvalue of the pair $(N_B H_{d,s} H_{d,s}^T N_B^T$, $N_B H_{f,s} H_{f,s}^T N_B^T)$ and N_B is the basis vector for parity space P_s.

6.1.3 Residual generation in multirate systems

A multirate sampled-data system is illustrated in Figure 6.2. The input-output description of the continuous-time process is given in (6.1). In the case of no uncertainty in the system model, the control signal and its sampling rate have no effect on the residual. So without loss of generality, it is assumed that the inputs are available at the fast rate; $u(t) = H_h v(k)$. The output channels, though, are sampled at different rates. The first output $y_1(t)$ is sampled every $n_1 h$ seconds, the second output $y_2(t)$ is sampled every $n_2 h$ seconds and so on.

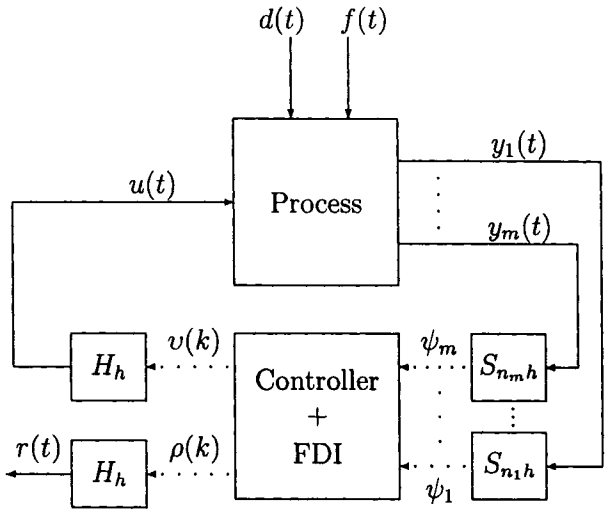

Figure 6.2: FDI in multirate sampled-data scheme

Therefore,

$$\begin{aligned} \psi_1(k_{n_1}) &= S_{n_1 h} y_1(t), \\ \psi_2(k_{n_2}) &= S_{n_2 h} y_2(t), \\ &\vdots \\ \psi_m(k_{n_m}) &= S_{n_m h} y_m(t). \end{aligned} \tag{6.10}$$

Note that since the discrete-time signals ψ_i, $i = 1, \cdots, m$, are available at different time instants, they have different time indices k_{n_i}, $i = 1, \cdots, m$.

Assume that the greatest common divisor and the least common multiple of $(n_1, \cdots, n_m)$ are 1 and N respectively. Then the sampling periods of the corresponding fast-rate and slow-rate systems are h and Nh respectively. The residual generator uses the discrete-time signals υ and ψ_i, $i = 1, \cdots, m$, to generate the residual. In order to pass the fault information as often as possible, the residual is generated at the fast rate, i.e., every h seconds. An $\mathcal{H}_\infty$ performance index similar to (6.7) can now be defined for the multirate system in Figure 6.2 (as in Section 4.4). A parity space performance index similar to (6.9) can also be defined (as in Section 4.3).

6.2 Performance analysis

It is generally accepted that the optimal performance of sampled-data control systems will be improved by faster sampling. In other words decreasing the sampling period will reduce the optimal performance in control problem. A special case of this (when the sampling period of the slow sampled system is an integer multiple of the sampling period of the fast sampled system) was proved in Theorem 5.3. Similar results are expected in the sampled-data FDI design. However, this is not the case with the performance indices in (6.7) and (6.9). The following examples show that decreasing the sampling period actually impairs the optimal performance.

Example 1. Consider the continuous-time system given in (6.1) with

$$G_u(s) = 0, \quad G_d(s) = \frac{4}{(s+2)(s+6)}, \quad G_f(s) = \frac{2}{(s+1)(s+27)}.$$

For $h = 1$ sec, $J^*_{\infty/\infty}(1) = 0.96$ and for $h = 2$ sec, $J^*_{\infty/\infty}(2) = 0.57$.

Example 2. Consider the continuous-time system given in (6.1) with

$$\left[\begin{array}{ccc} G_u(s) & G_d(s) & G_f(s) \end{array}\right] = \left[\begin{array}{cc|ccc} -2 & 8 & 0 & 0.1 & 0 \\ 0 & -20 & 0 & 1 & 1 \\ \hline 1 & 0 & 0 & 0 & 0 \\ 0 & 1 & 0 & 0 & 0 \end{array}\right].$$

For $h = 1$ sec, $J^*_{\text{ps}}(1) = 4.57$ and for $h = 2$ sec, $J^*_{\text{ps}}(2) = 1.34$.

Moreover, it was proved in Theorem 5.4 that the optimal performance of a system with a fast-rate controller is better than the optimal performance with a multirate controller. And the latter is better than the optimal performance with a slow-rate controller. One intuitively expects that this is also true for the multirate FDI problem. But again this is not the case with the performance indices in (6.7) and (6.9). Examples show that multirate design can sometimes work better than both fast-rate and slow-rate design, and sometimes work worse than both of them. Similar examples (but of higher order/dimension) can be constructed for the $\mathcal{H}_2$ performance index in (6.8). Therefore, it seems that the aforementioned performance indices for FDI design are not appropriate at least for comparison of different design techniques.

Now it is desirable to choose a performance index for the sampled-data FDI design so that:

- the optimal performance of a fast-rate sampled-data residual generator is better than the optimal performance of a slow-rate residual generator;
- the optimal performance of a multirate residual generator is better than that of a slow-rate residual generator and worse than that of a fast-rate residual generator.

The above properties hold for the performance indices defined for the standard sampled-data control problem ($\mathcal{H}_\infty$ and $\mathcal{H}_2$ norm of the closed-loop system) in Figure 6.3. Here G is a continuous-time linear time-invariant (LTI) plant, $w(t)$ the exogenous input, $z(t)$ the controlled output, $y(t)$ the measured output of the plant, $u(t)$ the control signal and $K(z)$ the discrete-time LTI controller. Partition G according to its inputs and outputs as

$$G = \begin{bmatrix} G_{11} & G_{12} \\ G_{21} & G_{22} \end{bmatrix}.$$

Let $\mathcal{F}\big(G(s), K(z)\big)$ denote the closed-loop system from $w(t)$ to $z(t)$, then as shown before

$$\mathcal{F}\big(G(s), K(z)\big) = G_{11}(s) + G_{12}(s)H_h K(z) S_h \Big(I - G_{22}(s)H_h K(z) S_h\Big)^{-1} G_{21}(s). \quad (6.11)$$

If the sampled-data FDI problem can be converted to a standard sampled-data control problem, the control performance indices can be readily used as appropriate choices of FDI performance index.

6.3 FDI design as a standard control problem

For the residual generator in (6.6), the goal is to make Γ_{rd} small while keeping Γ_{rf} large in some sense. As an alternative, the latter can be replaced by a new objective which is making Γ_{rf} as close to I as possible. If achieved, this means $H_h\rho(k) = r(t) \simeq f(t)$, which guarantees fault estimation as well as fault detection. More importantly, the alternative problem can be converted to the standard control problem of Figure 6.3. Therefore the residual generation

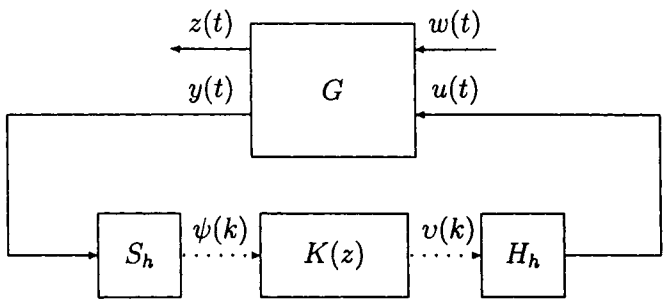

Figure 6.3: The standard sampled-data system.

problem is redefined as designing $R(z) \in \mathcal{RH}_\infty$ to minimize $\|\Gamma_{rd}\|$ and $\|\Gamma_{rf} - I\|$ for some definition of norm. Or in a more conservative form, the two goals can be combined together as minimizing

$$J = \|\begin{bmatrix} \Gamma_{rf} - I & \Gamma_{rd} \end{bmatrix}\| = \|\begin{bmatrix} H_h R(z) S_h G_f(s) - I & H_h R(z) S_h G_d(s) \end{bmatrix}\|. \tag{6.12}$$

Assume that the state space representation of $G_f(s)$ and $G_d(s)$ are given as

$$\begin{bmatrix} G_f(s) & G_d(s) \end{bmatrix} = \left[\begin{array}{c|cc} A & E_f & E_d \\ \hline C & 0 & 0 \end{array}\right].$$

where A, E_f, E_d and C are real matrices of appropriate dimensions. After some calculations, the problem can be reformulated in the standard form as in Figure 6.4, where

$$G(s) = \begin{bmatrix} [-I & 0] & I \\ [G_f(s) & G_d(s)] & 0 \end{bmatrix} = \left[\begin{array}{c|cc} A & [E_f & E_d] & 0 \\ \hline 0 & [-I & 0] & I \\ C & [0 & 0] & 0 \end{array}\right], \tag{6.13}$$

Let $\mathcal{F}\big(G(s), R(z)\big)$ be the closed-loop operator from $w(t)$ to $e(t)$ in Figure 6.4. Then using (6.11) and the partition of G given in (6.13) it follows that

$$\mathcal{F}\big(G(s), R(z)\big) = \begin{bmatrix} H_h R(z) S_h G_f(s) - I & H_h R(z) S_h G_d(s) \end{bmatrix}$$

and therefore

$$J = \|\mathcal{F}\big(G(s), R(z)\big)\|.$$

The common $\mathcal{H}_2$ or $\mathcal{H}_\infty$ norms might be used here. In the $\mathcal{H}_2$ case, since $\mathcal{F}\big(G(s), R(z)\big)$ is not strictly proper (in (6.13), notice that $D_{11} = [-I \quad 0] \neq 0$),

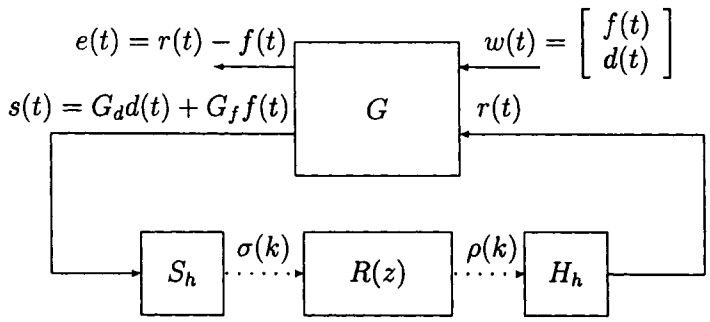

Figure 6.4: The standard sampled-data FDI problem.

$\|\mathcal{F}(G(s), R(z))\|_2$ is not finite. Therefore the problem is not regular for the $\mathcal{H}_2$ norm.

For the $\mathcal{H}_\infty$ norm, because $D_{21} = [0 \quad 0]$ does not have full row rank, the problem is also not regular. However, it can be regularized with minor modifications (e.g., by replacing D_{21} with $= [\epsilon I \quad \epsilon I]$, where ϵ is a small number). Nevertheless, for the $\mathcal{H}_\infty$ norm, the optimal solution is zero, i.e., $R^*(z) = 0$. The reason is that due to $D_{G_f} = 0$ and $D_{G_d} = 0$,

$$\| \begin{bmatrix} H_h R(z) S_h G_f(s) - I & H_h R(z) S_h G_d(s) \end{bmatrix} \|_\infty$$
$$\geq \sigma_{\max} \begin{bmatrix} D_R D_{G_f} - I & D_R D_{G_d} \end{bmatrix} = \sigma_{\max}[-I \quad 0] = 1.$$

where D_R, D_{G_f} and D_{G_d} are direct feed-through terms (D-terms in a realization) of $R(z)$, $G_f(s)$ and $G_d(s)$ respectively and $\sigma_{\max}(\cdot)$ denotes the maximum singular value. Note that the assumption of strictly properness of $G_f(s)$ and $G_d(s)$ is required for boundedness of the operators. So for the $\mathcal{H}_\infty$ norm, the lower limit of the optimal performance is 1. And this lower limit can be achieved when $R(z) = 0$, which means that $R^*(z) = 0$ is the optimal solution of the $\mathcal{H}_\infty$ problem.

To use the $\mathcal{H}_\infty$ and $\mathcal{H}_2$ norms effectively, the performance index has to be modified. Different modifications may be proposed here:

1. In one approach, instead of using $r(t) \simeq f(t)$, the objective is set as $r(t) \simeq Tf(t)$, for some strictly proper $T(s) \in \mathcal{RH}_\infty$, with the following state space representation

$$T(s) = \left[\begin{array}{c|c} A_T & B_T \\ \hline C_T & 0 \end{array}\right].$$

In that case

$$G_T(s) = \left[\begin{array}{cc|c} [-T(s) & 0] & I \\ [G_f(s) & G_d(s)] & 0 \end{array}\right]$$
$$= \left[\begin{array}{cc|cc|c} A_T & 0 & [-B_T & 0] & 0 \\ 0 & A & [E_f & E_d] & 0 \\ \hline C_T & 0 & [0 & 0] & I \\ 0 & C & [0 & 0] & 0 \end{array}\right],$$

and the performance index is

$$\begin{aligned} J_T &= \|\mathcal{F}(G_T(s), R(z))\| \\ &= \|[\ H_h R(z) S_h G_f(s) - T(s) \quad H_h R(z) S_h G_d(s)\ ]\|. \end{aligned} \tag{6.14}$$

2. Alternatively, a weighted version of the performance index in (6.12) might be used, i.e.,

$$\begin{aligned} J_W &= \|\mathcal{F}(G_W(s), R(z))\| \\ &= \|[\ W(s)(H_h R(z) S_h G_f(s) - I) \quad W(s) H_h R(z) S_h G_d(s)\ ]\|, \end{aligned} \tag{6.15}$$

where $W(s) \in \mathcal{RH}_\infty$ is a strictly proper weighting function with the following state space representation

$$W(s) = \left[\begin{array}{c|c} A_W & B_W \\ \hline C_W & 0 \end{array}\right],$$

and

$$G_W(s) = \left[\begin{array}{cc|c} [-W(s) & 0] & W(s) \\ [G_f(s) & G_d(s)] & 0 \end{array}\right]$$
$$= \left[\begin{array}{cc|cc|c} A_W & 0 & [-B_W & 0] & B_W \\ 0 & A & [E_f & E_d] & 0 \\ \hline C_W & 0 & [0 & 0] & 0 \\ 0 & C & [0 & 0] & 0 \end{array}\right]. \tag{6.16}$$

This is equivalent to making $Wr(t) \simeq Wf(t)$.

The good point is that, since in both $G_T(s)$ and $G_W(s)$, $D_{11} = 0$, the $\mathcal{H}_2$ norm of the closed-loop operator is finite and the problem is regular. Known methods of the sampled-data $\mathcal{H}_2$ design can be used here to convert the sampled-data problem to an equivalent pure discrete-time one [3, 9, 39]. As an example, the solution of the $\mathcal{H}_2$ problem for generalized plant $G_W(s)$ and the performance index in (6.15) is stated in the following lemma

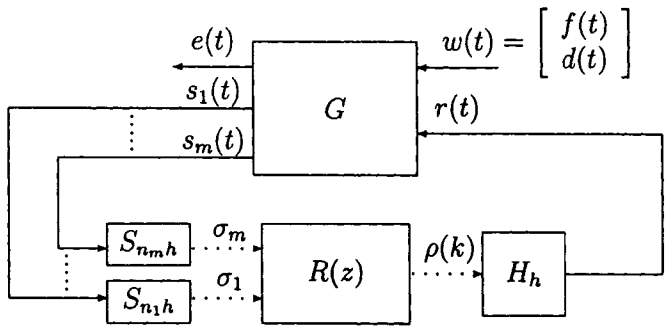

Figure 6.5: The general multirate sampled-data FDI problem.

Lemma 6.1 *Consider the generalized plant $G_W(s)$ in (6.16) and the performance index in (6.15). The following equality holds*

$$\|\mathcal{F}(G_W(s), R(z))\|_2 = \|\mathcal{F}(G_{Wd}(z), R(z))\|_2.$$

G_{Wd} is the equivalent discrete-time plant given by

$$G_d(z) = \left[\begin{array}{cc|cc} A_{WD} & 0 & B_{1,dd} & B_{WD} \\ 0 & A_D & & 0 \\ \hline C_{WJ} & 0 & 0 & 0 \\ 0 & C & 0 & 0 \end{array}\right],$$

where A_D, A_{WD}, B_{WD}, C_{WJ} and $B_{1,dd}$ are defined as

$$\begin{aligned} A_D &= e^{Ah}, \\ A_{WD} &= e^{A_W h}, \\ B_{WD} &= \int_0^h e^{A_W \tau} d\tau B_W, \\ C_{WJ}^T C_{WJ} &= \int_0^h e^{A_W^T \tau} C_W^T C_W e^{A_W \tau} d\tau, \\ B_{1,dd} B_{1,dd}^T &= \int_0^h \left[\begin{array}{cc} e^{A_W \tau} B_W B_W^T e^{A_W^T \tau} & -e^{A_W \tau} B_W E_f^T e^{A^T \tau} \\ -e^{A\tau} E_f B_W^T e^{A_W^T \tau} & e^{A\tau}(E_f E_f^T + E_d E_d^T) e^{A^T \tau} \end{array}\right] d\tau. \end{aligned}$$

□

The $\mathcal{H}_\infty$ norms of the performance indices in (6.14) and (6.15) are also well defined. To optimize the two performance indices, the well-known methods of sampled-data $\mathcal{H}_\infty$ optimization can be readily used [2, 9].

In the multirate case, the approach is quite similar. The block diagram of the multirate FDI problem in the standard form is illustrated in Figure 6.5.

Notice that, since the residual is generated at the fast rate, there is only one hold operator with sampling period h. This makes the multirate FDI problem fairly simpler than the general standard multirate control problem. The same performance indices in (6.14) and (6.15) are still valid with the appropriate definitions of $\mathcal{H}_\infty$ and $\mathcal{H}_2$ norms to accommodate the multirate sampling. Again the established methods of multirate sampled-data optimization can be readily used [10, 45].

The sampled-data FDI problem is hence converted to a standard sampled-data control problem. Now the main theorem can be stated: Consider the single-rate sampled-data system in (6.1), (6.2) and (6.3). The goal is to design a residual generator which optimizes the FDI performance index in (6.14) or (6.15). Let $J^*_{\text{FDI}}(h)$ be the optimal sampled-data FDI performance ($\mathcal{H}_2$ or $\mathcal{H}_\infty$ norm of the closed-loop operator).

Also consider the multirate sampled-data system described by (6.1), (6.10) and (6.3). The FDI performance index for the multirate sampled-data problem is similarly defined as the $\mathcal{H}_2$ or $\mathcal{H}_\infty$ norm of the closed-loop operator. Let $J^*_{\text{FDI}}(n_1h, \cdots, n_mh, h)$ denote the optimal multirate FDI performance.

Theorem 6.1 *For the sampled-data system described above and the FDI performance indices in (6.14) and (6.15), the following statements hold*

1. $J^*_{\text{FDI}}(h) \leq J^*_{\text{FDI}}(nh), \quad \forall n \in \mathbb{N},$
2. $J^*_{\text{FDI}}(h) \leq J^*_{\text{FDI}}(n_1h, \cdots, n_mh, h) \leq J^*_{\text{FDI}}(Nh).$

□

The two parts of this theorem are special cases of Theorems 5.3 and 5.4 and the proofs are similar.

6.4 Conclusions

In this chapter the choice of appropriate performance index in the sampled-data FDI problem was studied. In residual generator design, it is always desired to generate a residual which is only sensitive to the fault not disturbances and other known or unknown inputs. The design is usually carried out by solving an optimization problem, hence the importance of a well-selected performance measure. The common performance criteria consider the norms

of two transfer functions (from fault and disturbance to residual) separately. The problem with these type of performance criteria is that they do not satisfy the properties that one expects when dealing with sampled-data systems. One intuitively expects that the performance of a sampled-data system is improved by increasing the sampling frequency, and the multirate controller can work better than a slow-rate controller and worse than a fast-rate one.

Since in the standard sampled-data control problem, the $\mathcal{H}_2$ or $\mathcal{H}_\infty$ norm of the closed-loop system satisfies the expected properties, it is reasonable to convert the sampled-data FDI problem to the standard form. This is done by combining the two transfer functions (from fault and disturbance to residual) and considering the norm of one single transfer function rather than two transfer functions individually. Some modifications are required to regulate the standard problem and eliminate the trivial solutions. These modifications are performed by introducing appropriate weighting. The result is a standard control problem, which can be readily solved by any known technique for both single-rate and multirate systems.

Chapter 7

Conclusions and Future Work

In this thesis, some fundamental problems of fault detection and isolation in sampled-data systems have been investigated. This chapter summarizes the results reported in this thesis and proposes some possible future research directions.

7.1 Conclusions

In sampled-data systems, the process under control is a real world continuous-time system, while the controller and the FDI are digitally implemented by a computer. So, sampled-data systems involve both continuous and discrete-time signals and systems and hence are hybrid. Two traditional approaches of controller/FDI design for sampled-data systems are known as indirect designs. In one approach the continuous-time process is approximated by a discrete-time one and then a discrete-time controller/FDI is designed for this system. In the other approach first a continuous-time controller/FDI is designed for the continuous-time process and then is approximated by a discrete-time controller/FDI. Since both approaches involve approximations, the results might not be very satisfactory. In the FDI case, examples have been proposed in the literature to show that the indirect designs are in fact unsatisfactory [54]. This motivated us to switch to direct method of FDI design.

To design an optimal robust residual generator for a sampled-data system, it was shown that one can simply replace the sampled-data system with a certain discrete-time one. Any optimal norm based residual generator for the equivalent discrete-time system is also optimal for the sampled-data system.

This approach, unlike the indirect design techniques, does not involve any approximation. That is because the norm invariant transformation guarantees that the norms of the operators relating the fault and disturbance to the residual are equal in the original sampled-data and its equivalent discrete-time systems. Moreover, this approach is as simple as the indirect design, both mathematically and numerically. It was also shown that, based on the direct design in a sampled-data setup, it is generally more difficult to perfectly decouple residual from disturbance. In other words, even if perfect decoupling is possible for the continuous-time model, it may not be possible in a sampled-data configuration.

The idea of direct design was then generalized to multirate sampled-data systems. Similar to the single-rate case, it was shown that in order to design an optimal residual generator, one can replace the original multirate system with a discrete-time (slow-rate) one. The equivalent discrete-time system was obtained using the norm invariant transformation and the lifting operation. Any norm based method of residual generator design can be used. However, directly applying the methods will result in a slow-rate residual signal, for the equivalent discrete-time system is a slow-rate model. To reduce the detection delay the residual has to be generated at a faster rate. For this purpose, the concept of lifted residual was introduced which yields fast-rate residuals after applying the inverse lifting operator. Two methods of generating the lifted residual were developed. The first method was based on the parity space with the difference that instead of a parity vector, a parity matrix was used. The second method was based on the factorization approach with $\mathcal{H}_\infty$ optimization. Both methods involve optimizing a performance index subject to a set of causality constraints. For both methods, the analytical solutions of the optimization problems with constraints were proposed.

Most techniques of robust residual generation rely on a performance index to measure the compromise between robustness to disturbance and sensitivity to fault. So, selection of the performance index is a fundamental stage in FDI design. There are some properties that one expects a suitable performance index to satisfy. One of this properties is that for a suitable performance index, the optimal multirate design works better than the optimal slow-rate design but worse than the optimal fast-rate design. Unfortunately, this property does not hold for the performance indices traditionally used for FDI design (in par-

ity space, $\mathcal{H}_\infty$ optimization and $\mathcal{H}_2$ optimization methods). In contrast, it was proved that the property is indeed true for the performance indices used in control system design, i.e., $\mathcal{H}_\infty$ and $\mathcal{H}_2$ norms of closed-loop systems. This means that for the standard control problem, the optimal fast-rate controller performs better (i.e., yields smaller closed-loop norm) than the optimal multirate controller, which in turn performs better than the optimal slow-rate controller. In order to take advantage of this, the FDI design problem was formulated as a standard control problem. This was accomplished by combining the two requirements of the FDI problem (robustness to disturbance and sensitivity to fault). Any method of sampled-data controller design (e.g., $\mathcal{H}_\infty$ or $\mathcal{H}_2$) can then be readily applied to the converted FDI problem.

7.2 Future work

The research on fault diagnosis in sampled-data systems, supported by the well developed sampled-data control theory, has received great attention recently. Nonetheless, there are still many unanswered questions, some of them are proposed herein:

- Considering properties of a performance index for a sampled-data optimization problem, and how the optimal performance changes by varying the sampling period, there are many important questions to answer. For example, it is almost certainly believed that increasing the sampling frequency improves the performance of a sampled-data system (at least in a neighborhood of the origin). That is one reason why electronic manufacturers try to introduce faster and faster analog-to-digital and digital-to-analog converters in the market. Surprisingly, as far as we know, no theoretical work has been done in this regards. This conjecture was proved for a special case in this thesis (Theorem 5.3). However, how changing the sampling period affects the optimal performance in general is still unknown. The above conjecture is most likely true, but if it is not, then it would be interesting to investigate under what conditions and for what type of performance index it holds.

- The selection of performance index is a basic step in robust FDI design. In this thesis, it was shown that the common performance measures that

are used in the literature are not appropriate for this purpose. As an alternative, the performance measures in controller design ($\mathcal{H}_\infty$ and $\mathcal{H}_2$ norms of closed-loop systems) were used for FDI performance. But as mentioned before, this will add some conservatism to the solution. So another topic for research is to find a performance index that is not conservative, and in addition satisfies expected properties (proper behavior with respect to sampling period).

- In Chapter 3, the norm based methods of residual generation were generalized to sampled-data systems using the norm invariant transformation. It would be interesting to investigate if other methods of residual generation (e.g., observers) can be generalized for sampled-data systems via some direct design approach.

- Two methods of fast-rate residual generation for multirate sampled-data systems were developed in Chapter 4. The solutions of the corresponding optimization problems in those methods have the advantage that many parameters can be chosen freely. The freedom was used in this thesis to accommodate the practical causality constraints. One direction for research is using the free parameters to involve other useful constraints, to optimize other performance criteria or to isolate the faults. It would also be interesting to investigate other methods of residual generation for multirate systems.

- Fault detection process usually consists of different steps. In this thesis, however, only residual generation was considered. Residual analysis is also an important process in an FDI system which is carried out after the residual is generated. Residual analysis in sampled-data systems would be an interesting research topic. For instance, one can investigate how to select a threshold for residual and how the sampling period affects the threshold.

- Fault diagnosis is an essential part of any industrial control system. Moreover, most of the control systems are implemented in a sampled-data framework in industry. So another important research topic is to investigate the practical issues of fault diagnosis in (single-rate and multirate) sampled-data control systems.

Bibliography

[1] M. Araki and K. Yamamoto, "Multivariable multirate sampled-data systems: state space description, transfer characteristics and nyquist criterion", *IEEE Transactions on Automatic Control*, vol. 31, pp. 145–154, 1986.

[2] B.A. Bamieh and J.B. Pearson, "A general framework for linear periodic systems with applications to $\mathcal{H}_\infty$ sampled-data control", *IEEE Transactions on Automatic Control*, vol. 37, pp. 418–435, 1992.

[3] B.A. Bamieh and J.B. Pearson, "The $\mathcal{H}_2$ problem for sampled-data systems", *Systems & Control Letters*, vol. 19, pp. 1–12, 1992.

[4] M. Basseville and I.V. Nikiforov, *Detection of Abrupt Changes, Theory and Application*, Prentice-Hall, 1993.

[5] D. S. Bernstein, *Matrix Mathematics: Theory, Facts, and Formulas with Application to Linear Systems Theory*, Princeton University Press, Princeton, 2005.

[6] J. Braslavsky, G. Meinsma, R. Middleton and J. Freudenberg, "On a key sampling formula relating the Laplace and $\mathcal{Z}$ transforms", *Systems & Control Letters*, vol. 29, pp. 181–190, 1997

[7] J. Chen and R. Patton, *Robust Model-Based Fault Diagnosis for Dynamic Systems*, Kluwer Academic Publishers, Boston, 1999.

[8] T. Chen, "A simple derivation of the $\mathcal{H}_2$ optimal sampled-data controllers", *Systems & Control Letters*, vol. 20, pp. 49–56, 1993.

[9] T. Chen and B. Francis, *Optimal Sampled-data Control Systems*, Springer, New York, 1995.

[10] T. Chen and L. Qiu, "$\mathcal{H}_\infty$ design of general multirate sampled-data control systems", *Automatica*, vol. 30, pp. 1139–1152, 1994.

[11] E.Y. Chow and A.S. Willsky, "Analytical redundancy and the design of robust failure detection systems", *IEEE Transactions on Automatic Control*, vol. 29, pp. 603–614, 1984.

[12] S.X. Ding and P.M. Frank, "Fault detection via optimally robust detection filters", *Proceedings of the 28th IEEE Conference on Decision and Control*, pp. 1767–1772, 1989.

[13] S.X. Ding, T. Jeinsch, P.M. Frank and E.L. Ding, "A unified approach to the optimization of fault detection systems", *International Journal of Adaptive Control and Signal Processing*, vol. 14, pp. 725–745, 2000.

[14] M.S. Fadali, "Observer-based robust fault detection of multirate linear system using a lift reformulation", *Computers and Electrical Engineering*, vol. 29, pp. 235–243, 2003.

[15] M.S. Fadali and H.E. Emara-Shabaik, "Timely robust fault detection for multirate linear systems", *International Journal of Control*, vol. 75, pp. 305–313, 2002.

[16] M.S. Fadali and W. Liu, "Fault detection for systems with multirate sampling", *Proceedings of the American Control Conference*, pp. 3302–3306, 1998.

[17] C. Favre, "Fly-by-wire for commercial aircraft: the Airbus experience", *International Journal of Control*, vol. 59, pp. 139–57, 1994.

[18] P.M. Frank, "Fault diagnosis in dynamic systems using analytical and knowledge-based redundancy: A survey and some new results", *Automatica*, vol. 26, pp. 459–474, 1990.

[19] P.M. Frank, "Analytical and qualitative model-based fault diagnosis - A survey", *European Journal of Control*, vol. 2, pp. 6–28, 1996.

[20] P.M. Frank and S.X. Ding, "Frequency domain approach to optimally robust residual generation and evaluation for model-based fault diagnosis", *Automatica*, vol. 30, pp. 789–804, 1994.

[21] P.M. Frank and S.X. Ding, "Survey of robust residual generation and evaluation methods in observer-based fault detection systems", *Journal of Process Control*, vol. 7, pp. 403–424, 1997.

[22] P.M. Frank, S.X. Ding and T. Marcu, "Model-based fault diagnosis in technical processes", *Transactions of the Institute of Measurement and Control*, vol. 22, pp. 57–101, 2000.

[23] J.J. Gertler, "Survey of model-based diagnosis and isolation in complex plants", *IEEE Control Systems Magazine*, vol. 9, pp. 3–11, 1988.

[24] J.J. Gertler, "Analytical redundancy methods in fault detection and isolation; survey and synthesis", *Proceedings of the IFAC Fault Detection, Supervision and Safety for Technical Processes*, pp. 9–21, 1991.

[25] J.J. Gertler, *Fault Detection and Diagnosis in Engineering Systems*, Marcel Dekker, New York, 1998.

[26] P.R. Goulding, B. Lennox, D.J. Sandoz, K.J. Smith and O. Marjanovic, "Fault detection in continuous processes using multivariate statistical methods", *International Journal of Systems Science*, vol. 31, pp. 1459–1471, 2000.

[27] T. Hagiwara and M. Araki, "FR-operator approach to the $\mathcal{H}_2$ analysis of sampled-data systems", *IEEE Transactions on Automatic Control*, vol. 40, pp. 1411–1421, 1995.

[28] M. Hou and P.C. Muller, "Fault detection and isolation observers", *International Journal of Control*, vol. 60, pp. 827–846, 1994.

[29] V. Ionescu and C. Oara, "Spectral and inner-outer factorizations for discrete-time systems", *IEEE Transactions on Automatic Control*, vol. 41, pp. 1840–1845, 1996.

[30] R. Isermann and P. Balle, "Trends in the application of model-based fault detection and diagnosis of technical processes", *Control Engineering Practice*, vol. 5, pp. 709–719, 1997.

[31] R. Isermann, R. Schwarz, and S. Stolzl "Fault-tolerant drive-by-wire systems", *IEEE Control Systems Magazine*, vol. 22, pp. 64–81, 2002.

[32] I. Izadi, T. Chen and Q. Zhao, "Norm invariant discretization for sampled-data fault detection", *Automatica*, vol. 41, pp. 1633–1637, 2005.

[33] I. Izadi, T. Chen and Q. Zhao, "$\mathcal{H}_\infty$ performance comparison of single-rate and multirate sampled-data systems", *Proceedings of the American Control Conference*, pp. 183–187, 2006.

[34] I. Izadi, T. Chen and Q. Zhao, "Performance analysis in multirate sampled-data control systems", submitted to *IEEE Transactions on Automatic Control.*

[35] I. Izadi, Q. Zhao and T. Chen, "An optimal fast rate fault detection scheme for multirate sampled-data systems", *Proceedings of the 43rd IEEE Conference on Decision and Control*, pp. 4776-4781, 2004.

[36] I. Izadi, Q. Zhao and T. Chen, "An optimal scheme for fast-rate fault detection based on multirate sampled data", *Journal of Process Control*, vol. 15, pp. 307–319, 2005.

[37] I. Izadi, Q. Zhao and T. Chen, "An $\mathcal{H}_\infty$ approach to fast-rate fault detection for multirate sampled-data systems", *Journal of Process Control*, vol. 16, pp. 651–658, 2006.

[38] I. Izadi, Q. Zhao and T. Chen, "Analysis of performance criteria in sampled-data fault detection", submitted to *Systems & Control Letters.*

[39] P.P. Khargonekar and N. Sivasbankar, "$\mathcal{H}_2$ optimal control for sampled-data systems", *Systems & Control Letters*, vol. 18, pp. 627–631, 1992.

[40] A. Medvedev, "Fault detection and isolation by a continuous parity space method", *Automatica*, vol. 31, pp. 1039–1044, 1995.

[41] R.J. Patton, "Robustness issues in fault tolerant control", Plenary paper, *International Conference on Fault Diagnosis*, Toulouse, France, 1993.

[42] R.J. Patton and J. Chen, "Robust fault detection using eigenstructure assignment: A tutorial consideration and some new results", *Proceedings of the 30th IEEE Conference on Decision and Control*, pp. 2242–2247, 1991.

[43] R.J. Patton, P.M. Frank and R. Clark (Eds.), *Fault Diagnosis in Dynamic Systems, Theory and Application*, Prentice Hall, New York, 1989.

[44] R. Peuget, J.P. Rognon, N. Martin, "Signal based approaches to fault detection in electrical drives", *European Physical Journal, Applied Physics*, vol. 3, pp. 53–58, 1998.

[45] L. Qiu and T. Chen, "$\mathcal{H}_2$ optimal design of multirate sampled-data systems," *IEEE Transactions on Automatic Control*, vol. 39, pp. 2506–2511, 1994.

[46] L. Qiu and K. Tan, "Direct state space solution of multirate sampled-data $\mathcal{H}_2$ optimal control", *Automatica*, vol. 34, pp. 1431–1437, 1998.

[47] K.G. Shin, H. Kim, "A time redundancy approach to TMR failures using fault-state likelihoods", *IEEE Transactions on Computers*, vol. 43, pp. 1151–1162. 1994.

[48] A.K. Tangirala, R.S. Patwardhan, S.L. Shah, and T. Chen, "LQR performance comparison of multirate vs. single-rate systems", *Special Issue in DCDIS Series B on Control of Dynamic Multirate Systems*, vol. 8, pp. 517–537, 2001.

[49] N. Viswanadham and K.D. Minto, "Fault diagnosis in multirate sampled-data systems", *Proceedings of the 29th IEEE Conference on Decision and Control*, pp. 3666–3671, 1990.

[50] X. Wang, L. Zhang, T. Chen and B. Huang, "Minimum variance in fast, slow and dual-rate control loops", *International Journal of Adaptive Control and Signal Processing*, vol. 19, pp. 575–600, 2005.

[51] C. Zhang, and J. Zhang, "Performance of periodically time-varying controllers for sampled data control", *IEEE Transactions on Automatic Control*, vol. 44, pp. 1607–1611, 1999.

[52] C. Zhang, J. Zhang and K. Furuta, "Analysis of $\mathcal{H}_2$ and $\mathcal{H}_\infty$ performance of discrete periodically time varying controllers", *Automatica*, vol. 33, pp. 619–634, 1997.

[53] P. Zhang, S.X. Ding, G.Z. Wang and D.H. Zhou, "An FDI approach for sampled-data systems", *Proceedings of the American Control Conference*, pp. 2702–2707, 2001.

[54] P. Zhang, S.X. Ding, G.Z. Wang and D.H. Zhou, "Fault detection in multirate sampled data systems with time delays", *Proceedings of the IFAC World Congress*, 2002.

[55] P. Zhang, S.X. Ding, G.Z. Wang and D.H. Zhou, "Fault detection for multirate sampled-data systems with time delays", *International Journal of Control*, vol. 75, pp. 1457–1471, 2002.

[56] P. Zhang, S.X. Ding, G.Z. Wang and D.H. Zhou, "A frequency domain approach to fault detection in sampled-data systems", *Automatica*, vol. 39, pp. 1303–1307, 2003.

[57] P. Zhang, S.X. Ding, G.Z. Wang and D.H. Zhou, "An FD approach for multirate sampled-data systems in the frequency domain", *Proceedings of the American Control Conference*, pp. 2901–2906, 2003.

[58] P. Zhang, S.X. Ding, G.Z. Wang, D.H. Zhou and E.L. Ding, "An $\mathcal{H}_\infty$ approach to fault detection for sampled-data systems", *Proceedings of the American Control Conference*, pp. 2196–2201, 2002.

[59] P. Zhang, S.X. Ding, G.Z. Wang, D.H. Zhou and E.L. Ding, "Observer-based approaches to fault detection in multirate sampled-data systems", *Proceedings of the 4th Asian Control Conference*, pp. 1367–1372, 2002.

Appendix A

Co-inner-outer Factorization for Discrete-time Systems

In this appendix the method of calculating the co-inner-outer factorization of a discrete-time system is given. The results are adopted from [29]. Notice that there is a duality between inner-outer factorization and co-inner-outer factorization. If $G_i(z)$ and $G_o(z)$ form an inner-outer factorization of $G(z)$ (i.e., $G(z) = G_i(z)G_o(z)$), then $G_i^T(z)$ and $G_o^T(z)$ form a co-inner-outer factorization of $G^T(z)$, and vice versa. Therefore, here only the calculation of the inner-outer factorization for discrete-time systems is given.

Assume that $G(z) \in \mathcal{RH}_\infty$ is an LTI discrete-time system with sampling period h and has no transmission zeros on the unit circle. Then there exists an inner-outer factorization of $G(z)$

$$G(z) = G_i(z)G_o(z).$$

The inner matrix $G_i(z) \in \mathcal{RH}_\infty$ satisfies

$$G_i^T(e^{-j\omega h})G_i(e^{j\omega h}) = I.$$

The outer matrix $G_o(z) \in \mathcal{RH}_\infty$ has a right inverse $G_o^{-1}(z) \in \mathcal{RH}_\infty$ such that

$$G_o(z)G_o^{-1}(z) = I.$$

Assume that $G(z)$ has the following stat space realization

$$G(z) = \left[\begin{array}{c|c} A & B \\ \hline C & D \end{array}\right].$$

The procedure for obtaining the inner-outer factorization of $G(z)$ is given below:

1. Define

$$Q = C^T C,$$
$$L = C^T D,$$
$$R = D^T D.$$

2. Solve the following discrete-time algebraic Riccati equation

$$X = A^T X A - (A^T X B + L)(B^T X B + R)^{-1}(A^T X B + L)^T + Q.$$

3. Define

$$F = (B^T X B + R)^{-1}(A^T X B + L)^T.$$

4. Find the Cholesky decomposition

$$H^T H = B^T X B + R.$$

5. The inner and outer matrices $G_i(z)$ and $G_o(z)$ are given as

$$G_i(z) = \left[\begin{array}{c|c} A + BF & BH^{\#} \\ \hline C + DF & DH^{\#} \end{array}\right],$$
$$G_o(z) = \left[\begin{array}{c|c} A & B \\ \hline -HF & H \end{array}\right],$$

   where $H^{\#}$ is the right inverse of H satisfying $HH^{\#} = I$.

6. In addition right inverse of $G_o(z)$ is given as

$$G_o^{-1}(z) = \left[\begin{array}{c|c} A + BF & BH^{\#} \\ \hline F & H^{\#} \end{array}\right].$$

Appendix B

Computation of B_J

Assume that the matrices A and B (usually from a state-space realization) and the sampling period h are given. The objective is to calculate the full rank matrix B_J satisfying

$$B_J B_J^T = \int_0^h e^{A\tau} B B^T e^{A^T\tau} d\tau.$$

The procedure is given below [9]:

1. Define
$$P = \exp\left(h \begin{bmatrix} -A & BB^T \\ 0 & A^T \end{bmatrix}\right).$$
2. Partition P accordingly
$$P = \begin{bmatrix} P_{11} & P_{12} \\ 0 & P_{22} \end{bmatrix}.$$
3. Then,
$$B_J B_J^T = P_{22}^T P_{12}.$$

To compute B_J, if $P_{22}^T P_{12}$ is full rank then the Cholesky decomposition can be used and B_J would have the same dimensions as $P_{22}^T P_{12}$. But if $P_{22}^T P_{12}$ is rank deficient, then the number of columns of a full rank B_J is less than that of $P_{22}^T P_{12}$. In this case the simple version of Cholesky decomposition is not applicable. So using the singular value decomposition of $P_{22}^T P_{12}$

$$P_{22}^T P_{12} = \begin{bmatrix} U_1 & U_2 \end{bmatrix} \begin{bmatrix} \Sigma & 0 \\ 0 & 0 \end{bmatrix} \begin{bmatrix} U_1^T \\ U_2^T \end{bmatrix},$$

B_J can be calculated as

$$B_J = U_1 \Sigma^{1/2}.$$

Appendix C

Calculation of the Causal Optimal Solution in Section 4.4.2

Assume that $G(z) \in \mathcal{RH}_\infty$ is a given $q \times p$ transfer function matrix. In this appendix, the objective is to solve the following problem:

> **Problem 1**: Find a $n \times q$ transfer function matrix $Q(z) \in \mathcal{RH}_\infty$ that satisfies the following conditions
>
> i. Optimality Condition $\quad \|Q(z)G(z)\|_\infty = \|Q(z)\|_\infty \|G(z)\|_\infty$
>
> ii. Causality Condition $\quad Q(\infty) = XN_{\mathcal{M}}$

The number of columns of $Q(z)$, q, is given (since $G(z)$ is known). But the number of rows of $Q(z)$, n, can be chosen freely. Also $N_{\mathcal{M}}$ is a given fat matrix satisfying $N_{\mathcal{M}}N_{\mathcal{M}}^T = I$, but X can be arbitrarily chosen.

It is first shown that a constant matrix (not a transfer function matrix) can not solve the problem. Let $Q(z) = Q(\infty) = XN_{\mathcal{M}} = Q$. Since $Q(z)$ is constant, the $\mathcal{H}_\infty$ norm of the transfer function matrix $Q(z)$ will be equal to the induced 2-norm (spectral norm) of the constant matrix Q

$$\|Q(z)\|_\infty = \|Q\|_2.$$

The optimality condition implies that

$$\|QG(z)\|_\infty = \|Q\|_2\|G(z)\|_\infty = \|XN_{\mathcal{M}}\|_2\|G(z)\|_\infty = \|X\|_2\|G(z)\|_\infty.$$

Now it follows that

$$\begin{aligned}\|QG(z)\|_\infty = \|XN_{\mathcal{M}}G(z)\|_\infty &\leq \|X\|_2\|N_{\mathcal{M}}G(z)\|_\infty \\ &\leq \|X\|_2\|N_{\mathcal{M}}\|_2\|G(z)\|_\infty = \|X\|_2\|G(z)\|_\infty.\end{aligned} \tag{C.1}$$

For the optimality condition to be satisfied, all the inequalities in (C.1) should be converted to equalities. This is possible when $\|N_{\mathcal{M}}G(z)\|_\infty = \|G(z)\|_\infty$. But since $N_{\mathcal{M}}$ and $G(z)$ are independently given this is not always true. As a matter of fact, by submultiplicative property of $\mathcal{H}_\infty$ norm, most of the times $\|N_{\mathcal{M}}G(z)\|_\infty < \|G(z)\|_\infty$. In this case a constant matrix can not solve the problem. So the general form of the transfer function matrix has to be considered.

To simplify the calculations, the problem, originally in discrete-time, is transferred into continuous-time. Notice that the frequency response of a continuous-time transfer function is a polynomial function of frequency, while it is an exponential function in discrete-time case. Recall that the bilinear transformation preserves the $\mathcal{H}_\infty$ norm of a transfer function (Section 3.2.4). So, the bilinear transformation is used as a change of variable to convert the discrete-time problem (exponential function of frequency) to an equivalent continuous-time problem (polynomial function of frequency). Let $Q_{\mathrm{BT},i}(s)$ and $G_{\mathrm{BT}}(s)$ denote the bilinear transformations of $Q(z)$ and $G(z)$ respectively. Also note that $z \to \infty$ is equivalent to $s \to \frac{2}{h}$ in the bilinear transformation (h is the sampling period of $Q(z)$ and $G(z)$). Then the equivalent Continuous-time problem is:

> **Problem 2**: Find a $n \times q$ transfer function matrix $Q_{\mathrm{BT}}(s) \in \mathcal{RH}_\infty$ that satisfies the following conditions
>
> i. Optimality Condition
>
> $$\|Q_{\mathrm{BT}}(s)G_{\mathrm{BT}}(s)\|_\infty = \|Q_{\mathrm{BT}}(s)\|_\infty\|G_{\mathrm{BT}}(s)\|_\infty \tag{C.2}$$
>
> ii. Causality Condition
>
> $$Q_{\mathrm{BT}}(\frac{2}{h}) = XN_{\mathcal{M}} \tag{C.3}$$

$Q_{\mathrm{BT}}(s)$ is chosen to be a $1 \times q$ transfer function matrix (note that he number of rows of $Q_{\mathrm{BT}}(s)$ can be selected freely). To construct a $Q_{\mathrm{BT}}(s)$ that solves the problem, the following lemmas are useful:

Lemma C.1 *Assume that* $G_1(s), G_2(s) \in \mathcal{RH}_\infty$ *and*

$$\|G_i(s)\|_\infty = \sigma_{\max}(G_i(j\omega_o)) = \|G_i(j\omega_o)\|_2, \quad i = 1, 2,$$

and also

$$\|G_1(j\omega_o)G_2(j\omega_o)\|_2 = \|G_1(j\omega_o)\|_2\|G_2(j\omega_o)\|_2,$$

then

$$\|G_1(s)G_2(s)\|_\infty = \|G_1(s)\|_\infty\|G_2(s)\|_\infty.$$

$\sigma_{\max}(\cdot)$ represents the maximum singular value. ω_o is the frequency where the $\mathcal{H}_\infty$ norm of $G_1(s)$ and $G_2(s)$ is calculated. This lemma states sufficient conditions for which the submultiplicative property of $\mathcal{H}_\infty$ norm is converted to an equality.

Proof By submultiplicative property of $\mathcal{H}_\infty$ norm

$$\|G_1(s)G_2(s)\|_\infty \leq \|G_1(s)\|_\infty\|G_2(s)\|_\infty.$$

On the other hand

$$\begin{aligned}\|G_1(s)G_2(s)\|_\infty &\geq \|G_1(j\omega_o)G_2(j\omega_o)\|_2 \qquad \text{(by definition of } \mathcal{H}_\infty \text{ norm)} \\ &= \|G_1(j\omega_o)\|_2\|G_2(j\omega_o)\|_2 = \|G_1(s)\|_\infty\|G_2(s)\|_\infty.\end{aligned}$$

Comparing the two equations will complete the proof.

□

Lemma C.2 *Assume that* $G_i(s) \in \mathcal{RH}_\infty$, $i = 1, \cdots, n$, *and*

$$\|G_i(s)\|_\infty = \sigma_{\max}(G_i(j\omega_o)) = \|G_i(j\omega_o)\|_2, \quad i = 1, \cdots, n,$$

then the following identity holds

$$\|[G_1(s) \quad G_2(s) \quad \cdots \quad G_n(s)]\|_\infty = \|[G_1(j\omega_o) \quad G_2(j\omega_o) \quad \cdots \quad G_n(j\omega_o)]\|_2.$$

Proof Assume that

$$\|[G_1(s) \quad G_2(s) \quad \cdots \quad G_n(s)]\|_\infty \neq \|[G_1(j\omega_o) \quad G_2(j\omega_o) \quad \cdots \quad G_n(j\omega_o)]\|_2.$$

Then there should exist some frequency $\omega_1 \neq \omega_o$ such that

$$\begin{aligned}\|[G_1(s) \quad G_2(s) \quad \cdots \quad G_n(s)]\|_\infty &= \|[G_1(j\omega_1) \quad G_2(j\omega_1) \quad \cdots \quad G_n(j\omega_1)]\|_2 \\ &> \|[G_1(j\omega_o) \quad G_2(j\omega_o) \quad \cdots \quad G_n(j\omega_o)]\|_2.\end{aligned}$$

This implies that for at least one of the G_i's, the following statement holds

$$\|G_i(j\omega_1)\|_2 > \|G_n(j\omega_o)\|_2,$$

which subsequently implies that

$$\|G_i(s)\|_\infty \geq \|G_i(j\omega_1)\|_2 > \|G_n(j\omega_o)\|_2.$$

This is a contradiction and the proof is complete.

□

Let $\|G_{\rm BT}(s)\|_\infty = \|G_{\rm BT}(j\omega_o)\|_2$ (i.e., ω_o is the frequency where the $\mathcal{H}_\infty$ norm of $G_{\rm BT}(s)$ is calculated). Also assume that the singular value decomposition of $G_{\rm BT}(j\omega_o)$ is

$$G_{\rm BT}(j\omega_o) = U\Sigma V, \tag{C.4}$$

where U and V are complex unitary matrices and $U = [u_1 \quad u_2 \quad \cdots \quad u_q]$. Then,

$$\|G_{\rm BT}(j\omega_o)\|_2 = \|\Sigma\|_2.$$

Define the row vector Ψ as

$$\Psi = [\psi \quad 0 \quad \cdots \quad 0]U^T = \psi u_1^T, \tag{C.5}$$

for an arbitrary positive number ψ. Thus

$$\|\Psi\|_2 = \psi.$$

Then

$$\begin{aligned}\|\Psi G_{\rm BT}(j\omega_o)\|_2 &= \|[\psi\ 0\ \cdots\ 0]U^TU\Sigma V\|_2 = \|[\psi\ 0\ \cdots\ 0]\Sigma\|_2 \\ &= \psi\|\Sigma\|_2 = \|\Psi\|_2\|G_{\rm BT}(j\omega_o)\|_2.\end{aligned}$$

Therefore, if a stable $Q_{\rm BT}(s)$ satisfies

$$\begin{aligned}Q_{\rm BT}(j\omega_o) &= \Psi, \\ \|Q_{\rm BT}(s)\|_\infty &= \|Q_{\rm BT}(j\omega_o)\|_2,\end{aligned} \tag{C.6}$$

then according to Lemma C.1, optimality condition (C.2) holds. Let

$$\begin{aligned}Q_{\rm BT}(s) &= [Q_{{\rm BT},1}(s) \quad Q_{{\rm BT},2}(s) \quad \cdots \quad Q_{{\rm BT},q}(s)] \\ \Psi &= [u_1 + jv_1 \quad u_2 + jv_2 \quad \cdots \quad u_q + jv_q] \\ XN_{\mathcal{M}} &= [d_{Q,1} \quad d_{Q,2} \quad \cdots \quad d_{Q,q}]\end{aligned}$$

If SISO transfer functions $Q_{\mathrm{BT},i}(s)$, $i = 1, \cdots, q$, have their maximum gain at frequency ω_o (i.e., $\|Q_{\mathrm{BT},i}(s)\|_\infty = |Q_{\mathrm{BT},i}(j\omega_o)|$) and $Q_{\mathrm{BT},i}(j\omega_o) = u_i + jv_i$ then according to Lemma C.2 the equations in (C.6) will be true and optimality condition (C.2) holds. If in addition $Q_{\mathrm{BT},i}(\frac{2}{h}) = d_{Q,i}$, the causality constraint (C.3) also holds. Now the problem is simplified to finding stable SISO transfer functions $Q_{\mathrm{BT},i}(s)$, $i = 1, \cdots, q$, that satisfy

$$\begin{cases} \|Q_{\mathrm{BT},i}(s)\|_\infty = |Q_{\mathrm{BT},i}(j\omega_o)|, \\ Q_{\mathrm{BT},i}(j\omega_o) = u_i + jv_i, \\ Q_{\mathrm{BT},i}(\frac{2}{h}) = d_{Q,i}. \end{cases}$$

These conditions can be further simplified to

$$\begin{cases} \frac{\partial}{\partial\omega}|Q_{\mathrm{BT},i}(j\omega)|^2\Big|_{\omega_o} = 0, \\ Q_{\mathrm{BT},i}(j\omega_o) = u_i + jv_i, \\ Q_{\mathrm{BT},i}(\frac{2}{h}) = d_{Q,i}. \end{cases} \tag{C.7}$$

A candidate transfer function is chosen in the form

$$Q_{\mathrm{BT},i}(s) = \frac{a_i s^3 + b_i s^2 + c_i s + d_i}{P(s)}$$

where $P(s)$ is an arbitrary Hurwitz polynomial of order at least 3. The 4 free parameters in $Q_{\mathrm{BT},i}(s)$ are enough to satisfy conditions (C.7). In fact, it is easy to show that conditions (C.7) will be simplified to a set of linear simultaneous equations in terms of a_i, b_i, c_i and d_i

$$\begin{bmatrix} \beta_{ai}(\omega_o) & \beta_{bi}(\omega_o) & \beta_{ci}(\omega_o) & \beta_{di}(\omega_o) \\ -\omega_o^3 Y(\omega_o) & -\omega_o^2 X\omega_o) & \omega_o Y(\omega_o) & X(\omega_o) \\ -\omega_o^3 X(\omega_o) & \omega_o^2 Y(\omega_o) & \omega_o X(\omega_o) & -Y(\omega_o) \\ (\frac{2}{h})^3 & (\frac{2}{h})^2 & (\frac{2}{h}) & 1 \end{bmatrix} \begin{bmatrix} a_i \\ b_i \\ c_i \\ d_i \end{bmatrix} = \begin{bmatrix} (u_i^2 + v_i^2)\alpha'(\omega_o) \\ u_i\alpha(\omega_o) \\ v_i\alpha(\omega_o) \\ P(\frac{2}{h})d_{Q,i} \end{bmatrix}, \tag{C.8}$$

where

$$\begin{aligned} P(j\omega) &= X(\omega) + jY(\omega) \\ \alpha(\omega) &= X(\omega)^2 + Y(\omega)^2 = |P(j\omega)|^2 \\ \beta_{ai}(\omega) &= -\omega^3 X'(\omega)v_i - 3\omega^2 X(\omega)v_i - \omega^3 Y'(\omega)u_i - 3\omega^2 Y(\omega)u_i \\ \beta_{bi}(\omega) &= -\omega^2 X'(\omega)u_i - 2\omega X(\omega)u_i + \omega^2 Y'(\omega)v_i - 2\omega Y(\omega)v_i \\ \beta_{ci}(\omega) &= \omega X'(\omega)v_i + X(\omega)v_i + \omega Y'(\omega)u_i + Y(\omega)u_i \\ \beta_{di}(\omega) &= X'(\omega)u_i - Y'(\omega)v_i \end{aligned}$$

The determinant of coefficients matrix of linear equations in (C.7) is

$$2\omega_o^2\alpha(\omega_o)((\frac{2}{h})^2+\omega_o^2)\left((\omega_o v_i-\frac{2}{h}u_i)X(\omega_o)+(\omega_o u_i+\frac{2}{h}v_i)Y(\omega_o)\right),$$

which is always nonzero. Therefore, this set of linear equations always have a unique solution. The first condition in (C.7) does not always guarantee that $Q_{\mathrm{BT},i}(s)$ has its maximum gain at frequency ω_o (it can be a minimum or a local maximum). This can be resolved by changing $P(s)$ with one or two steps of trial and error. After calculating $Q_{\mathrm{BT},i}(s)$, $j=1,\cdots,q$, one can construct $Q_{\mathrm{BT}}(s)$ and use the bilinear transformation to calculate $Q(z)$.

The procedure of finding $Q(z)$ is summarized below

1. Calculate $G_{\mathrm{BT}}(s)$ the bilinear transformations of $G(z)$.
2. Find ω_o and perform the singular value decomposition in (C.4).
3. Arbitrarily select ψ and compute Ψ according to (C.5).
4. Choose $P(s)$ an arbitrary Hurwitz polynomial of order at least 3 and the $1\times q$ matrix X.
5. Construct and solve the set of linear simultaneous equations in (C.8) to obtain a_i, b_i, c_i, d_i and subsequently $Q_{\mathrm{BT},i}(s)$.
6. Perform the bilinear transformation on $Q_{\mathrm{BT}}(s)$ to find $Q(z)$.